FBEC OFFICE FILE COPY

AFFDL-TR-75-51

ADA 021 286

# FRACTURE MECHANICS ANALYSIS OF AN ATTACHMENT LUG

*AEROELASTIC AND STRUCTURES RESEARCH LABORATORY*
*DEPARTMENT OF AERONAUTICS AND ASTRONAUTICS*
*MASSACHUSETTS INSTITUTE OF TECHNOLOGY*
*CAMBRIDGE, MASSACHUSETTS 02139*

JANUARY 1976

TECHNICAL REPORT AFFDL-TR-75-51

Approved for public release; distribution unlimited

AIR FORCE FLIGHT DYNAMICS LABORATORY
Air Force Systems Command
Wright-Patterson Air Force Base, Ohio 45433

NOTICE

When Government drawings, specifications, or other data are used for any purpose other than in connection with a definitiely related Government procurement operation, the United States Government thereby incurs no responsibility nor any obligation whatsoever; and the fact that the Government may have formulated, furnished, or in any way supplied the said drawings, specifications, or other data, is not to be regarded by implication or otherwise as in any manner licensing the holder or any other person or corporation, or conveying any rights or permission to manufacture, use, or sell any patented invention that may in any way be related thereto.

This report has been reviewed by the Information Office (OI) and is releasable to the National Technical Information Service (NTIS). At NTIS, it will be available to the general public, including foreign nations.

"This technical report has been reviewed and is approved for publication."

James L. Rudd

JAMES L. RUDD
Project Engineer

FOR THE COMMANDER

R.M. Bader

ROBERT M. BADER, Chief
Structural Integrity Branch
Structures Division

Gerald G. Leigh

Gerald G. Leigh, Lt Col, USAF
Chief, Structures Division

Copies of this report should not be returned unless return is required by security considerations, contractual obligations, or notice on a specific document.

UNCLASSIFIED

SECURITY CLASSIFICATION OF THIS PAGE (When Data Entered)

| REPORT DOCUMENTATION PAGE | | READ INSTRUCTIONS BEFORE COMPLETING FORM |
|---|---|---|
| 1. REPORT NUMBER<br>AFFDL-TR-75-51 | 2. GOVT ACCESSION NO.<br>N/A | 3. RECIPIENT'S CATALOG NUMBER<br>N/A |
| 4. TITLE (and Subtitle)<br>FRACTURE MECHANICS ANALYSIS OF AN ATTACHMENT LUG | | 5. TYPE OF REPORT & PERIOD COVERED<br>INTERIM<br>May 1974-October 1974 |
| | | 6. PERFORMING ORG. REPORT NUMBER<br>ASRL TR 177-1 |
| 7. AUTHOR(s)<br>Oscar Orringer | | 8. CONTRACT OR GRANT NUMBER(s)<br>F33615-74-C-3063 |
| 9. PERFORMING ORGANIZATION NAME AND ADDRESS<br>Aeroelastic and Structures Research Lab.<br>Department of Aeronautics & Astronautics<br>MIT, Cambridge, Massachusetts 02139 | | 10. PROGRAM ELEMENT, PROJECT, TASK AREA & WORK UNIT NUMBERS<br>13670315 |
| 11. CONTROLLING OFFICE NAME AND ADDRESS<br>Air Force Flight Dynamics Laboratory<br>Air Force Systems Command<br>Wright-Patterson AFB, Ohio 45433 | | 12. REPORT DATE<br>January 1976 |
| | | 13. NUMBER OF PAGES<br>83 |
| 14. MONITORING AGENCY NAME & ADDRESS(if different from Controlling Office)<br>Same | | 15. SECURITY CLASS. (of this report)<br>Unclassified |
| | | 15a. DECLASSIFICATION/DOWNGRADING SCHEDULE<br>N/A |

16. DISTRIBUTION STATEMENT (of this Report)

Approved for public release; distribution unlimited.

17. DISTRIBUTION STATEMENT (of the abstract entered in Block 20, if different from Report)

Same

18. SUPPLEMENTARY NOTES

None

19. KEY WORDS (Continue on reverse side if necessary and identify by block number)

Fracture Mechanics
Stress Intensity Factors
Finite Element Analysis
Hybrid Elements
Aircraft Structural Integrity
Stress Analysis
Computer Structural Analysis

20. ABSTRACT (Continue on reverse side if necessary and identify by block number)

This report documents a finite-element analysis procedure for computation of Mode I and Mode II stress intensity factors associated with a sharp crack in an attachment lug detail. The procedure is a complete FORTRAN-IV program which generates and parametrically analyzes the lug, based on designer-oriented input data. The formulation of a special crack-containing element is reviewed and its performance is summarized. A detailed description of the

DD FORM 1 JAN 73 1473 EDITION OF 1 NOV 65 IS OBSOLETE

UNCLASSIFIED

SECURITY CLASSIFICATION OF THIS PAGE (When Data Entered)

UNCLASSIFIED

SECURITY CLASSIFICATION OF THIS PAGE(*When Data Entered*)

lug analysis procedure covers the physical problem, modeling, program flow and options, input/output conventions, execution times and limitations which must be observed. Results from example analyses of some attachment lugs are presented.

UNCLASSIFIED

SECURITY CLASSIFICATION OF THIS PAGE(*When Data Entered*)

# FOREWORD

The developments documented in this report were carried out at the Aeroelastic and Structures Research Laboratory (ASRL), Department of Aeronautics and Astronautics, Massachusetts Institute of Technology, Cambridge, Massachusetts 02139, under Contract No. F33615-74-C-3063 (Project 1367, Task 136703) from the U.S. Air Force Flight Dynamics Laboratory. Mr. James L. Rudd (AFFDL/FBE) served as technical monitor. The contractor's report number is ASRL TR 177-1.

TABLE OF CONTENTS

## LIST OF FIGURES

LIST OF FIGURES (continued)

## Section 1

## INTRODUCTION

The application of linear elastic fracture mechanics analysis to structural details in new aircraft designs has received growing emphasis from the Air Force and from aircraft manufacturers during the past few years. Not only have fracture mechanics data become more readily available in recent years [1,2], but also, there has been a trend toward treatment of the problem of fracture in its own right, distinct from fatigue. Within the past year, this trend has culminated in the establishment of structural design criteria by the Air Force which require an aircraft designer to take specific design-analysis actions to protect structures against fracture [3]. Required design calculations now include, generally, comparison of load-induced stress intensity factors to material fracture toughness and assessment of crack growth rates, based on assumptions concerning the size and location of possible cracks in the structure. Both types of calculation require prior estimation of the load-induced stress intensity factor. Hence, there has also been considerable emphasis on adding to the body of available fracture mechanics solutions.

Because so few geometrical configurations are amenable to a purely analytical solution of the equations of elastic fracture mechanics, the finding of new solutions depends upon development of numerical analysis techniques. Extensive contributions have been made by Bowie and his colleagues [4,5,6] using the complex variable formulation of elasticity in combination with conformal mapping, analytic continuation and boundary collocation methods. Tada, et al. [7] have recently collected and classified a comprehensive body of solutions based on the semi-analytical methods (complex variables, boundary collocation, Fourier transforms, etc.) among which appear many new solutions by Tada. However, the semi-analytical methods have not as yet proved capable of application to the irregular geometrical configurations which are found so often in real airframe structural details. Stress analysis of irregular structure has been the province of the finite-element methods for the past decade. Within the last six years, numerous contributors have extended the finite-element technique to fracture mechanics analysis.

Work on finite-element fracture mechanics analysis at MIT has followed the path of assumed-stress hybrid elements, first proposed by Pian [8] for ordinary continuum elements. The hybrid method was subsequently extended by Tong, Pian, Luk, and Lasry [9,10,11,12] to formulation of rectangular elements which incorporate an elastic crack-tip singularity, but which also have an assumed linear or quadratic variation of displacements along the element edges and are thus compatible with ordinary elements (Figure 1). Numerical experiments have demonstrated that the hybrid crack-containing elements are capable of producing estimates of $K_I$ and $K_{II}$ with less than 1 percent error, using 20 to 50 total degrees of freedom in the analysis, for simple geometrical configurations. Hence, it becomes possible to create economically practical analysis procedures for structural details by refining the mesh or ordinary elements to pick up the stress gradients caused by nonuniform loading and complicated boundary geometry, leaving to the special hybrid element the task of picking up the local gradients caused by the crack-tip singularity.

This report summarizes recent developments at the MIT Aeroelastic and Structures Research Laboratory (ASRL) in which the crack-containing hybrid element has been applied for the first time to some typical structural details, found in current production aircraft, with geometries too complicated for economical solution by other techniques. The "PCRK59" crack element used in these analyses is a generalized version of the original Lasry element [12] which was formulated and programmed by Tong and subsequently modified for greater utility by the ASRL computing staff.

## Section 2

## BASIC ELEMENTS AND METHODS

### 2.1 Element QUAD4

The ASRL QUAD4 four-node quadrilateral element (Figure 2) is used as the basic building block in the analysis procedure. QUAD4 is the well-known bilinear isoparametric assumed-displacement element which has been used for continuum stress analysis for many years [13]. The ASRL version has been programmed as an independent subroutine which includes the options of individual rotation transformations at each node and calculation of a "$\underset{\sim}{B}$" matrix for stress analysis.

The nodal coordinates $X_1$, $Y_1$, $X_2, \ldots, Y_4$, element thickness T and the elastic constants matrix:

$$\underset{\sim}{C} = \begin{bmatrix} C_{11} & C_{12} & C_{13} \\ C_{12} & C_{22} & C_{23} \\ C_{13} & C_{23} & C_{33} \end{bmatrix} \quad ; \quad \begin{Bmatrix} \sigma_{XX} \\ \sigma_{YY} \\ \sigma_{XY} \end{Bmatrix} = \underset{\sim}{C} \begin{Bmatrix} \varepsilon_{XX} \\ \varepsilon_{YY} \\ \varepsilon_{XY} \end{Bmatrix} \qquad (1)$$

comprise the required basic input information. For isotropic materials

$$\underset{\sim}{C} = \frac{E}{1-\nu^2} \begin{bmatrix} 1 & \nu & 0 \\ \nu & 1 & 0 \\ 0 & 0 & \frac{1-\nu}{2} \end{bmatrix} \text{(plane stress)} \quad \text{or} \quad \frac{E}{(1+\nu)(1-2\nu)} \begin{bmatrix} 1-\nu & \nu & 0 \\ \nu & 1-\nu & 0 \\ 0 & 0 & \frac{1-2\nu}{2} \end{bmatrix} \text{(plane strain)} \qquad (2)$$

Subroutine QUAD4 allows for general plane orthotropic behavior, a capability which is included in the attachment lug program. Plane stress is assumed in the analysis. The lug program does not use the rotation transformation option.

The element stiffness matrix $\underset{\sim}{k}$ is calculated by numerical area integration, using 3x3-point Gaussian quadrature [14] for

$$\underset{\sim}{k} = T \iint_{\substack{\text{ELEMENT}\\\text{AREA}}} \underset{\sim}{D}^T \underset{\sim}{C} \underset{\sim}{D} \, dX \, dY \tag{3}$$

where $\underset{\sim}{D}$ contains the interior strain-nodal displacement relations:

$$\{\varepsilon_{XX} \ \varepsilon_{YY} \ \varepsilon_{XY}\} = \underset{\sim}{D}(X,Y)\{q_1 \ q_2 \cdots q_8\} \tag{4}$$

The stiffnesses are returned in Lower Triangle Vector (LTV) form:

$$\underset{\sim}{k} = \lfloor k_{11} \ k_{21} \ k_{22} \ k_{31} \ k_{32} \ \cdots \ k_{88} \rfloor \tag{5}$$

For the purpose of stress analysis, Eqs. 1 and 4 may be combined to give:

$$\underset{\sim}{\sigma}(X,Y) = \underset{\sim}{C}\,\underset{\sim}{D}(X,Y)\,\underset{\sim}{q} = \underset{\sim}{B}(X,Y)\,\underset{\sim}{q} \tag{6}$$

QUAD4 also returns the matrix $\underset{\sim}{B}(X_C,Y_C)$, formed at the fifth Gaussian station, for later calculation of stresses at the element "centroid", defined in terms of the nodal coordinates:

$$X_c = \frac{1}{4}\sum_{i=1}^{4} X_i \qquad Y_c = \frac{1}{4}\sum_{i=1}^{4} Y_i \tag{7}$$

The behavior of QUAD4 has been studied extensively on other projects and is well understood. Uniform or nearly uniform stress fields can be picked up to within the roundoff accuracy of the digital computer being used for the analysis. The inability of the bilinear assumed displacement fields to follow the quadratic deflection of the neutral axis of a cantilever beam loaded by an end moment has been well documented elsewhere [15] and constitutes a limitation on the QUAD4. In practical terms, this requires that the element aspect ratio (Figure 2) be held close to unity for models of structures which are expected to have quadratic or higher-order displacement behavior. In some cases, even an aspect ratio of unity is not sufficient to insure convergence of the solution. For example, the

QUAD4 element was used recently to model a thick-walled cylinder subjected to centrifugal loading from its own mass, due to rotation [16]. The analytical solution of this axisymmetric problem includes an $r^3$ term in the radial displacement field which the bilinear element is unable to pick up; errors of 25% were found for a cylinder with a 2:1 ratio of outside-to-inside radius, using four unit-aspect-ratio QUAD4 elements through the wall thickness.

The misbehavior of the bilinear element in the presence of higher-order gradients requires the use of many elements to model complicated geometries. Also, "calibration" of the finite-element model is a good idea, where possible, by comparing the numerical results with independent solutions. Calibrations for this project have included comparisons with the classical elasticity solution for stresses and displacements near a circular hole in a semi-infinite strip under tension [17] and with finite-element analyses using higher-order assumed-displacement elements.

## 2.2 Element PCRK59

Formulation of the assumed-stress hybrid finite-element method begins with the Principle of Minimum Complementary Energy:

$$\Pi_c = \sum_n \left[ \int_{S_u} \hat{\underset{\sim}{u}}^T \underset{\sim}{T} \, dS - \int_V \tfrac{1}{2} \underset{\sim}{\sigma}^T \underset{\sim}{S} \, \underset{\sim}{\sigma} \, dV \right] \tag{8}$$

where

$\sum_n$ indicates summation over the element set.

$S_u$ = part of the element boundary over which displacements are prescribed.

$V$ = element volume.

$\hat{\underset{\sim}{u}}$ = vector of prescribed displacements on $S_u$.

$\underset{\sim}{\sigma}$ = stress vector.

$\underset{\sim}{S}$ = compliance constants = $\underset{\sim}{C}^{-1}$ ($\underset{\sim}{\varepsilon} = \underset{\sim}{S}\underset{\sim}{\sigma}$).

$\underset{\sim}{T}$ = vector of surface tractions = $\underset{\sim}{N}\underset{\sim}{\sigma}$, where $\underset{\sim}{N}$ is a matrix of surface normal direction cosines.

If $\Pi_c$ is used directly, only the stress field is assumed, subject to admissibility criteria requiring that the assumed stresses satisfy:

(i) Interior equilibrium $\partial\sigma_{ij}/\partial x_j + \hat{F}_i = 0$, in V, where $\hat{F}_i$ are prescribed body forces.

(ii) Mechanical boundary conditions $\underset{\sim}{N}\underset{\sim}{\sigma} = \hat{\underset{\sim}{T}}$ on $S_\sigma$, that part of the element boundary over which the surface tractions $\hat{\underset{\sim}{T}}$ are prescribed.

(iii) Equilibrium of surface tractions $\underset{\sim}{N}\underset{\sim}{\sigma}$ across the interelement boundaries S, which are distinct from $S_u$ and $S_\sigma$.

Formal application of the variational calculus to Eq. 8 leads to two sets of Euler equations:

(iv) Interior compatibility, $\underset{\sim}{S}\underset{\sim}{\sigma} = \underset{\sim}{\varepsilon}$ in V, where $\varepsilon_{ij} = 1/2\ (\partial u_i/\partial x_j + \partial u_j/\partial x_i)$.

(v) Displacement boundary conditions, $\underset{\sim}{u} = \hat{\underset{\sim}{u}}$ on $S_u$.

If assumed stress functions are substituted and Eq. 8 is integrated before $\Pi_c$ is varied, there results a linear equation system in which the generalized coordinates to be solved for are forces. This approach leads to a Matrix Force Method analysis which brings with it the programming problem of systematic identification and elimination of redundant quantities.

The assumed-stress hybrid approach avoids the complications of force redundancy by modifying $\Pi_c$ so that the primary unknowns in a finite-element application become displacements once again. The Principle of Minimum Complementary Energy is modified by addition of Lagrange multiplier terms [8,18] which change admissibility criteria. Specifically, conditions (ii) and (iii) above are relaxed and confition (v) is enforced. Under the new principle, stress functions satisfying only the interior equilibrium conditions (i) may be assumed, and displacement functions which satisfy interelement compatibility and conditions (v) must now be assumed as well. The modified energy principle which replaces Eq. 8 is:

$$\Pi_1 = \sum_n \left[ \int_{\partial V} \tilde{T}^T \tilde{\bar{u}}\, dS - \int_V \tfrac{1}{2} \tilde{\sigma}^T \tilde{S}\, \tilde{\sigma}\, dV - \int_{S_\sigma} \tilde{\bar{u}}^T \hat{\tilde{T}}\, dS \right] \tag{9}$$

where "$\partial V$" represents the entire element boundary, $S + S_u + S_\sigma$. To convert $\Pi_1$ into a finite-element formulation, the stress vector $\tilde{\sigma}$ is assumed within each element and the displacement vector $\tilde{\bar{u}}$ is assumed on the boundary, $\partial V$, of each element:

$$\tilde{\sigma} = \tilde{P}(x,y,z)\tilde{\beta} \qquad \tilde{\bar{u}} = L(x,y,z)\tilde{q} \tag{10}$$

where $\tilde{P}$ and $\tilde{L}$ are matrices of interpolation functions. Vector $\tilde{\beta}$ contains generalized stress coordinates, while $\tilde{q}$ is a vector of nodal displacements. Matrices $\tilde{P}$ and $\tilde{L}$ are assumed independently, with $\tilde{L}$ defined only along the element boundary $\partial V$. Substitution of Eq. 10 into Eq. 9 then leads to:

$$\Pi_1 = \sum_n \left[ \tilde{\beta}^T \tilde{G} \tilde{q} - \tfrac{1}{2} \tilde{\beta}^T \tilde{H} \tilde{\beta} - \tilde{q}^T \hat{\tilde{Q}} \right] \tag{11}$$

where

$$\tilde{G} = \int_{\partial V} (\tilde{N}\tilde{P})^T \tilde{L}\, dS \qquad \tilde{H} = \int_V \tilde{P}^T \tilde{S} \tilde{P}\, dV$$

$$\hat{\tilde{Q}} = \int_{S_\sigma} \tilde{L}^T \hat{\tilde{T}}\, dS = \text{Consistent nodal force vector} \tag{12}$$

and where $\tilde{N}\tilde{\sigma} = \tilde{N}\tilde{P}\tilde{\beta}$ has been substituted for the surface traction vector $\tilde{T}$ in the expression for $\tilde{G}$.

Direct assembly and solution of the equation system represented by $\Pi_1$ is possible, but results in a mixed matrix method, with both force and displacement unknowns. A more versatile formulation is obtained by recognizing that, since the stresses are assumed independently within each element, $\tilde{P}\tilde{\beta}$ for one element is not coupled with any other elements. Therefore, the unknowns $\tilde{\beta}$ may be formally eliminated by applying the variational calculus to $\Pi_1$:

$$\delta\Pi_1(\tilde{\beta} \text{ for only one element varied}) = \delta\tilde{\beta}^T\{\partial\Pi_1/\partial\tilde{\beta}\} =$$

$$\delta\tilde{\beta}^T(\tilde{G}\tilde{q} - \tilde{H}\tilde{\beta}) = \tilde{0}$$

which leads to

$$\underset{\sim}{\beta} = \underset{\sim}{H}^{-1} \underset{\sim}{G}\, \underset{\sim}{q} \tag{13}$$

Substitution of Eq. 13 back into Eq. 11 then yields*:

$$\Pi_1 = \sum_n \left[ \frac{1}{2} \underset{\sim}{q}^T \underset{\sim}{G}^T \underset{\sim}{H}^{-1} \underset{\sim}{G}\, \underset{\sim}{q} - \underset{\sim}{q}^T \hat{\underset{\sim}{Q}} \right] \tag{14}$$

The alternate expression for $\Pi_1$ given by Eq. 14 represents a pure Matrix Displacement Method. The quantity $\underset{\sim}{G}^T \underset{\sim}{H}^{-1} \underset{\sim}{G}$ can be recognized as an element stiffness matrix. The $\sum_n$ notation may now be identified as a conventional Matrix Displacement Method structure model assembly procedure. Hence, structure models can be created by assembling conventional and hybrid elements, provided only that compatibility across the interelement boundaries is maintained by proper choices for the assemed displacement fields. The versatility of the hybrid method lies in its ability to provide special-purpose elements, for restricted regions, which may be coupled into a model containing conventional elements in the remaining regions which are free of singularities or other unusual behavior.

The original hybrid crack elements [9,10] were derived from $\Pi_1$ by assuming a stress field containing $r^{-1/2}$ terms, where r measures radial distance from the crack tip and, by assuming displacement fields which vary linearly from one node to the next, along the element boundary. However, subsequent analysis of error sources [19] has indicated that the area integration required for computation of $\underset{\sim}{H}$ (see Eqs. 12) gives poor results for the $r^{-1/2}$ terms since some of the Gaussian stations are close to the crack tip. This situation may be remedied by increasing the number of Gaussian stations, but the computation of $\underset{\sim}{k}$ then becomes too costly. A better approach, used for the second-generation crack elements [11,12] has been followed in the present work. The energy principle $\Pi_1$ may be further modified by introducing two displacement fields: $\bar{\underset{\sim}{u}}$ assumed on $\partial V$ and $\underset{\sim}{u}$ assumed in V. There now arises another compatibility condition, $\underset{\sim}{u} = \bar{\underset{\sim}{u}}$ on $\partial V$, which is relaxed by the Lagrange

---

*Note that $\underset{\sim}{H}$ and $\underset{\sim}{H}^{-1}$ are symmetric matrices.

multiplier method. At the same time, the condition that $\underset{\sim}{u}$ must satisfy the interior equilibrium equations, as well as the strain-displacement relations, is enforced. As a result, the area integration is converted to a boundary integral and $\Pi_1$ is modified to the form:

$$\Pi_2 = \sum_n \left[ \int_{\partial V} \underset{\sim}{T}^T \underset{\sim}{\bar{u}} \, dS - \frac{1}{2} \int_{\partial V} \frac{1}{2} (\underset{\sim}{T}^T \underset{\sim}{u} + \underset{\sim}{u}^T \underset{\sim}{T}) \, dS - \int_{S_\sigma} \underset{\sim}{\bar{u}}^T \underset{\sim}{\hat{T}} \, dS \right] \quad (15)$$

The same boundary displacement field $\underset{\sim}{\bar{u}}$ can be used for both $\Pi_1$ and $\Pi_2$. However, the interior assumed fields in $\Pi_2$ must be a complete elasticity solution: stresses $\underset{\sim}{\sigma}$ and displacements $\underset{\sim}{u}$ which satisfy all of the equations of elasticity, with $\underset{\sim}{T} = \underset{\sim}{N}\underset{\sim}{\sigma}$ a derived quantity. The distributions for $\underset{\sim}{\sigma}$ and $\underset{\sim}{u}$ are obtained from a complex variable solution of the equations of elasticity near a crack tip or equivalently, by solving the biharmonic equation for an Airy stress function. Computation of the element stiffness matrix is the same as for $\Pi_1$, except that $\underset{\sim}{H}$ is now computed by a boundary integral:

$$\underset{\sim}{H} = \frac{1}{2} \int_{\partial V} \left[ (\underset{\sim}{N}\underset{\sim}{P})^T \underset{\sim}{A} + \underset{\sim}{A}^T \underset{\sim}{N}\underset{\sim}{P} \right] dS \quad (16)$$

where $\underset{\sim}{A}$ is a matrix of shape functions corresponding to the interior assumed displacement field, $\underset{\sim}{u} = \underset{\sim}{A}\underset{\sim}{q}$.

The principle $\Pi_2$ also possesses the advantage of convenience for treatment of arbitrary shapes, since only boundary integration is required. Figure 3 illustrates the PCRK59 element based on $\Pi_2$. Input information required by this element is similar to the information required by QUAD4:

(i) Geometry: global coordinates of the crack tip $X_t$, $Y_t$; global coordinates of each node $X_1, Y_1, X_2, \ldots Y_9$.

(ii) Material properties: the shear modulus $G = E/2(1+\nu)$ and a second constant $\eta = (3-\nu)/(1+\nu)$ for plane stress $(3-4\nu$ for plane strain$)$

PCRK59 is programmed only for isotropic material and does not incorporate the rotation transformations available in QUAD4. In fact, rotation transformations cannot be applied once the PCRK59 stiffness matrix has been formed. This limitation is caused by the appearance of the crack tip coordinates in the numerical integration scheme, but the restriction does not affect many practical fracture mechanics problems. The numerical integration is by five-point Gaussian quadrature [14] between each pair of nodes, except that the crack surfaces are skipped. Omission of the crack surfaces is justified because they constitute $S_\sigma$, over which $\hat{\underset{\sim}{T}} = \underset{\sim}{0}$, and because the derived tractions $\underset{\sim}{T}$ satisfy this stress-free condition at least in an average sense.

The PCRK59 element has two other important features. First, unit thickness is assumed. Second, a symmetric "half-element" option is available, under which nodes 1,5 and the crack tip are assumed to lie on a line parallel to the global X-axis, while the element and applied loading are assumed to be symmetric about this line. Under these conditions, a half-model of a structure may be analyzed to obtain Mode I stress intensity solutions only; e.g., for the coupon in uniform tension with edge cracks, shown in Figure 4. The "half-element" consists of nodes 1,2,...5, only, with node 1 requiring a roller restraint to maintain the assumed symmetry. Another input parameter determines which option is executed:

KEY = 1 for "half-element"

2 for full element

The "half-element" option is used mainly for illustrative examples and performance testing. The full element option has been used exclusively in the present work.

Element PCRK59 computes and returns a stiffness matrix in LTV form (see Eq. 5) for either the 10 degree-of-freedom "half-element" or the 18 degree-of-freedom full element. In addition, a special $\underset{\sim}{B}$ matrix for calculation of stress intensities is returned. Eq. 13, used in the derivation of the stiffness matrix, can also be used to compute the generalized stress coordinates $\underset{\sim}{\beta}$ after the element nodal displacements $\underset{\sim}{q}$ have been obtained. For the PCRK59,

$$\underset{\sim}{\beta} = \{ k_1 \ \beta_2 \ \beta_3 \ \cdots \ \beta_9 \ k_2 \ \beta_{11} \ \cdots \ \beta_{18} \} \qquad (17)$$

where $k_1, k_2$, are the Mode I, Mode II stress intensity factors, defined by:

$$\sigma_{XX} = \frac{k_1}{\sqrt{2r}} f_1(\theta) + \frac{k_2}{\sqrt{2r}} f_2(\theta) + (\text{terms in } \beta_2, \beta_3 \cdots) \qquad (18)$$
$$\sigma_{YY} = \text{etc.} \cdots$$

The functions $f_1, f_2$, are from the classical crack tip solution, and the other generalized coordinates $\beta_2, \beta_3, \ldots, \beta_{18}$ represent far-field behavior. Thus, $\underset{\sim}{B}$ is formed by extracting the first and tenth rows of $\underset{\sim}{H}^{-1}\underset{\sim}{G}$, so that the stress intensities may be calculated from:

$$\{k_1 \; k_2\} = \underset{\sim}{B}_{(2\times 18)} \{g_1 \; g_2 \; \cdots \; g_{18}\} \qquad (19)$$

for the full element. Only the first row of $\underset{\sim}{H}^{-1}\underset{\sim}{G}$ is extracted if the "half-element" option is in effect:

$$k_1 = \underset{\sim}{B}_{(1\times 10)} \{g_1 \; g_2 \; \cdots \; g_{10}\} \qquad (20)$$

NASA/ASTM standard stress intensity factors may be computed after Eq. 19 or Eq. 20 by:

$$K_I = k_1 \sqrt{\pi} \qquad K_{II} = k_2 \sqrt{\pi} \qquad (21)$$

If a structure model with thickness $T \neq 1$ is to be analyzed, this may be done simply by scaling the PCRK59 stiffness to:

$$\underset{\sim}{k}' = T \underset{\sim}{k} \qquad (22)$$

Performance of the PCRK59 element has been tested extensively by comparison with classical and boundary collocation solutions [19]. Solutions for $K_I$ accurate to better than 1 percent have been obtained with a rectangular crack element surrounded by only a few QUAD4 elements. Other tests have shown that solution accuracy within 3 percent is maintained when the crack element shape is distorted by relocating some nodes as much as 0.3 x (length of crack within element) away from the positions they occupy for a rectangle. Also, the 3 percent accuracy limit can be maintained with the crack tip located anywhere from 20 to 70 percent across a line between nodes 5 and 1, with the element shape kept rectangular. The distortions of element shape and crack tip location required for the structure models analyzed in the present work are well within these limits.

The PCRK59 element possesses one unavoidable quirk which arises from its linearity. If the element is placed in a region with compressive stress normal to the crack, a negative value of $K_I$ is obtained. In a real structure, the crack would close and cease to be a problem in this situation. Therefore, negative $K_I$ values should be interpreted as signaling the absence of Mode I stress intensity. On the other hand, the solution for $K_{II}$ will be positive (negative) according to whether the crack is being subjected to positive (negative) shear stress, as defined by the standard conventions of elasticity. In this case, the correct interpretation is to take the absolute value of $K_{II}$.

In summary, the PCRK59 element permits efficient computation of stress intensity factors by well established procedures of the Matrix Displacement Method. The unusual features of the element are internal to its subroutine. The element subroutine requires familiar input information and returns $\underset{\sim}{k}$ and $\underset{\sim}{B}$ matrices like a conventional element. The structure model is assembled and a global displacement solution is computed by standard techniques. Computation of either the centroid stresses in the conventional elements or the stress intensity factors in the crack element is then merely a matter of extracting the element displacements $\underset{\sim}{q}$ from the global solution and performing a straightforward matrix multiplication.

## Section 3

## ATTACHMENT LUG PROGRAM

Program LUG has been developed for analysis of stresses or stress intensity factors in an attachment lug typical of many structural details found in current aircraft. This section describes the lug structure model and explains how the program is used. Results obtained from some example analyses are presented in Section 4.

### 3.1 Lug Structure Model

Figure 5 illustrates the structure which Program LUG models. The detail consists of a straight shank, built in at the foot and a rounded ear whose outer edge is concentric with a bearing pinhole. Provision is made to treat the lug as a two-material system composed of an isotropic bushing ring surrounding the bearing pinhole, and the lug proper, which may be treated as either isotropic or plane orthotropic. A perfect mechanical bond between the bushing and lug is assumed. A monolithic single-material lug is obtained if identical isotropic material properties are specified for the bushing and the lug proper.

Bearing loads are assumed to be applied to the structure at the bearing pinhole surface. Tension, compression, positive shear or negative shear may be applied. These loads are defined in Figure 5. Each load component is represented as a radial bearing pressure over one-half the circumference of the bearing pinhole, with the pressure distribution centered on and symmetric about the line of action of the load. Options for a cosine pressure distribution or a uniform pressure distribution are available.

The attachment lug is assumed to be under plane stress, with two analysis options allowed. Under option 1, a model of an uncracked lug is assembled, using only QUAD4 elements, and a conventional stress analysis is executed. Under option 2, a small radial crack is assumed to emanate from the bearing pinhole surface, with the crack tip located in the bushing. The length of the crack is specified by the program user (Figure 6). Program LUG automatically executes a sequence of solutions in which the crack location is varied step-wise around the entire bearing hole circumference.

## 3.2 Input Conventions

The input data conventions for Program LUG are summarized in Figure 7. Formats for all numerical data have been standardized to I5 fields for integers and E10.0 fields for floating point numbers. Integer data and floating point data supplied in E format should be right-justified in the field. However, floating point data may also be given in F format, if desired, without changing the program code. F format data need not be right-justified. Also, the implied decimal point location for floating point data may be overridden. A maximum of 3 decimal figures may be input under E format and up to 7 decimal figures may be input under F format.

A series of independent cases may be analyzed in one run. The first input data card specifies the total number of cases which follow. The remainder of the input deck consists of six cards per case which give the program a complete description of the case. The conventions for these cards are as follows:

Card 2 - may contain any alphanumeric information which identifies the case. This information is printed as a heading title.

Card 3 - specifies the options selected by the user for four control parameters:

IANL = 1 (Conventional stress analysis without crack).
2 (Stress intensity analysis).

LOAD = 1 (Cosine pressure distribution).
2 (Uniform pressure distribution).

MODE = 1 (Lug treated as isotropic).
2 (Lug treated as orthotropic).

NT = Total number of QUAD4 elements wanted per 45° arc around the bearing pinhole. A minimum value of 3 is recommended.

Card 4 - specifies the lug dimensions and crack size.

DI = Inside diameter of bearing pinhole.

DB = Outside diameter of bushing.

W = Lug width.

H = Total (root to tip) length of lug.

T = Lug thickness (lug and bushing assumed to have equal thickness).

CSIZE = Length of crack.

Card 5 - specifies the material properties of the bushing, which is always assumed to be isotropic:

E = Young's modulus.

$\nu$ = Poisson's ratio.

Card 6 - specifies the lug material properties. If MODE = 1 on card 3, the convention is:

E = Young's modulus.

$\nu$ = Poisson's ratio.

If MODE = 2 on card 3, the convention is:

$E_L$ = Longitudinal modulus.

$E_{LT}$ = Cross-coupling modulus.

$E_T$ = Transverse modulus.

$G_{LT}$ = Shear modulus.

$\theta$ = Angle between lug XY axes and material LT axes (degree measure, positive CCW from X to L).

Card 7 - specifies the bearing force value:

TENSN = Tension or compression bearing force.

SHEAR = Positive or negative shear bearing force.

The lug dimensions and crack size were defined in Figures 5 and 6. Any value of thickness may be specified. Program LUG rescales the model internally to unit thickness. Figure 8 illustrates a finite element mesh which might result when NT = 3 elements per 45° arc is specified on card 3. The positive convention for the relationship between the lug XY axes and material LT axes is also shown. The quantities $E_L$, $E_{LT}$, $E_T$, $G_{LT}$ are the conventional plane-orthotropic moduli for; e.g., a fiber composite laminate. The stress-strain relations take the form:

$$\begin{Bmatrix} \sigma_L \\ \sigma_T \\ \sigma_{LT} \end{Bmatrix} = \begin{bmatrix} E_L & E_{LT} & 0 \\ E_{LT} & E_T & 0 \\ 0 & 0 & G_{LT} \end{bmatrix} \begin{Bmatrix} \varepsilon_L \\ \varepsilon_T \\ \varepsilon_{LT} \end{Bmatrix} \tag{23}$$

in the LT axis system. For $\theta \neq 0°$ the stress-strain relations in the XY axis system take a more complicated form:

$$\begin{Bmatrix} \sigma_{XX} \\ \sigma_{YY} \\ \sigma_{XY} \end{Bmatrix} = \begin{bmatrix} C_{11} & C_{12} & C_{13} \\ C_{12} & C_{22} & C_{23} \\ C_{13} & C_{23} & C_{33} \end{bmatrix} \begin{Bmatrix} \varepsilon_{XX} \\ \varepsilon_{YY} \\ \varepsilon_{XY} \end{Bmatrix} = \underset{\sim}{C}\ \underset{\sim}{\varepsilon} \tag{24}$$

where, in general, $C_{13}$, $C_{23} \neq 0$. The matrix $\underset{\sim}{C}$ in Eq. 24 is computed from $E_L$, $E_{LT}$,...,$\theta$ by ASRL subroutine CTFORM.

The bearing load conventions were indicated in Figure 5. The value of TENSN or SHEAR supplied on card 7 refers to total bearing force; the corresponding pressure distributions are computed internally. A positive (negative) value TENSN has the effect of applying a tension (compression) bearing load to the structure. A positive (negative) value for SHEAR similarly applies a positive (negative) shear bearing load.

Figure 9 illustrates a portion of the actual finite element mesh generated for a hypothetical large all-aluminum wing root attachment lug. Since the "bushing" diameter does not have any physical significance in this single-material case, it is used to control the mesh so that the tip of a 0.5-inch long crack lies at the middle of the PCRK59 element. The crack is shown with a finite opening for clarity. However, nodes 5 and 6 of the crack element (Figure 3) actually overlap to provide the correct model of a sharp crack. The PCRK59 element has replaced a group of four adjacent

QUAD4 elements in the mesh. When analysis option 2 is in effect, a series of structure models are generated and analyzed one after the other, with the PCRK59 shifted circumferentially by one pair of QUAD4's after each analysis. Thus, for the case shown in Figure 9 (NT = 3), 24 stress intensity solutions are obtained with the crack located successively at $\theta = 0°, 15°, 30°, \ldots, 345°$. Figure 10 summarizes the input data deck required to run a stress analysis (case 1) and a stress intensity analysis (case 2) for the hypothetical lug detail.

### 3.3 Required Subprograms and Other Features

Program LUG requires the following FORTRAN-IV subroutines to form an executable load module:

(i) ASRL FEABL-2 subroutines ASMLTV, BCON, FACT, ORK, SETUP, SIMULQ, and XTRACT [20,21].

(ii) ASRL element and utility library subroutines QUAD4, PCRK59, and CTFORM.

(iii) IBM Scientific Subroutine Package routines MFSD and SINV which are required by the PCRK59 element subroutine.

The entire source deck is supplied in IBM 029-punch format.

The following features of Program LUG may cause machine-dependence problems on non-IBM hardware:

(i) The 20A4 format for input of case title information may be incompatible with some systems. This may be remedied by changing FORMAT statement 502 to 80A1 and redimensioning vector TITLE to 80.

(ii) FORTRAN unit numbers 5 and 6 are assumed for the card reader and line printer respectively. Program LUG may be converted to other hardware standards simply by reprogramming the two lines of code:

```
KR = 5
KW = 6
```

which appear shortly after the FORMAT statements near the beginning of the program.

(iii) Program LUG requires a sequential-access scratch dataset, designated as FORTRAN file 20, when analysis option 1 (uncracked structure stresses) is in effect. The file must consist of (30 single-precision words per record) x (records = maximum number of QUAD4 elements expected). A total of 600 records should be adequate for most analyses. A job control instruction, specific to the installation where the program is being executed, is required to create this file on a system disk. However, Program LUG may be executed without creating this file if only stress intensity solutions are sought.

(iv) IBM/SSP subroutines MFSD and SINV may not be compatible with other systems. If this problem arises, reprogramming or substitution will be required.

## 3.4 Model Generation and Program Flow

Program LUG automatically generates the geometrical information, element interconnections, etc., which are required to compute and assemble the element stiffnesses, restrain the structure properly, apply the bearing load and execute a stress or stress intensity analysis. The program flow is summarized in Figure 11. Parenthesized numbers in the figure refer to FORTRAN statement numbers in the program listing (Appendix A).

After the input data has been read for a case and some auxiliary values have been calculated, the case title and input data are printed for checking. A sample output from this section of the program is shown in Figure 12. The number of QUAD4 elements required radially in the bushing and lug and the number required axially in the lug shank are then computed by rounding off to the nearest whole number which gives an average element aspect ratio closest to unity for each region. The total number of elements, total degrees of freedom and some additional parameters are then calculated, and the vectors which will contain the K-solutions are erased.

The major section of the code, a loop over the crack locations, then follows. The location loop is executed 8*NT times for a stress intensity analysis, but only once for a conventional uncracked structure stress analysis. Previous results are erased and the interconnections for an uncracked structure are generated. Figure 13 illustrates the node and element numbering conventions, using the example mesh from Figure 8. The numbering patterns are as follows:

(i) Nodes are numbered, globally, radially outward from the bearing pinhole on each ray. The rays are taken in counterclockwise order, beginning at $\theta = 0°$. Vertical lines of nodes in the lug shank are numbered afterward, from the top down and from right to left. The last line of nodes is restrained.

(ii) Degrees of freedom are numbered 2n-1 (displacement parallel to X) and 2n (displacement parallel to Y) at each node n.

(iii) Elements in the bushing are numbered radially outward and counterclockwise, partially following the node numbering pattern.

(iv) Elements in the lug ear are numbered radially outward and counterclockwise after the bushing elements.

(v) Elements in the lug shank are numbered last, from the top down and from right to left.

If a stress intensity analysis is being executed, the location of the PCRK59 element is now computed from the crack location loop index and connections for this element are generated. As shown in Figure 14, the PCRK59 element overlays four QUAD4 elements. The central node of this group of elements is transferred to the bearing pinhole to accommodate the PCRK59. The element numbers of the four overlaid QUAD4 elements are also flagged.

The global XY coordinates for each node in the model are now computed, assuming an uncracked structure. If a stress intensity analysis is being executed, the transferred node coordinates are adjusted and global coordinates are computed for the crack tip. The area corresponding to the global force vector $\hat{\underset{\sim}{Q}}_G$ in the FEABL-2 storage system is used as temporary storage for the node coordinate data.

After auxiliary storage for element-level data has been prepared, a loop over all QUAD4 elements is executed. The node coordinates for each element are extracted from the global data, other required input is provided from auxiliary storage and $\underset{\sim}{k}$ and $\underset{\sim}{B}$ are computed for the element. Also, centroid coordinates $X_c$, $Y_c$ are computed for the element; $\underset{\sim}{B}$, $X_c$, $Y_c$ are stored in FORTRAN file 20 (stress analysis option only) and $\underset{\sim}{k}$ is assembled into the global stiffness matrix. If a stress intensity analysis is being executed, these procedures are skipped for the four flagged elements, while $\underset{\sim}{k}$ and $\underset{\sim}{B}$ are computed and $\hat{\underset{\sim}{k}}$ is assembled for the PCRK59.

After assembly, $\underset{\sim}{Q}_G$ is erased and replaced by prescribed nodal forces which are statically equivalent to the specified bearing load and the assumed (cosine or uniform) pressure distribution. For stress intensity analysis, the two nodes at the crack opening each receive one-half the nodal force which would have been applied to a single node at that location in an uncracked structure.

The final section of the code executes a solution of the global equation system and either a stress or a stress intensity analysis. In the latter case, the stress intensity factors are saved and a complete table is printed after the crack location loop has been completed.

## 3.5 Output Conventions and Error Messages

If a stress analysis has been executed, nodal forces, nodal displacements and element stresses are printed. The table of forces and displacements appears immediately below the problem input data and merely lists the force or displacement value for each degree of freedom ("ROW" in the table heading). The stress table contains one line of information for each element:

$$\text{Element No., } X_c, Y_c, \sigma_{xx}, \sigma_{yy}, \sigma_{xy}, \sigma_{rr}, \sigma_{\theta\theta}, \sigma_{r\theta}$$

The stress values are computed for the element's centroid location $X_c$, $Y_c$. Figures 15 and 16 present samples of these output tables.

If a stress intensity analysis has been executed, only a table of K-solutions is printed. Each line of the table corresponds to one crack location, containing:

$$\text{Angle to crack opening, } K_I, K_{II}$$

A sample is shown in Figure 17.

If abnormal conditions occur during execution, certain error messages may be printed by Program LUG. The messages and actions required are as follows:

(i) Insufficient core memory available for storage of the problem data causes the message:

THE LENGTH OF THE "DATA" VECTOR FOR THIS CASE IS xxxxx WHICH EXCEEDS yyyyy = THE MAXIMUM ALLOWED IN THE DIMENSION STATEMENT.

The entire run will be terminated if this condition occurs. The dimensions of vectors RE and IN (line 2 of the program code) are yyyyy. Redimension these vectors to 1.15 (xxxxx).

(ii) Ill-conditioning of the structure model causes the message:

INDEFINITE MATRIX; THIS CASE CANCELLED.

Execution continues with the next case. The most likely cause is misplacement of the crack tip, relative to the bushing O.D. Recheck the input data to make sure that the crack tip does not extend beyond the bushing, even if a single-material lug is being analyzed. Material property errors are another probable source. Ill-conditioning may result if the bushing is too stiff, compared to the lug, or vice versa. Errors may also results from incorrect specification of orthotropic material properties.

## 3.6 Visual Interpretation of Output

Level contour plots are recommended as the best means of visually interpreting the output from a stress analysis case. For this purpose, a scale plan of the lug outline should be prepared and the element centroid positions marked on the plan. The stress values may then be transferred and a contour plot prepared. Plots of $\sigma_{rr}$, $\sigma_{\theta\theta}$, $\sigma_{r\theta}$ in the region around the bearing pinhole and of $\sigma_{xx}$, $\sigma_{yy}$, $\sigma_{xy}$ in the shank region are recommended. The nodal displacement solution table may be used to provide a plot of the deformed structure, if desired. The output from a stress intensity analysis is best treated by means of polar plots for $K_I$ and $K_{II}$. These plots are discussed in detail with examples in Section 4.

## 3.7 Program Status

At the date of this report, the following program options have been exercised successfully:

(i) Stress and stress intensity analysis.

(ii) Bearing load: tension, compression, positive shear, and negative shear.

(iii) Cosine and uniform pressure distribution.

(iv) Isotropic, single-material lug.

(v) NT = 3, 4, and 6.

The following options have not been exercised to date:

(vi) Isotropic, two-material lug.

(vii) Isotropic bushing with orthotropic lug.

(viii) NT > 6.

Section 4

# RESULTS OF EXAMPLE ANALYSES

Two example analyses were run to demonstrate the program. The first was limited to stress and stress intensity analysis of the hypothetical wing root attachment lug shown in Figure 9. Second, a detail similar to the aft engine support pylon truss lug in the C-5A was subjected to a more extensive analysis. Experience with the program to date, on IBM S-370/165 and S-370/168 computers, indicates that approximately 1.8 to 3.6 CPU seconds per $K_I$, $K_{II}$ solution pair are required, depending upon the amount of detail in the model.

## 4.1 Analysis of Wing Root Attachment Lug

Figure 18 summarizes the stress distribution in the hypothetical wing lug. Stress contours for $\sigma_{rr}$, $\sigma_{\theta\theta}$, and $\sigma_{r\theta}$ are shown. A survey of the numerical data confirmed that $\sigma_{rr}$, $\sigma_{\theta\theta}$ were symmetric about the lug centerline. Hence, only half-plots are shown for those contours. The survey also indicated that $\sigma_{r\theta}$ behaved anti-symmetrically, as shown in the second part of Figure 18.

Figure 19 presents polar "butterfly" plots for $K_I$ and $K_{II}$ as functions of angle to the crack opening. The crack was 0.5 inches long and oriented radially. Again, the data behave symmetrically about the lug centerline (crack at 0° and 180° locations). The interpretation of these polar plots is explained in Figure 20. If the origin of the plot is identified with the center of the bearing pinhole, a radius vector through the assumed crack location may be constructed. The length of the vector between the origin and the K-plot then gives the corresponding stress intensity value.

If the crack size is small compared with the lug dimensions, there follows an intuitive hypothesis that the stress intensities ought to behave in the same manner as the uncracked structure stresses. This hypothesis can be confirmed, for the present case, by comparison of Figures 18 and 19. For a radially-oriented crack,

$K_I$ should be influenced primarily by $\sigma_{\theta\theta}$, while $K_{II}$ should be influenced primarily by $\sigma_{r\theta}$. Maxima of $\sigma_{\theta\theta}$ and $K_I$ are observed to occur near $\theta = 90°, 270°$. Maxima of $\sigma_{r\theta}$ occur approximately at $\theta = 45°, 135°, 225°$, and $315°$, while $K_{II}$ maxima occur approximately at 60°, 120°, 240°, and 300°. The apparent discrepancy between $K_{II}$ and $\sigma_{r\theta}$ can be explained by recognizing that the crack tip actually lies near the 1.5 and 2.0 ksi stress contours. Local maxima for $\sigma_{r\theta}$ in those regions are less sharply defined.

## 4.2 Analysis of Engine Pylon Truss Lug

Figure 21 is a scale plot of the structure model used to analyze a detail similar to the C-5A engine pylon aft truss lug. The actual lug has two tongues to place the bearing pin in double shear. It can be reasonably assumed that the load transferred into the engine pylon at this point is borne equally by both tongues. Hence, the lug program has been used to analyze one tongue. The model is 0.19 inch thick, with:

$D_I = 1.75$ inches $\qquad D_B = 2.35$ inches

$H = 10.5$ inches $\qquad W = 3.5$ inches

A 0.15-inch long crack was assumed, with radial orientation. Material properties for high-strength steel alloys were used:

$E = 30 \times 10^6$ psi $\qquad \nu = 0.295$

The "bushing" O.D. was chosen merely to locate the crack tip at the middle of the bushing region. Models were run with 24 elements (NT = 3, "coarse mesh") and 32 elements (NT = 4, "fine mesh") around the bearing pinhole. The fine mesh model is shown in Figure 21. All runs were made with a 1,000-pound bearing load, as a standard for plotting the results.

Figure 22 summarizes the stress distribution near the hole, as obtained from a fine mesh model of the uncracked structure, with a cosine bearing pressure distribution. The symmetries discussed in Subsection 4.1 were observed again. Three additional checks were made to assure that the model accurately reflects the stress gradients caused by the lug geometry. First, in a typical section through the shank, the tension stress $\sigma_{xx}$ was found to be uniform and statically equivalent to the bearing load, to better than one percent accuracy, for both models. Second, a section was taken through the bearing pinhole center ($\theta = 90°$, $270°$) and $\sigma_{\theta\theta}$ was plotted. The radial variation of $\sigma_{\theta\theta}$ was found to agree generally with Timoshenko's classical solution for an eye bolt under tension bearing [17]. Also, numerical evaluation of $T\int\sigma_{\theta\theta}dr$ gave the bearing load, with 1.7 percent error for the coarse mesh and 1.4 percent error for the fine mesh. Finally, the solution for $\sigma_{rr}$ was compared with the bearing pressure distribution. The peak value of the bearing pressure is given by $p_o = P/\pi D_I T$, where P is the bearing load. For the present case, $p_o = 3.83$ ksi and acts at $\theta = 0°$. The two elements with centroid locations nearest to $r = D_I/2$, $\theta = 0°$ were found to have $\sigma_{rr} = 3.5$ ksi, and the radial stress could be extrapolated to a value close to $p_o$ at the peak point. Based on these results and the measured performance of the PCRK59 element (Subsection 2.2), the fine mesh model was accepted as giving a converged solution for $K_I$, having a cumulative error of 5 percent.

Butterfly plots for $K_I$ and $K_{II}$ are shown in Figure 23. Again, the stress intensities behave symmetrically to better than 1 percent accuracy for both models, and $K_I$ follows $\sigma_{\theta\theta}$, while $K_{II}$ follows $\sigma_{r\theta}$. The data for $K_I$, shown in the upper half of the figure, demonstrate that convergence has been obtained. The data for $K_{II}$, in the lower half of the figure, indicate that additional refinement of the mesh might be required to demonstrate Mode II stress intensity convergence. However, since the $K_{II}$ values are generally smaller than $K_I$, and since they tend to decrease as the solution converges, no further refinements were made. The coarse model contained 408 degrees of freedom and took 48 CPU seconds to compute a complete set of 24 pairs of $K_I$ and $K_{II}$ solutions. The fine model contained 608 degrees of freedom and took 102 CPU seconds to compute 32 solutions.

The length of the lug detail was reduced from 10.5 inches to 7.0 inches for the remaining analyses, to eliminate superfluous elements in the shank and thus reduce computation costs. Fine mesh models (and a few "very fine" models) were analyzed in the remaining series. The shortened lug fine mesh model is illustrated by Figure 24.

The stress intensity analysis for cosine tension bearing was repeated to assess the influence of the change in shank length. Figure 25 compares the $K_I$ and $K_{II}$ butterfly plots from Figure 23 with corresponding plots for the shortened lug. A slight increase in stress intensities with decrease in shank length can be observed. Figure 26 compares butterfly plots for the 7-inch lug under cosine and uniform bearing. Three significant differences can be observed:

(i) The increased ability of a uniform bearing pressure to spread the part outward changes the hoop stress from compression to tension at $\theta = 0°$. Compare the uncracked structure stress contours for cosine bearing (Figure 22) with the contours for uniform bearing, shown in Figure 27.

(ii) The maximum $K_I$ value changes from 5 ksi $\sqrt{in.}$ at $\theta = 85°$ (cosine bearing) to about 4.7 ksi $\sqrt{in.}$ at $\theta = 107°$ (uniform bearing).

(iii) Mode II stress intensities are lower for uniform bearing.

The third series of runs analyzed the case of positive shear bearing. Figure 28 illustrates the stress contours obtained for shear bearing with a cosine distribution. The behavior of $\sigma_{rr}$ near the bearing pressure peak (now at $\theta = 90°$) is similar to the tension bearing case (compare with Figure 22). The Cartesian stress components in the shank region were surveyed to provide additional equilibrium checks. Figure 29 compares the finite element stress distributions for $\sigma_{XX}$, $\sigma_{XY}$ through a typical shank section and for $\sigma_{XX}$ axially, with engineering beam theory calculations:

$$\sigma_{XX} = -\frac{M(X)Y}{I} \qquad \sigma_{XY} = \frac{3V(X)}{2A}\left[1 - \left(\frac{2Y}{W}\right)^2\right] \qquad (25)$$

where

$M(X)$ = Section bending moment at X

$V(X)$ = Section shear at X

$I$ = Section moment of inertia = $TW^3/12$

$A$ = Section area = TW

It is evident from the figure that the finite element results are within 1 or 2 percent of engineering beam theory. The only exception is the axial behavior of $\sigma_{XX}$ which exhibits some stress concentration effects:

(i) Due to the cantilever restraints, as the left end of the shank is approached.

(ii) Due to the influence of the hole, as the shank/ear interface is approached.

Based on these results, the fine mesh model was judged to be capable of giving stress intensities for shear bearing which are comparable to the tension bearing results (5 percent error).

Figures 30 and 31 present $K_I$ and $K_{II}$ butterfly plots for cosine and uniform pressure distributions, respectively. Data for a "very fine" model (NT = 6, 48 elements around the hole) as well as for the fine mesh model, are shown in Figure 31. The refined model was run to improve the fairing of the curves, after plots of the fine mesh model were seen to have large gaps between $K_I$ data points. The refined model data indicate that the fine mesh has not quite converged the $K_I$ solutions. Two interesting features are illustrated by these plots. First, the stress intensity maxima and minima no longer coincide with the stress distribution. Apparently, even a small crack is sufficient to change the stress distribution significantly when the bearing load is shear. Second, the significant difference between cosine and uniform pressure now occurs at the $K_I$ maxima, which are about 10 percent larger for uniform pressure. This arises from the fact that the $K_I$ maxima are located near and nearly opposite to the bearing load line of action.

A fourth series of analyses treated the case of compression bearing, using only the fine mesh model. Both the stresses and stress intensities were found to behave symmetrically, similar to the case of tension bearing. Equilibrium checks and stress contour plots have been omitted, in view of the results already presented. Figures 32 and 33 show $K_I$ and $K_{II}$ butterfly plots for compression bearing with cosine and uniform distribution, respectively. The most interesting feature is the extreme sensitivity to load distribution when the crack is at or opposite to the load center. The Mode I stress intensity for uniform bearing increases by factors of 2 at the first location and 4 at the second. This extreme sensitivity results from the high hoop stresses which are present in these regions.

## 4.3 Example Application

To provide an example of how the butterfly plots may be applied to structural integrity verification analysis, the following data have been abstracted from load calculations for the original C-5A engine pylon truss design [22]:

| Load Condition | Tension (Compression) | Shear |
|---|---|---|
| "Maximum Compression" (MC) | $-221 \times 10^3$ lb. | -340 lb. |
| "Maximum Tension" (MT) | $148 \times 10^3$ lb. | 220 lb. |

The values in the above table represent total load transferred through the attachment lug, and must be divided by 2 to obtain the loads per tongue. Since shear bearing can obviously be ignored for the above conditions, there results:

Condition MC: $110.5 \times 10^3$ lb. Compression Bearing

Condition MT: $74 \times 10^3$ lb. Tension Bearing

Assuming that a cosine pressure distribution is representative, the following calculations can be made for 0.15-inch cracks assumed to be located at 0°, 45°, 90°, and 180°:

| Crack Location | Condition MC (K values in ksi$\sqrt{\text{in.}}$) | Condition MT (K values in ksi$\sqrt{\text{in.}}$) |
|---|---|---|
| 0° | $K_I \cong 0.4 \times 110.5 = 44.2$<br>$K_{II} = 0$ | $K_I = K_{II} \cong 0$ |
| 45° | $K_I \cong 0.3 \times 110.5 = 33.2$<br>$K_{II} \cong 0$ | $K_I \cong 2.6 \times 74 = 192.4$<br>$K_{II} \cong 1.25 \times 74 = 92.5$ |
| 90° | $K_I = K_{II} = 0$ | $K_I \cong 5 \times 74 = 370$<br>$K_{II} \cong 0.2 \times 74 = 14.8$ |
| 180° | $K_I \cong 1.63 \times 110.5 = 180.1$<br>$K_{II} = 0$ | $K_I = K_{II} \cong 0$ |

"Unit" K values are read from Figure 26 for Condition MT and from Figure 32 for Condition MC. The actual values are then computed by using the actual load to scale the unit values.

Potential fracture sites may be assessed by comparing $K_I$ with $K_{IC}$ for a proposed lug material. Since high strength steel alloys have fracture toughness generally below 100 ksi $\sqrt{\text{in.}}$, the above data indicate that a 0.15-inch crack is longer than critical size if the crack is located at 45°, 90°, or 180°. If a criterion that 0.15-inch cracks be less than critical is to be met, the designer might do this by increasing the lug thickness. Since the numerical data result from a linear analysis, the design can be scaled. For example, a revised thickness

$$T' = \frac{370}{K_{IC}} \times T = \frac{370}{50} \times 0.19 \cong 1.41 \text{ in.} \quad (26)$$

can be calculated, assuming that protection against a 0.15-inch crack at 90°, in a material with $K_{IC} = 50$ ksi $\sqrt{\text{in.}}$, is required. At other points; e.g., $\theta = 45°$ (Condition MT), $K_I$ and $K_{II}$ are comparable, and interaction formulas such as:

$$\left(\frac{K_I}{K_{IC}}\right)^2 + \left(\frac{K_{II}}{K_{IIC}}\right)^2 \leq 1 \quad (27)$$

may be used to assess structural integrity.

## Section 5

## CONCLUSIONS

A finite-element analysis program for computation of Mode I and Mode II stress intensity factors in attachment lug details has been presented. Since the program is based on an assumed-stress hybrid crack element, relatively crude structure models can be used. Performance tests of the crack element and the lug program have indicated that $K_I$ and $K_{II}$ solutions can be obtained to $\pm$ 5 percent accuracy, for 1.8 to 3.6 CPU seconds per solution pair on current-generation large computers.

A series of demonstration examples, involving a lug detail similar to the C-5A engine pylon aft truss attachment lug, served to illustrate a number of important features of the K solutions. With the crack size held at 0.15 inch and the crack orientation kept radial, parametric analyses were conducted for $K_I$ and $K_{II}$ with the lug subjected to tension, shear and compression bearing forces. In each case, data were obtained for both a cosine and a uniform pressure distribution, to represent possible extremes of load transfer across the bearing surface. The parametric capability of the program was used to compute for each case a number of $K_I$ and $K_{II}$ values corresponding to location of the crack at various positions around the bearing pinhole. Polar plots of $K_I$ and $K_{II}$ versus angle to the crack location were presented to provide a concise picture of the parametric behavior.

The following specific conclusions can be drawn from the results of the analysis. First, uniform bearing pressure has more tendency than cosine pressure to spread the lug apart, and this is reflected by increased $K_I$ values. This effect interacts with the relation between the crack location and the line of action of the bearing load. The most significant sensitivity to pressure distribution occurs when a $K_I$ maxima coincides with or is close to the line of action of the load, or when a maximum lies opposite to the load line. Second, the most critical locations for a given crack often lie in unexpected places or correspond to unexpected load conditions. For example, cracks at ±90° to the lug axis appear to be most critical in tension bearing. However, cracks at ±45° may actually be the most critical if the lug material happens to have a low Mode II fracture toughness. A significant Mode I stress intensity value for a crack at 180°, under compression bearing, is another unexpected result. Finally, the maxima and minima of $K_I$ and $K_{II}$ sometimes tend to follow local maxima and minima of the stress distribution in an equivalent uncracked structure, if the crack is small compared to the structure detail dimensions. However, the coincidence of maxima and minima occurs only for some load conditions, while significant discrepancies occur under other load conditions. One is, therefore, led to conclude that a stress analysis of an uncracked structure does not always provide a good map of where to expect the most critical stress intensities, even for small cracks.

## REFERENCES


1. Campbell, J. E., et al., "Damage Tolerant Design Handbook", Metals and Ceramics Information Center, Battelle Columbus Laboratories, 505 King Avenue, Columbus, Ohio, 1972.

2. Matthews, W. T., "Plane Strain Fracture Toughness ($K_{IC}$) Data Handbook for Metals", Army Materials and Mechanics Research Center, Watertown, Massachusetts 02172, AMMRC MS 73-6, December 1973.

3. Anon., "Airplane Damage Tolerance Design Requirements", MIL-A-83444, U.S. Air Force Aeronautical Systems Division, Wright-Patterson AFB, Ohio 45433, June 1974.

4. Bowie, O. L., J. Appl. Mech., Vol. 31, pp. 208-212 (1964).

5. Bowie, O. L. and Neal, D. M., Int. J. Fracture Mech., Vol. 6, pp. 199-206 (1970).

6. Bowie, O. L., Freese, C. E. and Neal, D. M., "Solution of Plane Problems of Elasticity Utilizing Partitioning Concepts", ASME Paper No. 73-APM-C, 1973.

7. Tada, H., Paris, P. C., and Irwin, G. R., The Stress Analysis of Cracks Handbook, DEL Research Corporation, Hellertown, Pennsylvania, 1973.

8. Pian, T. H. H., AIAA J., Vol. 2, pp. 1333-1336 (1964).

9. Tong, P. and Pian, T. H. H., Int. J. Solids Struc., Vol. 9, pp. 313-321 (1973).

10. Luk, C. H., "Assumed Stress Hybrid Finite Element Methodology for Fracture Mechanics and Elastic-Plastic Analysis", Aeroelastic and Structures Research Laboratory, MIT, ASRL TR 170-1, December 1972.

11. Tong, P., Pian, T. H. H. and Lasry, S. J., Int. J. Num. Meth. Eng., Vol. 7, pp. 297-308 (1973).

12. Lasry, S. J., "Derivation of Crack Element Stiffness Matrix by the Complex Variable Approach", Aeroelastic and Structures Research Laboratory, MIT, ASRL TR 170-2, AFOSR-TR-73-1602, February 1973.

13. Zienkiewicz, O. C. and Cheung, Y. K., The Finite Element Method in Structural and Continuum Mechanics, McGraw-Hill, 1967.

14. Abramowitz, M. and Stegun, I. A. (ed.), Handbook of Mathematical Functions, National Bureau of Standards, U.S. Department of Commerce, Ninth Ed., November 1970.

15. Desai, C. S. and Abel, J. F., Introduction to the Finite Element Method, Van Nostrand Reinhold Company, 1970.

16. Orringer, O., "FEABL (Finite Element Analysis Basic Library) Documentation of Sample Program for Export Version", Aeroelastic and Structures Research Laboratory, MIT, ASRL TM 162-3-4, February 1974.

17. Timoshenko, S. and Goodier, J. N., Theory of Elasticity, McGraw-Hill, 1961.

18. Washizu, K., Variational Methods in Elasticity and Plasticity, Pergamon Press, 1968.

19. Lin, K. Y., Tong, P. and Orringer, O., "Effect of Shape and Size on Hybrid Crack-Containing Finite Elements", submitted for presentation at ASME Pressure Vessels and Piping Conference, San Francisco, California, June 1975.

20. Orringer, O. and French, S. E., "FEABL (Finite Element Analysis Basic Library) User's Guide", Aeroelastic and Structures Research Laboratory, MIT, ASRL TR 162-3, AFOSR-TR-72-2228, August 1972.

21. Orringer, O. and French, S. E., "FEABL (Finite Element Analysis Basic Library) Version 2/Release 2", Aeroelastic and Structures Research Laboratory, MIT, ASRL TM 162-3-3, February 1974.

22. Neilson, J. A., Shockley, E. J. and Dallas, C. H., "C-5A Pylon Evaluation and Redesign Recommendations", Lockheed-Georgia Aircraft Company, Marietta, Georgia, Report No. SRD 72-21-775, p. 29.

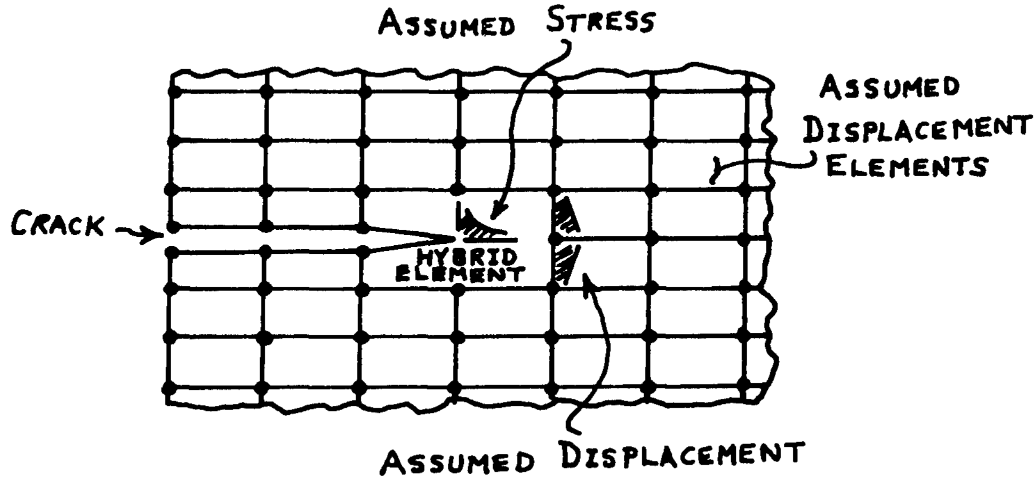


FIG. 1 COMBINATION OF ASSUMED-DISPLACEMENT ELEMENTS WITH HYBRID CRACK-CONTAINING ELEMENT

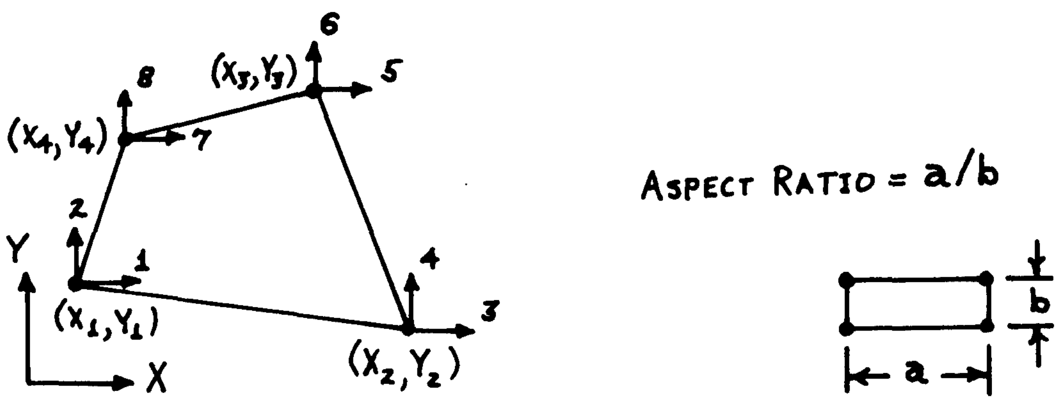


FIG. 2 CONVENTIONS FOR ASRL QUAD4 ASSUMED-DISPLACEMENT ELEMENT

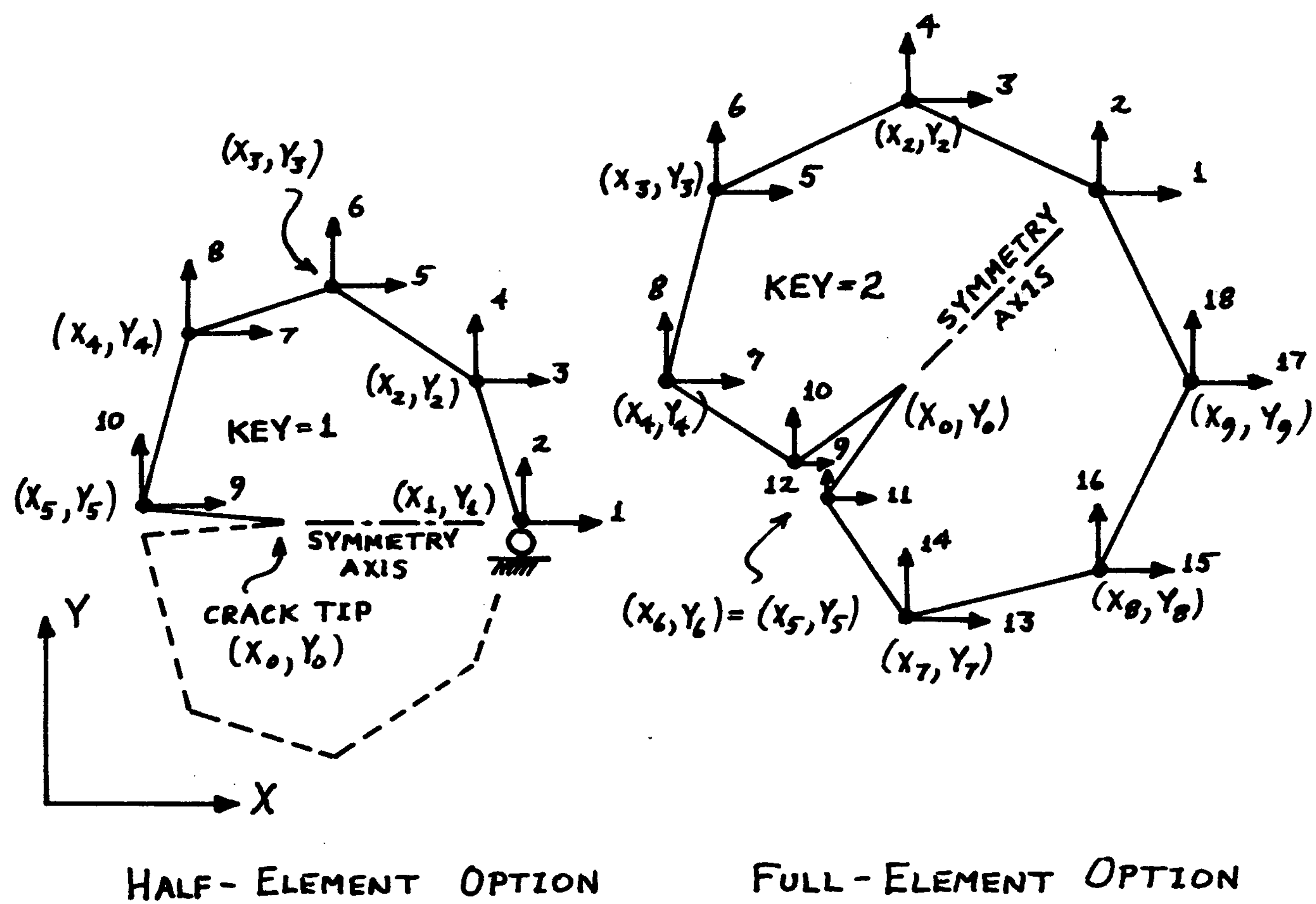


FIG. 3 ASRL PCRK59 HYBRID CRACK-CONTAINING ELEMENT

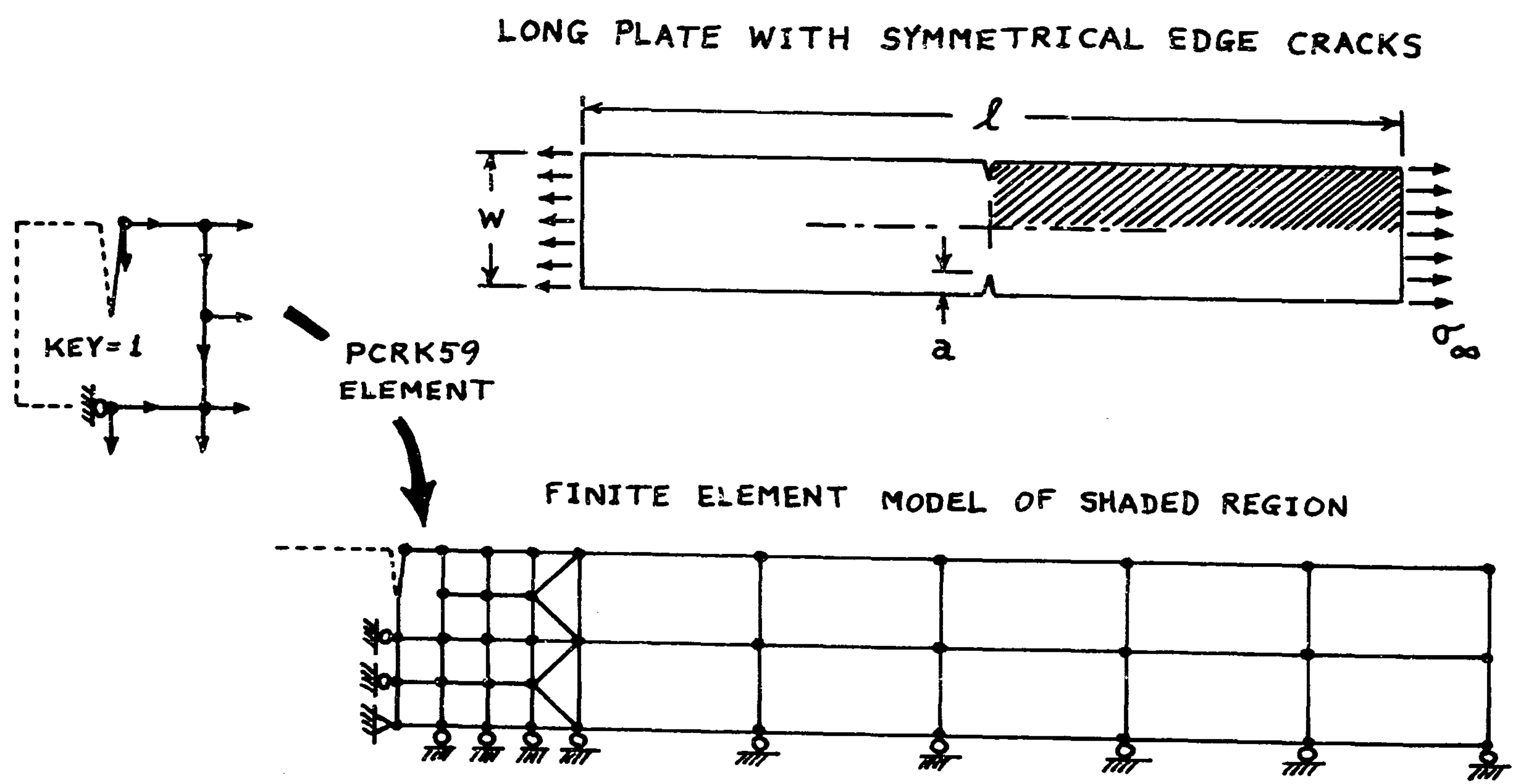


FIG. 4 APPLICATION OF PCRK59 ELEMENT TO SYMMETRIC ANALYSES

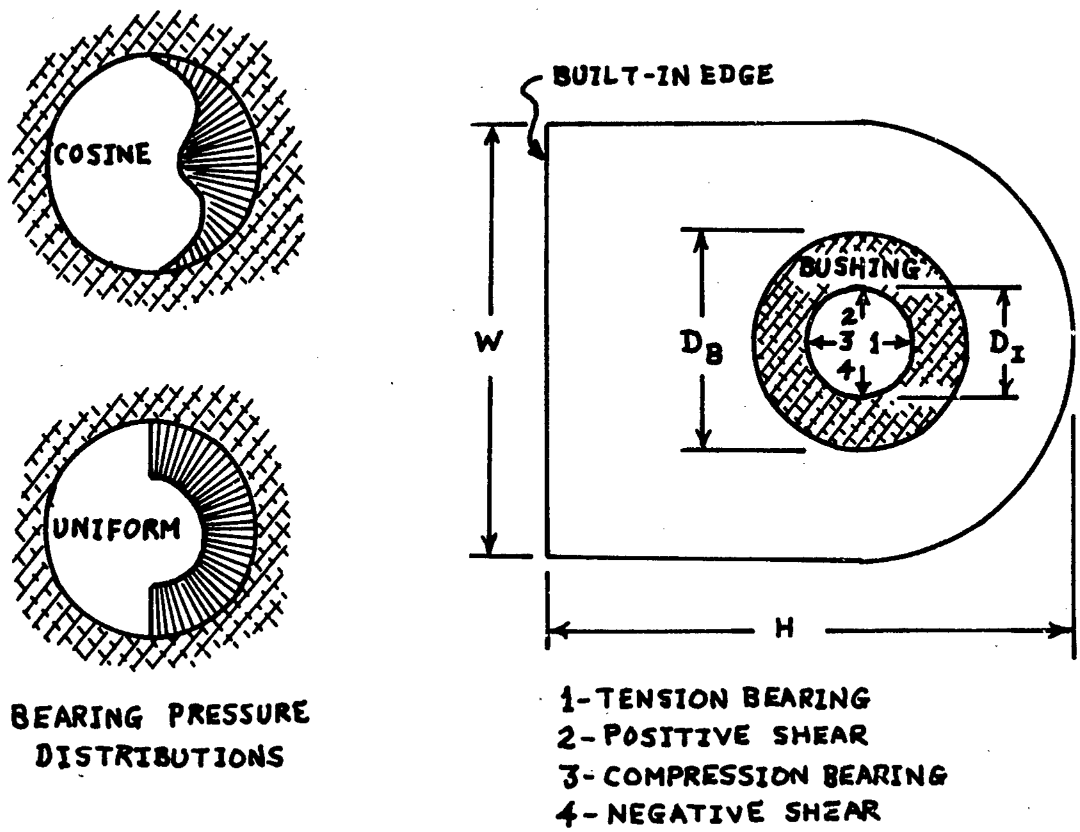


FIG. 5 ATTACHMENT LUG DETAIL

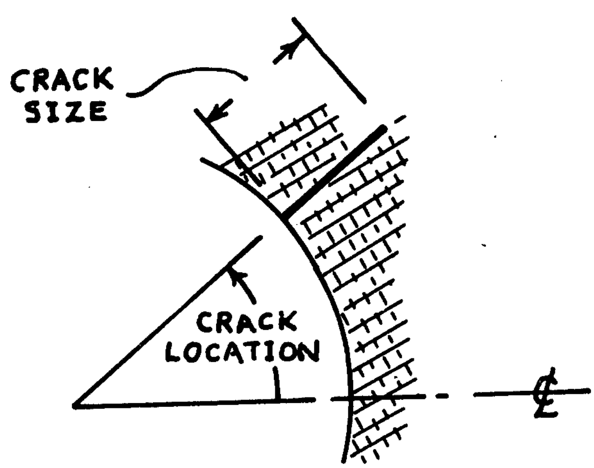


FIG. 6 CRACK PARAMETERS

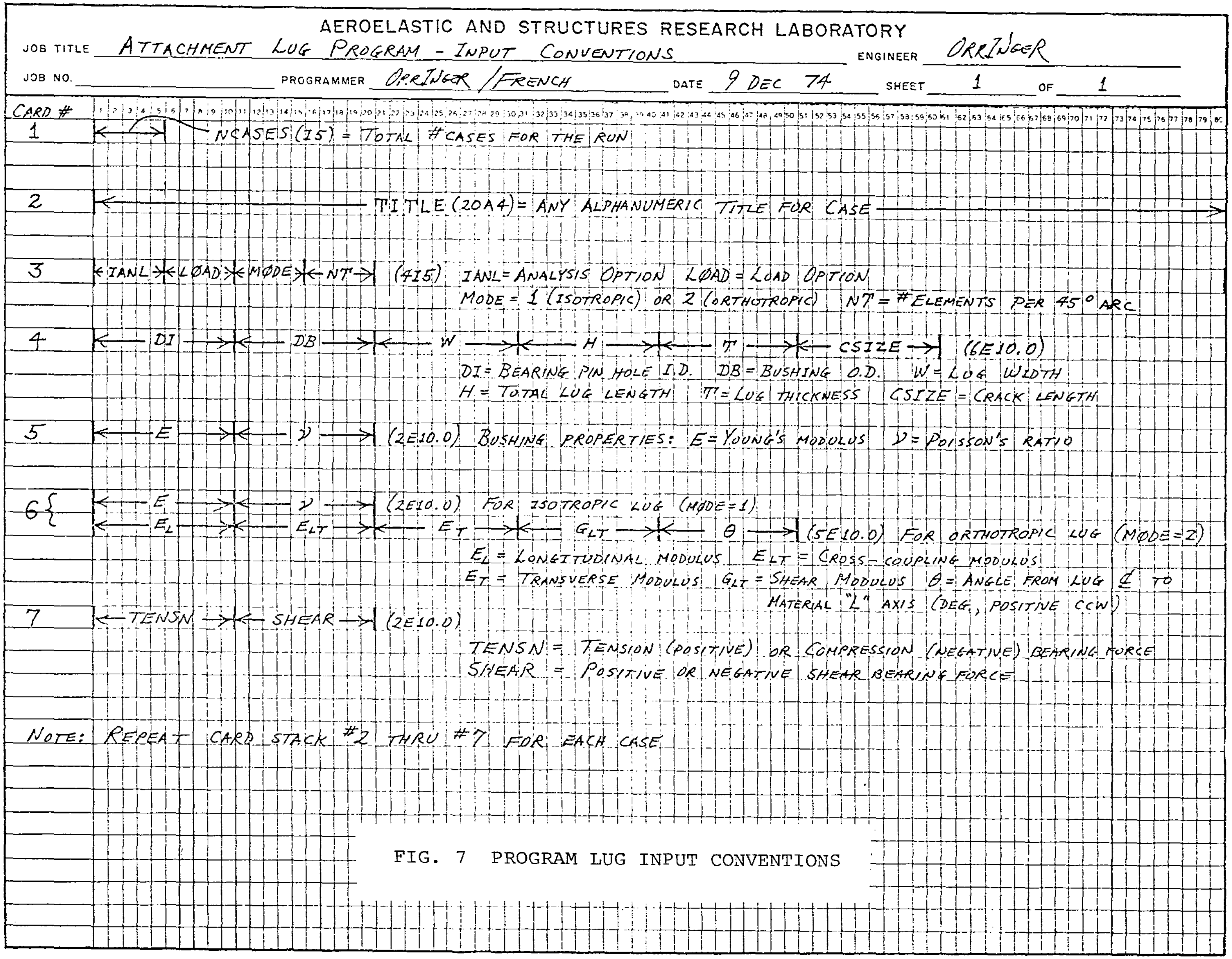


FIG. 7 PROGRAM LUG INPUT CONVENTIONS

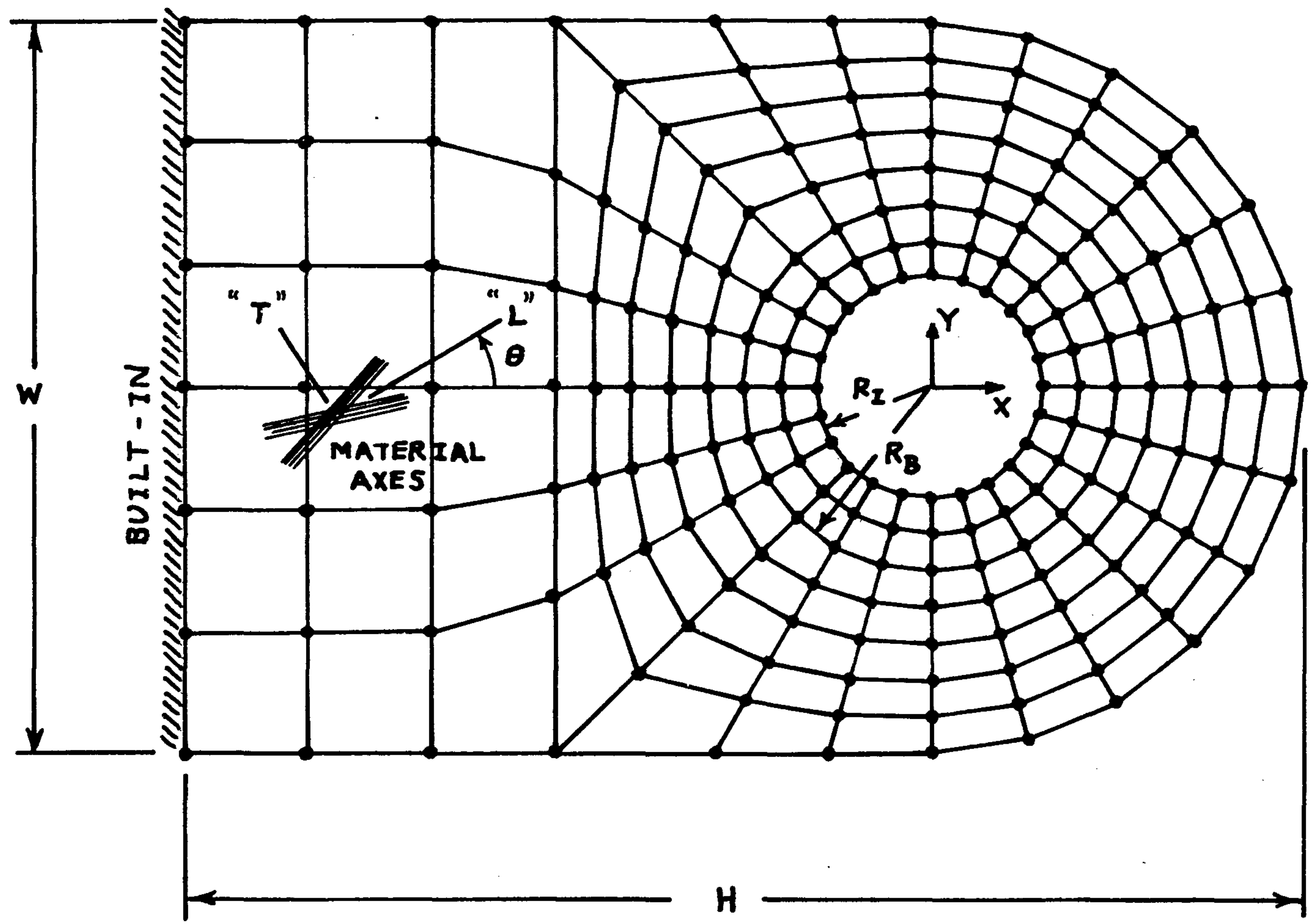


FIG. 8 FINITE ELEMENT MESH FOR NT = 3

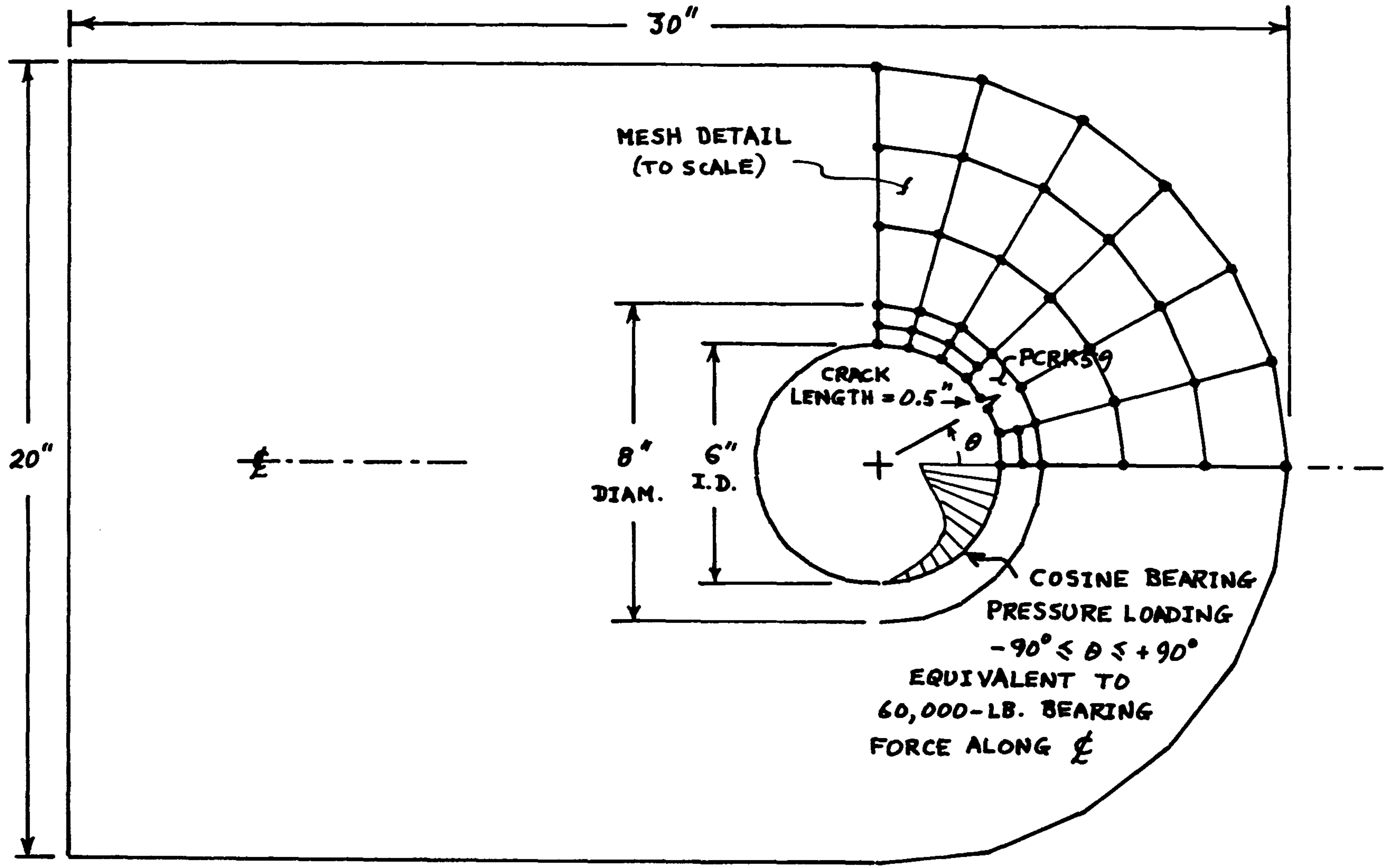


FIG. 9 HYPOTHETICAL WING ROOT ATTACHMENT LUG

AEROELASTIC AND STRUCTURES RESEARCH LABORATORY

JOB TITLE: INPUT DATA FOR PROGRAM LUG: HYPOTHETICAL WING ROOT ATTCH. LUG ENGINEER ______

JOB NO. ______ PROGRAMMER ______ DATE 9 DEC 74 SHEET 1 OF 1

| CARD # | Cols 1–10 | Cols 11–20 | Cols 21–30 | Cols 31–40 | Cols 41–50 | Cols 51–60 |
|---|---|---|---|---|---|---|
| 1 | 2 | | | | | |
| 2 | LARGE WING RØØT LUG: STRESS ANALYSIS ØF UNCRACKED STRUCTURE (CØSINE LØAD) | | | | | |
| 3 | 1 1 | 1 3 | | | | |
| 4 | 6.0 | 8.0 | 20.0 | 30.0 | 1.0 | 0.5 |
| 5 | 1.E7 | 0.3 | | | | |
| 6 | 1.E7 | 0.3 | | | | |
| 7 | 6.E4 | | | | | |
| 8 | LARGE WING RØØT LUG: STRESS INTENSITY ANALYSIS | | | | | |
| 9 | 2 1 | 1 3 | | | | |
| 10 | 6.0 | 8.0 | 20.0 | 30.0 | 1.0 | 0.5 |
| 11 | 1.E7 | 0.3 | | | | |
| 12 | 1.E7 | 0.3 | | | | |
| 13 | 6.E4 | | | | | |

FIG. 10 INPUT DATA FOR ANALYSIS OF LUG SHOWN IN FIG. 9

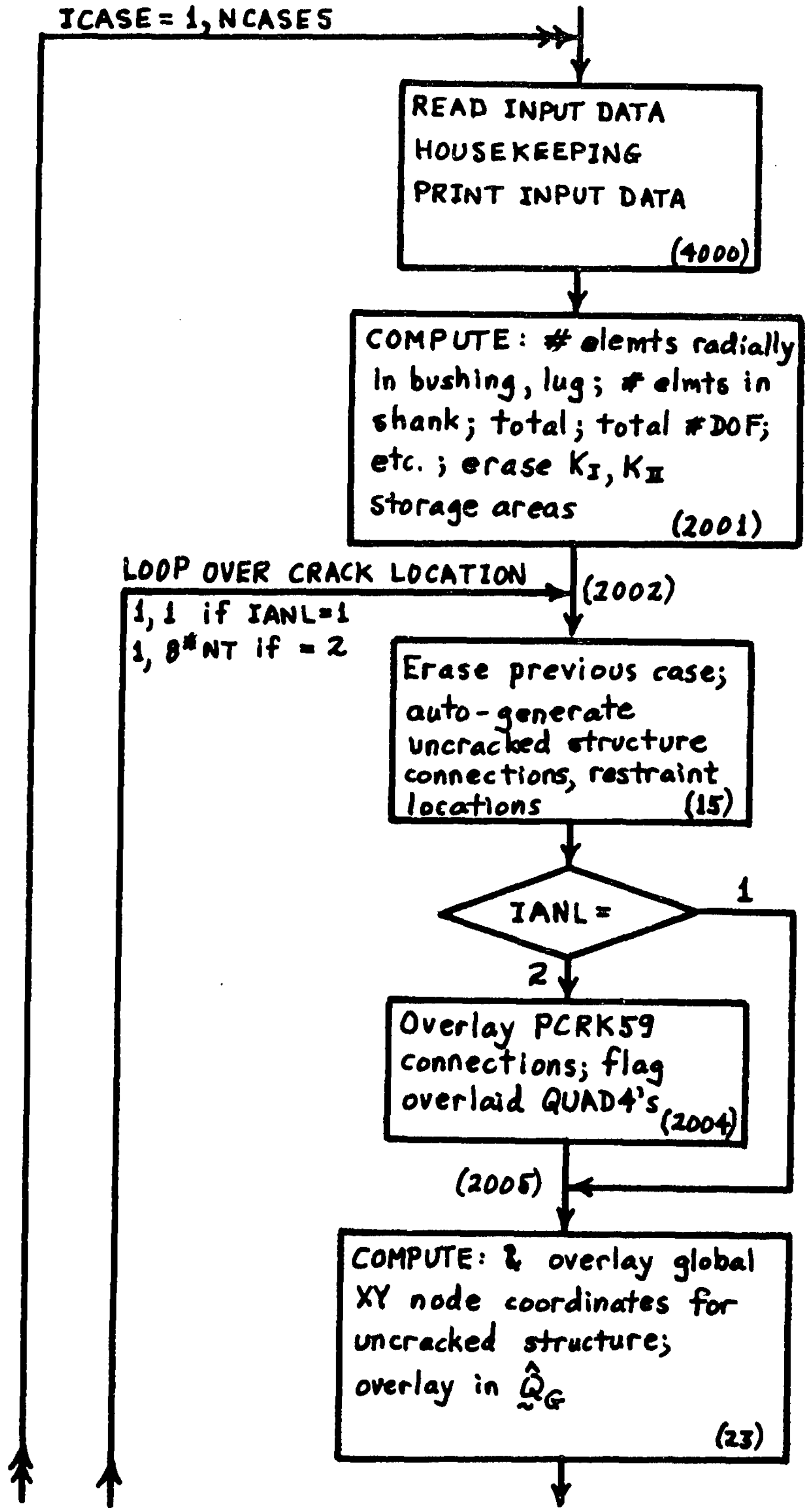


FIG. 11 PROGRAM LUG FLOW CHART

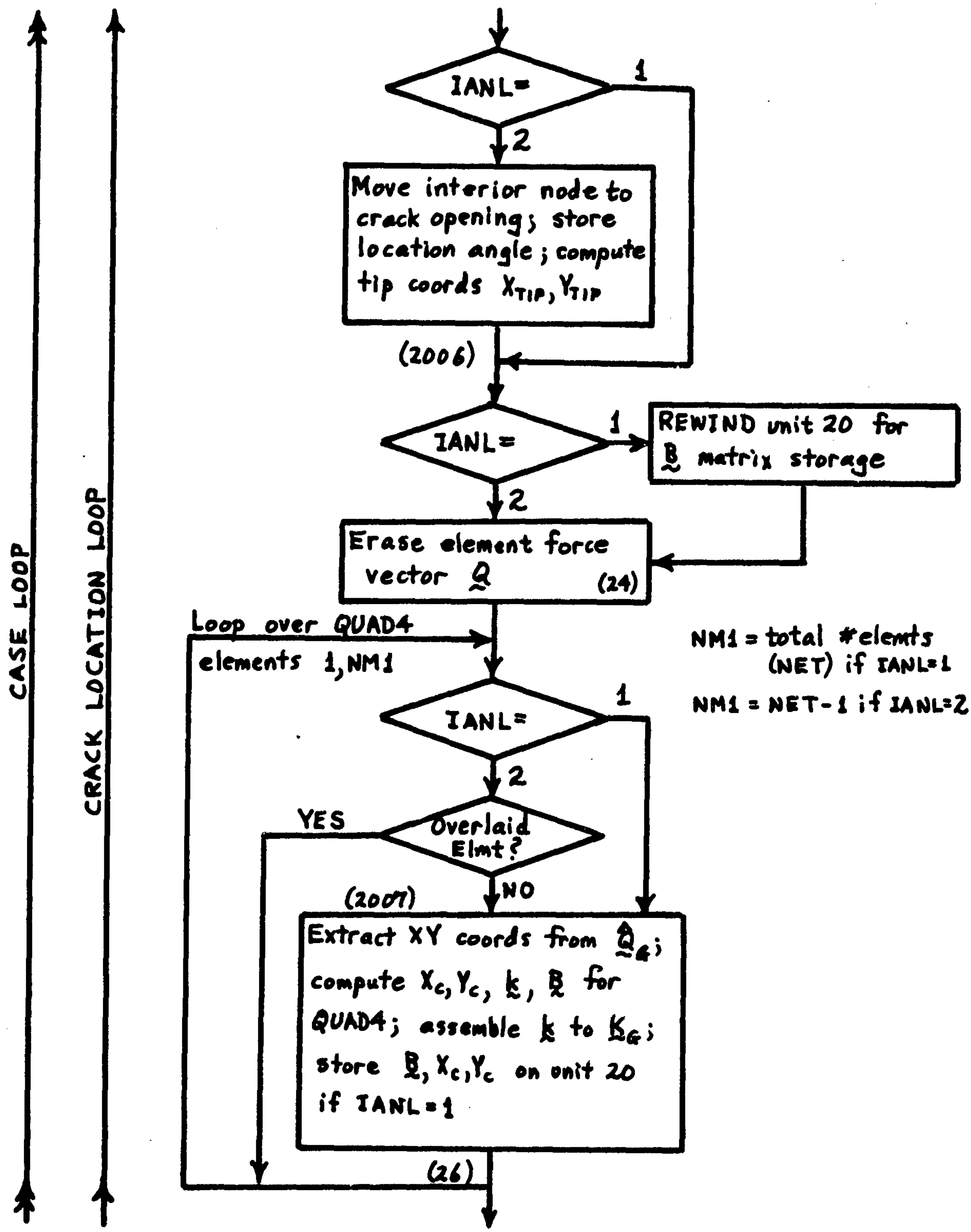


FIG. 11 (CONTINUED)

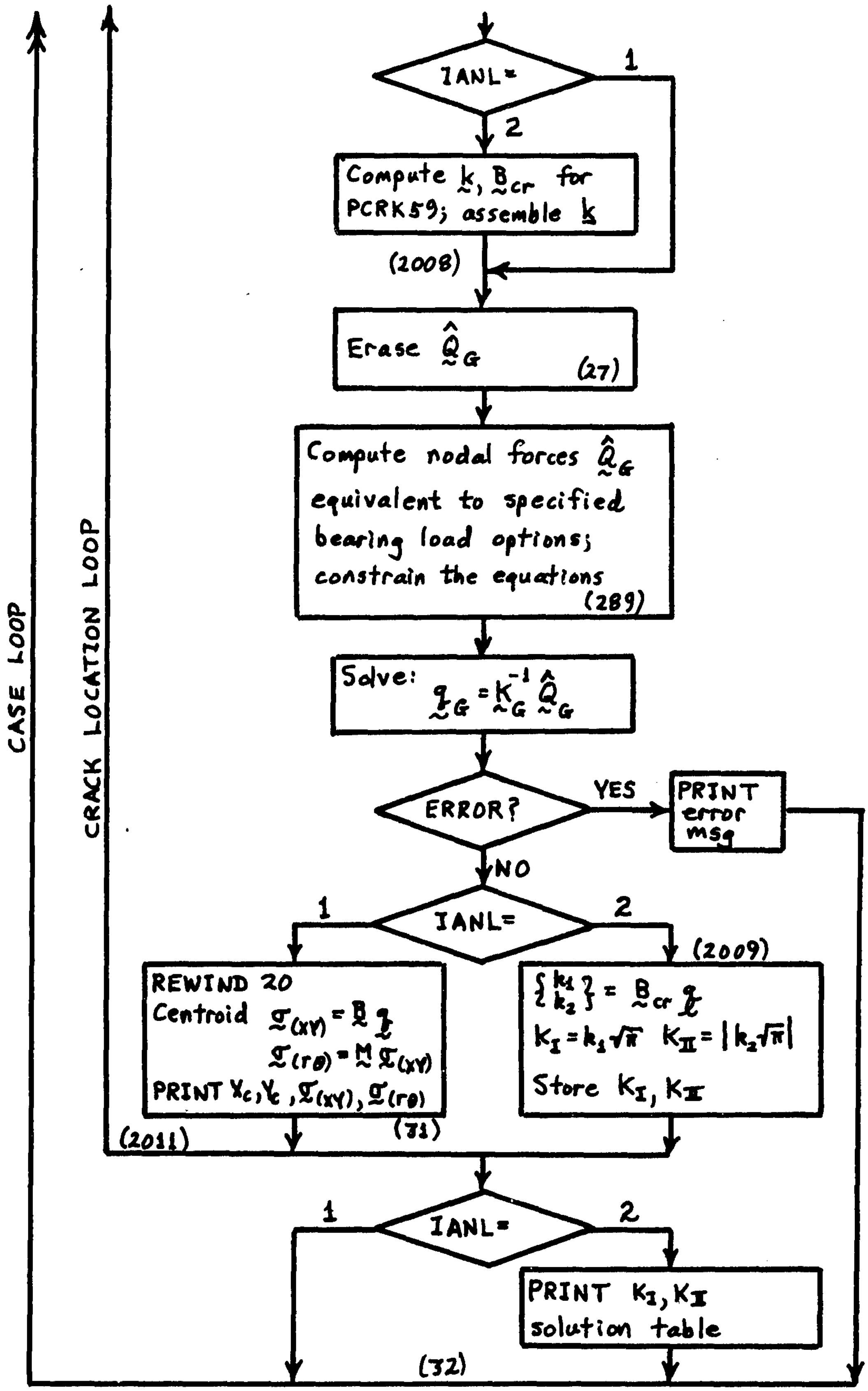


FIG. 11 (CONCLUDED)

```
CASE  36:  LUG PROGRAM STRESS INTENSITY ANALYSIS

ANALYSIS OPTION= 2; LOAD OPTION= 2

MODE= 1 (1=ISOTROPIC, 2=ORTHOTROPIC LUG)
TOTAL OF 32 ELEMENTS AROUND PIN HOLE
HOLE I.D.= 0.200E+01     BUSHING O.D.= 0.300E+01     LUG WIDTH= 0.400E+01  LUG LENGTH= 0.700E+01  THICKNESS= 0.100E+01

CRACK LENGTH= 0.200E+00; DIRECTION= 0.0

BUSHING MATERIAL: E= 0.100E+08 NU= 0.300E+00

ISOTROPIC LUG:    E= 0.100E+08 NU= 0.300E+00

APPLIED TENSION= 0.100E+04 LB. AND SHEAR= 0.0       LB.
```

FIG. 12  PRINTOUT OF INPUT DATA

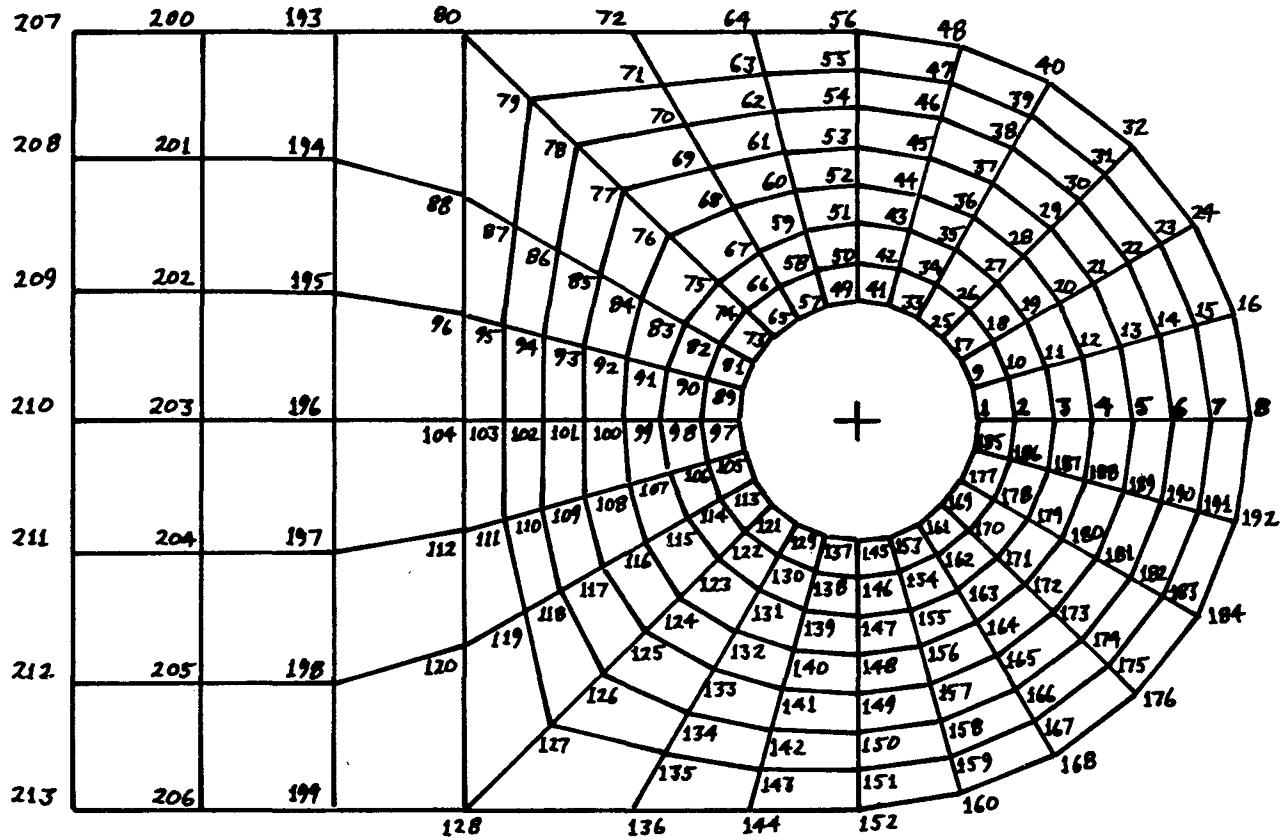


(a) Node Numbering Diagram

FIG. 13 NUMBERING CONVENTIONS ILLUSTRATED FOR SAMPLE MESH SHOWN IN FIG. 8

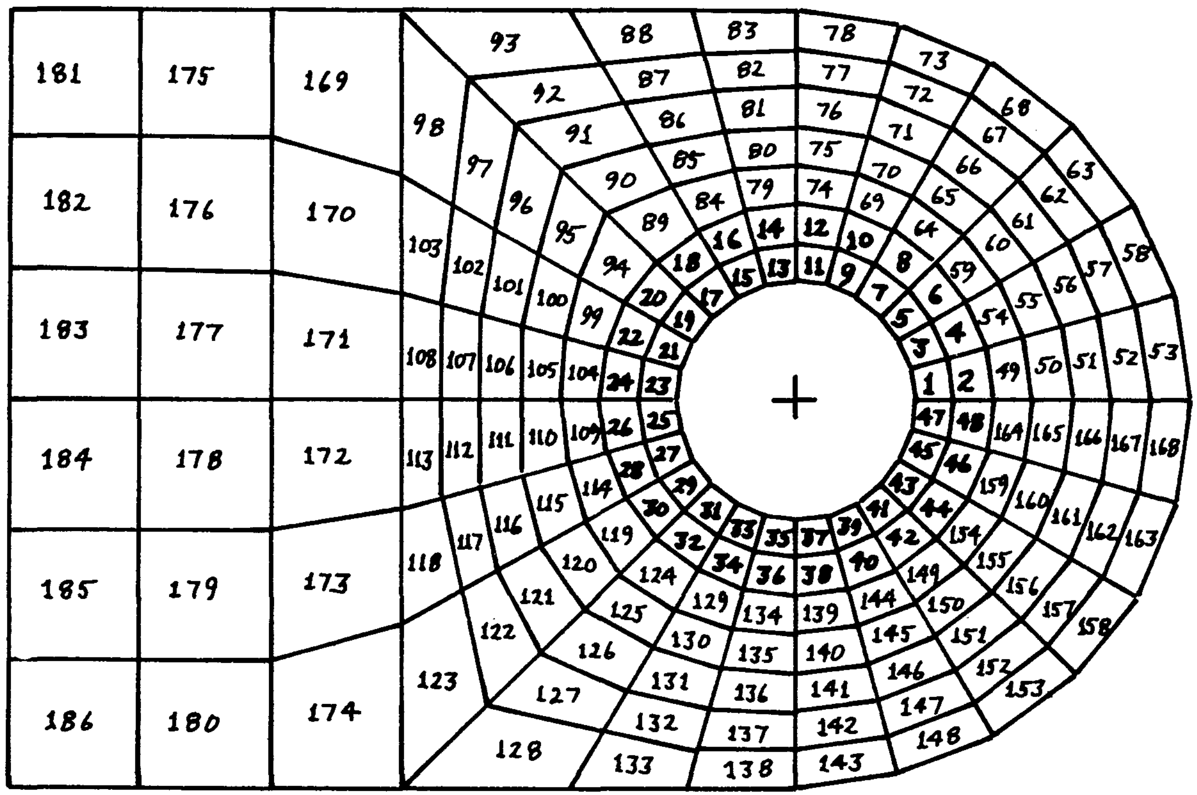


(b) Element Numbering Diagram

FIG. 13 (CONCLUDED)

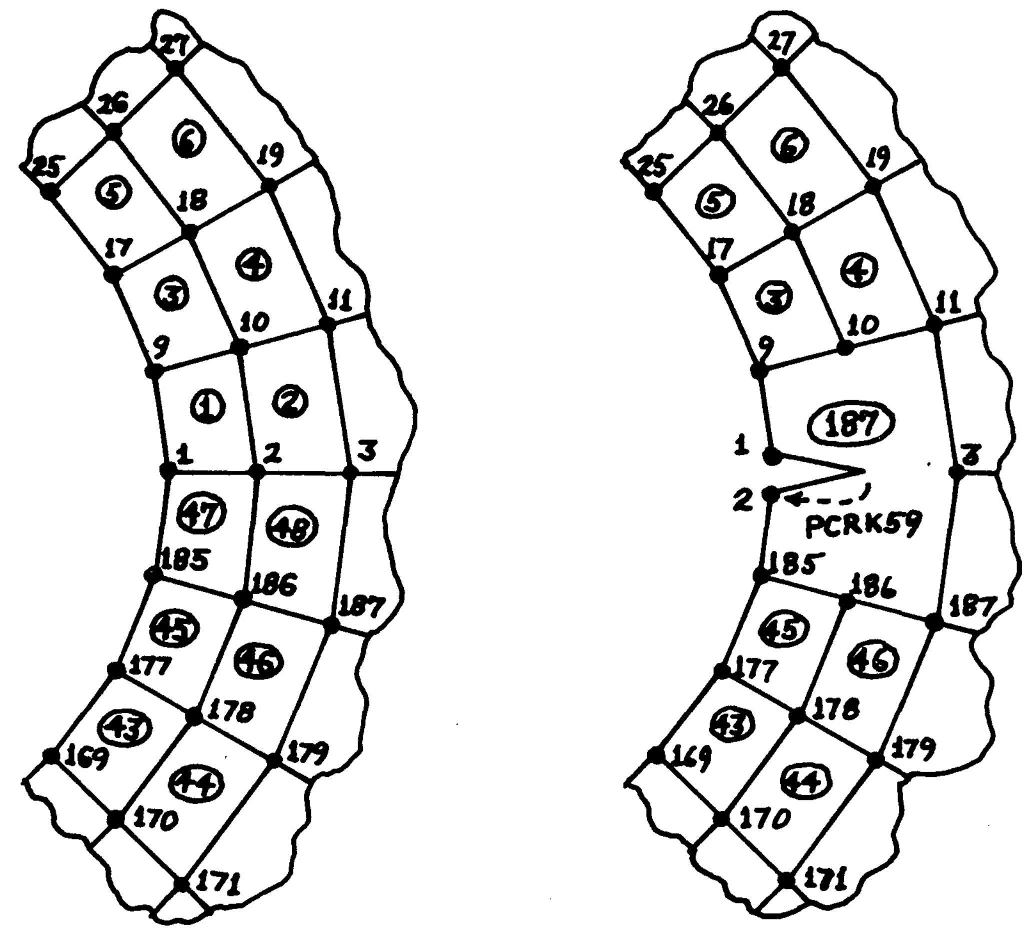


FIG. 14 OVERLAY FOR STRESS INTENSITY ANALYSIS

CASE 1: CASE 1 11 DECEMBER 1974

ANALYSIS OPTION= 1: LOAD OPTION= 2

MODE= 1 (1=ISOTROPIC, 2=ORTHOTROPIC LUG)
TOTAL OF 32 ELEMENTS AROUND PIN HOLE
HOLE I.D.= 0.175E+01 BUSHING O.D.= 0.235E+01 LUG WIDTH= 0.350E+01 LUG LENGTH= 0.700E+01 THICKNESS= 0.190E+00

BUSHING MATERIAL: E= 0.300E+08 NU= 0.295E+00

ISOTROPIC LUG: E= 0.300E+08 NU= 0.295E+00

APPLIED TENSION= 0.100E+04 LB. AND SHEAR= 0.0 LB.

SIMULQ ENTRY POINT

PRESCRIBED FORCE/DISPLACEMENT VECTOR:

| | | | | | | | | | | |
|---|---|---|---|---|---|---|---|---|---|---|
| ROW | 1 | 2 | 3 | 4 | 5 | 6 | 7 | 8 | 9 | 10 |
| VALUE | 0.987E+02 | -0.124E-03 | 0.0 | 0.0 | 0.0 | 0.0 | 0.0 | 0.0 | 0.0 | 0.0 |
| ROW | 11 | 12 | 13 | 14 | 15 | 16 | 17 | 18 | 19 | 20 |
| VALUE | 0.963E+02 | 0.192E+02 | 0.0 | 0.0 | 0.0 | 0.0 | 0.0 | 0.0 | 0.0 | 0.0 |
| ROW | 21 | 22 | 23 | 24 | 25 | 26 | 27 | 28 | 29 | 30 |
| VALUE | 0.907E+02 | 0.376E+02 | 0.0 | 0.0 | 0.0 | 0.0 | 0.0 | 0.0 | 0.0 | 0.0 |
| ROW | 31 | 32 | 33 | 34 | 35 | 36 | 37 | 38 | 39 | 40 |
| VALUE | 0.816E+02 | 0.545E+02 | 0.0 | 0.0 | 0.0 | 0.0 | 0.0 | 0.0 | 0.0 | 0.0 |
| ROW | 41 | 42 | 43 | 44 | 45 | 46 | 47 | 48 | 49 | 50 |
| VALUE | 0.694E+02 | 0.694E+02 | 0.0 | 0.0 | 0.0 | 0.0 | 0.0 | 0.0 | 0.0 | 0.0 |
| ROW | 51 | 52 | 53 | 54 | 55 | 56 | 57 | 58 | 59 | 60 |
| VALUE | 0.545E+02 | 0.816E+02 | 0.0 | 0.0 | 0.0 | 0.0 | 0.0 | 0.0 | 0.0 | 0.0 |
| ROW | 61 | 62 | 63 | 64 | 65 | 66 | 67 | 68 | 69 | 70 |
| VALUE | 0.376E+02 | 0.907E+02 | 0.0 | 0.0 | 0.0 | 0.0 | 0.0 | 0.0 | 0.0 | 0.0 |
| ROW | 71 | 72 | 73 | 74 | 75 | 76 | 77 | 78 | 79 | 80 |
| VALUE | 0.192E+02 | 0.963E+02 | 0.0 | 0.0 | 0.0 | 0.0 | 0.0 | 0.0 | 0.0 | 0.0 |
| ROW | 81 | 82 | 83 | [illegible] | [illegible] | [illegible] | 87 | 88 | 89 | [illegible] |
| VALUE | 0.0 | 0.491E+02 | 0.0 | [illegible] | [illegible] | [illegible] | 0.0 | 0.0 | [illegible] | [illegible] |
| ROW | [illegible] | [illegible] | 433 | 434 | 435 | 436 | [illegible] | [illegible] | [illegible] | 440 |
| VALUE | [illegible] | [illegible] | 0.0 | 0.8 | 0.0 | 0.0 | 0.0 | [illegible] | 0.0 | 0.0 |
| ROW | 441 | 442 | 443 | 444 | 445 | 446 | 447 | 448 | 449 | 450 |
| VALUE | 0.0 | 0.0 | 0.0 | 0.0 | 0.0 | 0.0 | 0.0 | 0.0 | 0.0 | 0.0 |
| ROW | 451 | 452 | 453 | 454 | 455 | 456 | 457 | 458 | 459 | 460 |
| VALUE | 0.0 | 0.0 | 0.0 | 0.0 | 0.0 | 0.0 | 0.0 | 0.0 | 0.0 | 0.0 |
| ROW | 461 | 462 | 463 | 464 | | | | | | |
| VALUE | 0.0 | 0.0 | 0.0 | 0.0 | | | | | | |

DISPLACEMENT SOLUTION VECTOR:

| | | | | | | | | | | |
|---|---|---|---|---|---|---|---|---|---|---|
| ROW | 1 | 2 | 3 | 4 | 5 | 6 | 7 | 8 | 9 | 10 |
| VALUE | 0.572E-03 | 0.854E-06 | 0.556E-03 | 0.861E-06 | 0.543E-03 | 0.875E-06 | 0.527E-03 | 0.907E-06 | 0.516E-03 | 0.929E-06 |
| ROW | 11 | 12 | 13 | 14 | 15 | 16 | 17 | 18 | 19 | 20 |
| VALUE | 0.567E-03 | 0.213E-04 | 0.550E-03 | 0.225E-04 | 0.537E-03 | 0.239E-04 | 0.519E-03 | 0.279E-04 | 0.508E-03 | 0.339E-04 |
| ROW | 21 | 22 | 23 | 24 | 25 | 26 | 27 | 28 | 29 | 30 |
| VALUE | 0.553E-03 | 0.396E-04 | 0.534E-03 | 0.412E-04 | 0.520E-03 | 0.434E-04 | 0.499E-03 | 0.503E-04 | 0.484E-03 | 0.609E-04 |
| ROW | 31 | 32 | 33 | 34 | 35 | 36 | 37 | 38 | 39 | 40 |
| VALUE | 0.530E-03 | 0.536E-04 | 0.509E-03 | 0.544E-04 | 0.492E-03 | 0.563E-04 | 0.468E-03 | 0.640E-04 | 0.448E-03 | 0.772E-04 |
| ROW | 41 | 42 | 43 | 44 | 45 | 46 | 47 | 48 | 49 | 50 |
| VALUE | 0.500E-03 | 0.618E-04 | 0.477E-03 | 0.602E-04 | 0.459E-03 | 0.605E-04 | 0.433E-03 | 0.666E-04 | 0.405E-03 | 0.795E-04 |
| ROW | 51 | 52 | 53 | 54 | 55 | 56 | 57 | 58 | 59 | 60 |
| VALUE | 0.465E-03 | 0.635E-04 | 0.441E-03 | 0.580E-04 | 0.421E-03 | 0.555E-04 | 0.390E-03 | 0.576E-04 | 0.361E-03 | 0.674E-04 |
| ROW | 61 | 62 | 63 | 64 | 65 | 66 | 67 | 68 | 69 | 70 |
| VALUE | 0.427E-03 | 0.580E-04 | 0.403E-03 | 0.481E-04 | 0.384E-03 | 0.418E-04 | 0.353E-03 | 0.383E-04 | 0.322E-03 | 0.429E-04 |
| ROW | 71 | 72 | 73 | 74 | 75 | 76 | 77 | 78 | 79 | 80 |
| VALUE | 0.388E-03 | 0.454E-04 | 0.365E-03 | 0.303E-04 | 0.349E-03 | 0.210E-04 | 0.322E-03 | 0.127E-04 | 0.294E-03 | 0.116E-04 |
| ROW | 81 | 82 | 83 | 84 | 85 | 86 | 87 | 88 | 89 | 90 |
| VALUE | 0.348E-03 | 0.181E-04 | 0.331E-03 | 0.497E-05 | 0.319E-03 | -0.314E-05 | 0.298E-03 | -0.126E-04 | 0.277E-03 | -0.176E-04 |
| ROW | 91 | 92 | 93 | 94 | 95 | 96 | 97 | 98 | 99 | 100 |
| VALUE | 0.311E-03 | -0.822E-05 | 0.303E-03 | -0.163E-04 | 0.295E-03 | -0.214E-04 | 0.278E-03 | -0.296E-04 | 0.265E-03 | -0.356E-04 |

FIG. 15 FORCE AND DISPLACEMENT TABLES FROM STRESS ANALYSIS

STRESS ANALYSIS FOR CASE 1 WING LUG PGM TEST CASE #4A: ALUMINUM LUG FOR STRESSES ONLY

| LNUM | CENTROID LOCATION, ----XC---- | ----YC---- | CARTESIAN STRESSES ----XX---- | ----YY---- | ----XY---- | POLAR STRESSES ----RR---- | ----TT---- | ----RT---- |
|---|---|---|---|---|---|---|---|---|
| PART A: BUSHING | | | | | | | | |
| 1 | 0.319E+01 | 0.421E+00 | -0.112E+05 | 0.156E+04 | -0.197E+04 | -0.115E+05 | 0.185E+04 | -0.246E+03 |
| 2 | 0.369E+01 | 0.485E+00 | -0.899E+04 | 0.213E+04 | -0.195E+04 | -0.931E+04 | 0.244E+04 | -0.448E+03 |
| 3 | 0.298E+01 | 0.123E+01 | -0.811E+04 | 0.685E+03 | -0.536E+04 | -0.106E+05 | 0.319E+04 | -0.683E+03 |
| 4 | 0.343E+01 | 0.142E+01 | -0.586E+04 | 0.708E+03 | -0.504E+04 | -0.846E+04 | 0.331E+04 | -0.124E+04 |
| 5 | 0.256E+01 | 0.196E+01 | -0.260E+04 | -0.740E+03 | -0.723E+04 | -0.890E+04 | 0.556E+04 | -0.974E+03 |
| 6 | 0.295E+01 | 0.226E+01 | -0.842E+03 | -0.120E+04 | -0.610E+04 | -0.687E+04 | 0.483E+04 | -0.175E+04 |
| 7 | 0.196E+01 | 0.256E+01 | 0.390E+04 | -0.198E+04 | -0.693E+04 | -0.649E+04 | 0.841E+04 | -0.105E+04 |
| 8 | 0.226E+01 | 0.295E+01 | 0.421E+04 | -0.228E+04 | -0.499E+04 | -0.469E+04 | 0.662E+04 | -0.184E+04 |
| 9 | 0.123E+01 | 0.298E+01 | 0.949E+04 | -0.212E+04 | -0.457E+04 | -0.365E+04 | 0.110E+05 | -0.875E+03 |
| 10 | 0.142E+01 | 0.343E+01 | 0.770E+04 | -0.163E+04 | -0.262E+04 | -0.212E+04 | 0.818E+04 | -0.145E+04 |
| 11 | 0.421E+00 | 0.319E+01 | 0.125E+05 | -0.267E+03 | -0.120E+04 | -0.360E+03 | 0.126E+05 | -0.495E+03 |
| 12 | 0.485E+00 | 0.369E+01 | 0.884E+04 | 0.425E+03 | -0.685E+03 | 0.391E+03 | 0.887E+04 | -0.427E+03 |
| 13 | -0.421E+00 | 0.319E+01 | 0.120E+05 | 0.111E+04 | 0.643E+03 | 0.113E+04 | 0.120E+05 | 0.790E+03 |
| 14 | -0.485E+00 | 0.369E+01 | 0.857E+04 | 0.143E+04 | -0.253E+03 | 0.162E+04 | 0.839E+04 | 0.117E+04 |
| 15 | -0.123E+01 | 0.298E+01 | 0.878E+04 | 0.116E+04 | 0.218E+04 | 0.732E+03 | 0.920E+04 | 0.115E+04 |
| 16 | -0.142E+01 | 0.343E+01 | 0.750E+04 | 0.743E+03 | 0.329E+03 | 0.150E+04 | 0.674E+04 | 0.216E+04 |
| 17 | -0.196E+01 | 0.256E+01 | 0.488E+04 | 0.113E+04 | 0.211E+04 | 0.487E+03 | 0.553E+04 | 0.126E+04 |
| 18 | -0.226E+01 | 0.295E+01 | 0.544E+04 | -0.733E+02 | 0.926E+03 | 0.107E+04 | 0.429E+04 | 0.242E+04 |
| 19 | -0.256E+01 | 0.196E+01 | 0.190E+04 | 0.150E+03 | 0.110E+04 | 0.195E+03 | 0.186E+04 | 0.113E+04 |
| 20 | -0.295E+01 | 0.226E+01 | 0.315E+04 | -0.727E+03 | 0.113E+04 | 0.617E+03 | 0.180E+04 | 0.217E+04 |
| 21 | -0.298E+01 | 0.123E+01 | 0.378E+03 | -0.150E+04 | 0.188E+03 | -0.302E+02 | -0.109E+04 | 0.796E+03 |
| 22 | -0.343E+01 | 0.142E+01 | 0.127E+04 | -0.116E+04 | 0.932E+03 | 0.254E+03 | -0.150E+03 | 0.152E+04 |
| 23 | -0.319E+01 | 0.421E+00 | -0.124E+03 | -0.278E+04 | -0.594E+02 | -0.153E+03 | -0.275E+04 | 0.286E+03 |
| 24 | -0.369E+01 | 0.485E+00 | 0.189E+03 | -0.139E+04 | 0.355E+03 | 0.701E+02 | -0.127E+04 | 0.548E+03 |
| 25 | -0.319E+01 | -0.421E+00 | -0.124E+03 | -0.278E+04 | 0.598E+02 | -0.153E+03 | -0.275E+04 | -0.285E+03 |
| 26 | -0.369E+01 | -0.485E+00 | 0.189E+03 | -0.139E+04 | -0.354E+03 | 0.701E+02 | -0.127E+04 | -0.547E+03 |
| 27 | -0.298E+01 | -0.123E+01 | 0.378E+03 | -0.150E+04 | -0.188E+03 | -0.301E+02 | -0.109E+04 | -0.796E+03 |
| 28 | -0.343E+01 | -0.142E+01 | 0.127E+04 | -0.117E+04 | -0.931E+03 | 0.254E+03 | -0.150E+03 | -0.152E+04 |
| 29 | -0.256E+01 | -0.196E+01 | 0.190E+04 | 0.148E+03 | -0.110E+04 | 0.194E+03 | 0.186E+04 | -0.113E+04 |
| 30 | -0.295E+01 | -0.226E+01 | 0.315E+04 | -0.727E+03 | -0.113E+04 | 0.616E+03 | 0.180E+04 | -0.217E+04 |
| 31 | -0.196E+01 | [illegible] | 0.488E+04 | [illegible] | 0.211E+04 | [illegible] | 0.553E+04 | [illegible] |
| [illegible] | [illegible] | [illegible] | [illegible] | [illegible] | [illegible] | [illegible] | [illegible] | [illegible] |

FIG. 16 PART OF STRESS TABLE

STRESS INTENSITIES FOR CASE 36 LUG PROGRAM STRESS INTENSITY ANALYSIS

| POS | --ANGLES-- | ----K1---- | ----K2---- |
|---|---|---|---|
| 1 | 0.0 | 0.382E+03 | 0.869E-01 |
| 2 | 0.112E+02 | 0.421E+03 | 0.207E+02 |
| 3 | 0.225E+02 | 0.488E+03 | 0.509E+01 |
| 4 | 0.337E+02 | 0.506E+03 | 0.370E+02 |
| 5 | 0.450E+02 | 0.489E+03 | 0.172E+02 |
| 6 | 0.562E+02 | 0.495E+03 | 0.390E+02 |
| 7 | 0.675E+02 | 0.532E+03 | 0.720E+02 |
| 8 | 0.787E+02 | 0.594E+03 | 0.579E+02 |
| 9 | 0.900E+02 | 0.713E+03 | 0.679E+01 |
| 10 | 0.101E+03 | 0.876E+03 | 0.233E+03 |
| 11 | 0.112E+03 | 0.927E+03 | 0.409E+03 |
| 12 | 0.124E+03 | 0.773E+03 | 0.403E+03 |
| 13 | 0.135E+03 | 0.528E+03 | 0.267E+03 |
| 14 | 0.146E+03 | 0.298E+03 | 0.152E+03 |
| 15 | 0.157E+03 | 0.106E+03 | 0.998E+02 |
| 16 | 0.169E+03 | -0.313E+02 | 0.582E+02 |
| 17 | 0.180E+03 | -0.813E+02 | 0.208E-01 |
| 18 | 0.191E+03 | -0.312E+02 | 0.582E+02 |
| 19 | 0.202E+03 | 0.106E+03 | 0.998E+02 |
| 20 | 0.214E+03 | 0.298E+03 | 0.151E+03 |
| 21 | 0.225E+03 | 0.528E+03 | 0.267E+03 |
| 22 | 0.236E+03 | 0.773E+03 | 0.403E+03 |
| 23 | 0.247E+03 | 0.927E+03 | 0.409E+03 |
| 24 | 0.259E+03 | 0.876E+03 | 0.233E+03 |
| 25 | 0.270E+03 | 0.714E+03 | 0.675E+01 |
| 26 | 0.281E+03 | 0.595E+03 | 0.580E+02 |
| 27 | 0.292E+03 | 0.533E+03 | 0.723E+02 |
| 28 | 0.304E+03 | 0.496E+03 | 0.393E+02 |
| 29 | 0.315E+03 | 0.490E+03 | 0.168E+02 |
| 30 | 0.326E+03 | 0.506E+03 | 0.366E+02 |
| 31 | 0.337E+03 | 0.487E+03 | 0.529E+01 |
| 32 | 0.349E+03 | 0.421E+03 | 0.205E+02 |

FIG. 17 STRESS INTENSITY FACTOR TABLE FROM ANALYSIS WITH NT = 4

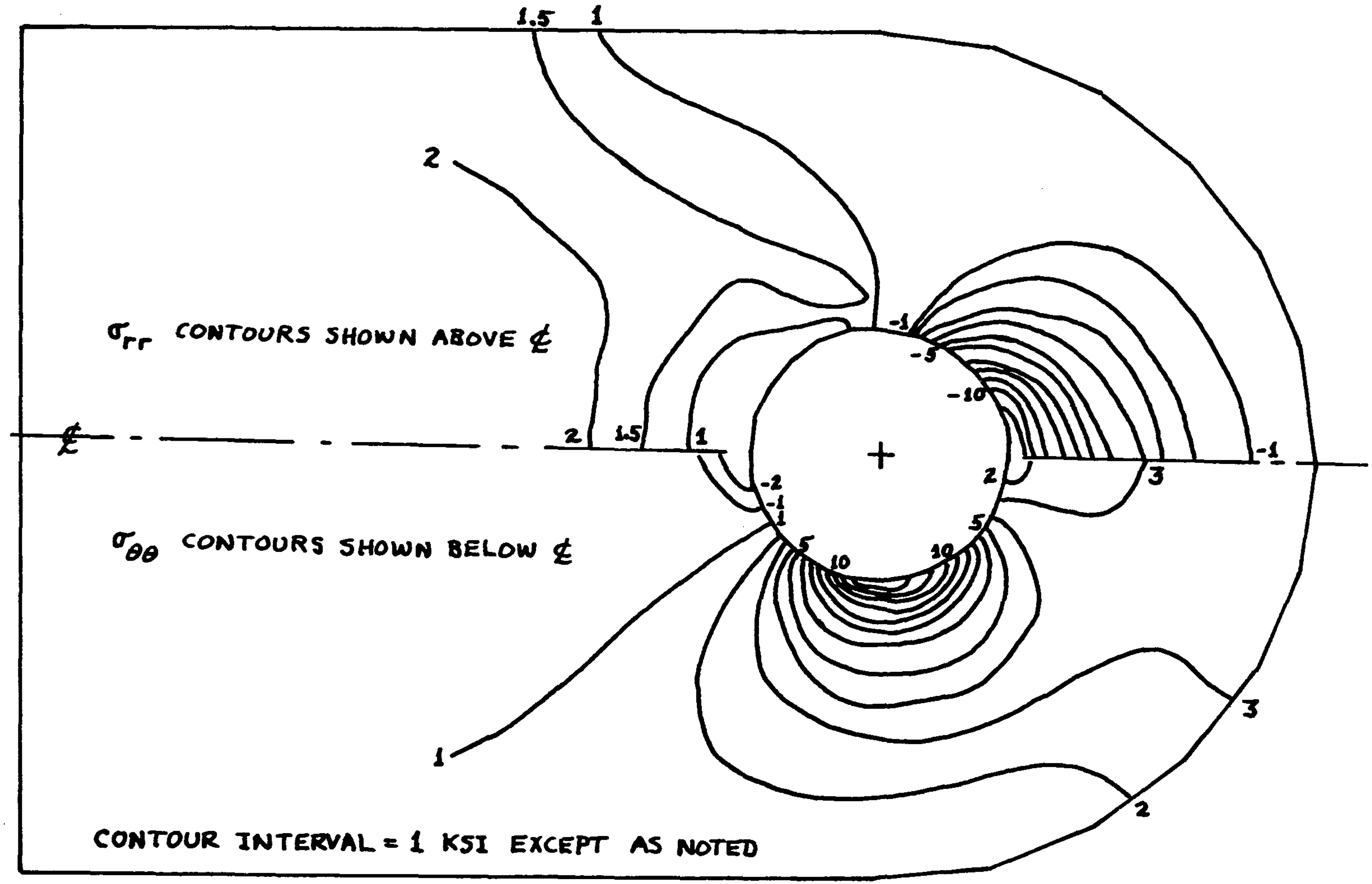


FIG. 18 STRESS CONTOURS FOR WING ROOT LUG

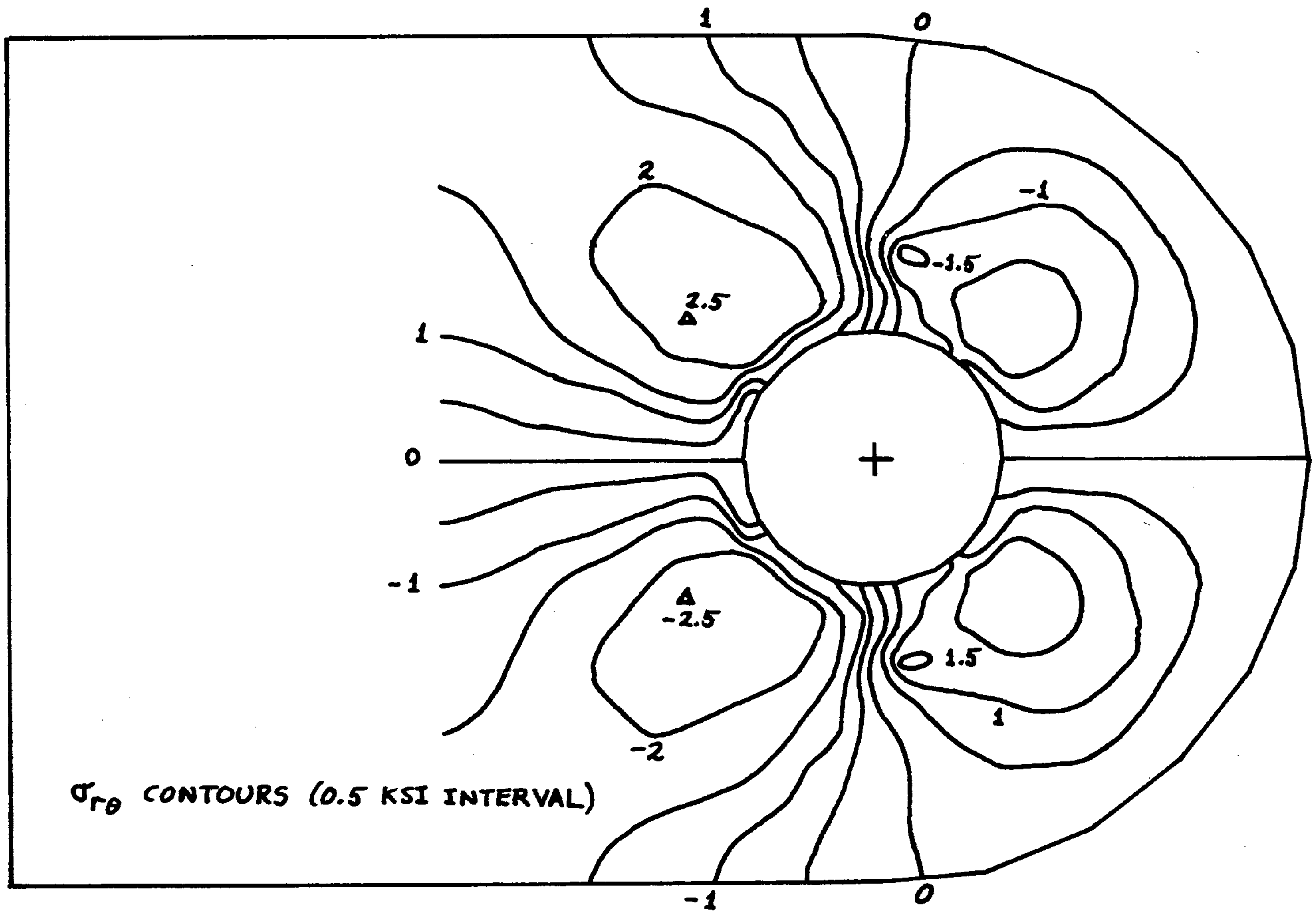


FIG. 18 (CONCLUDED)

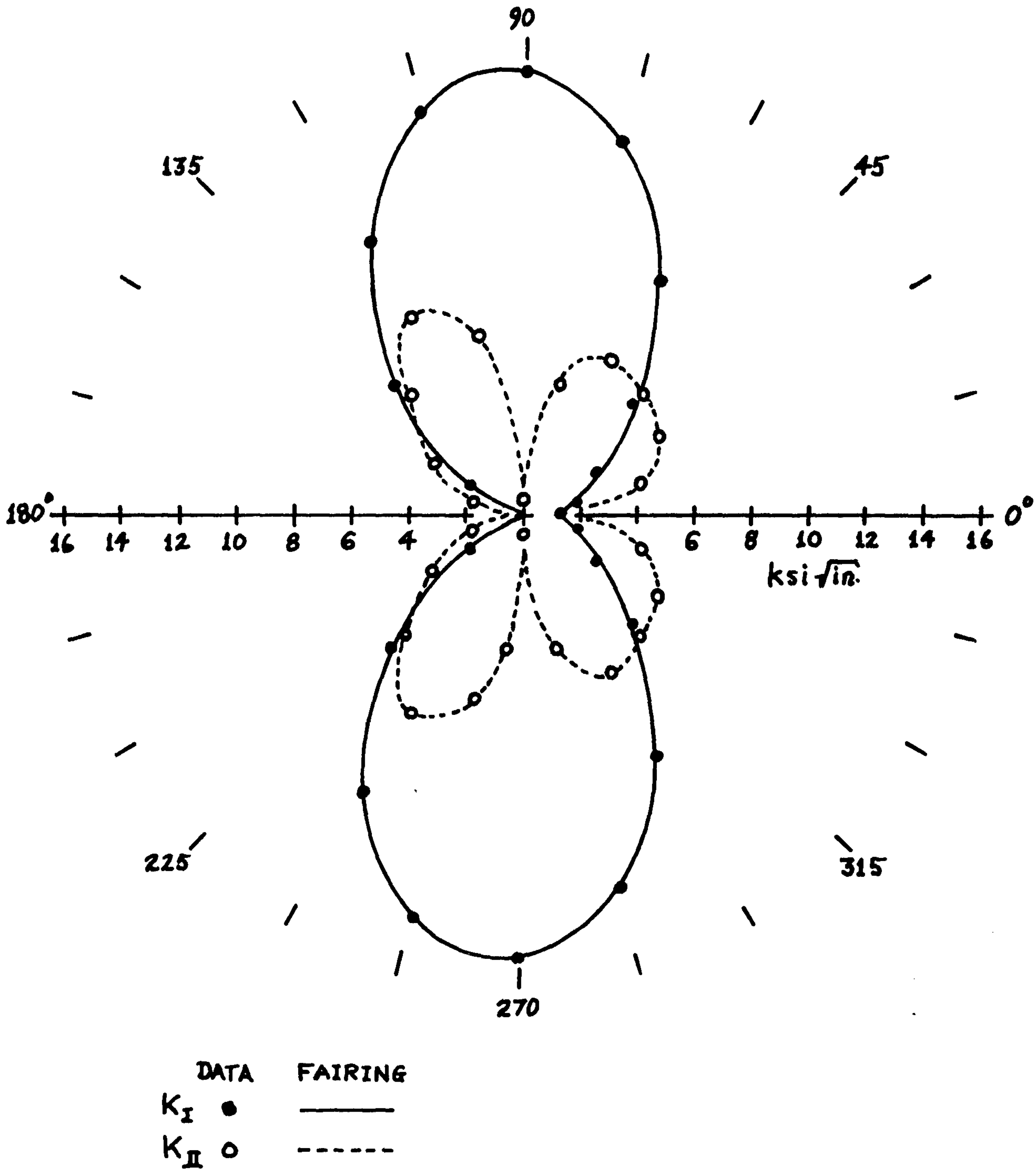


FIG. 19 BUTTERFLY PLOT FOR WING ROOT LUG STRESS INTENSITIES

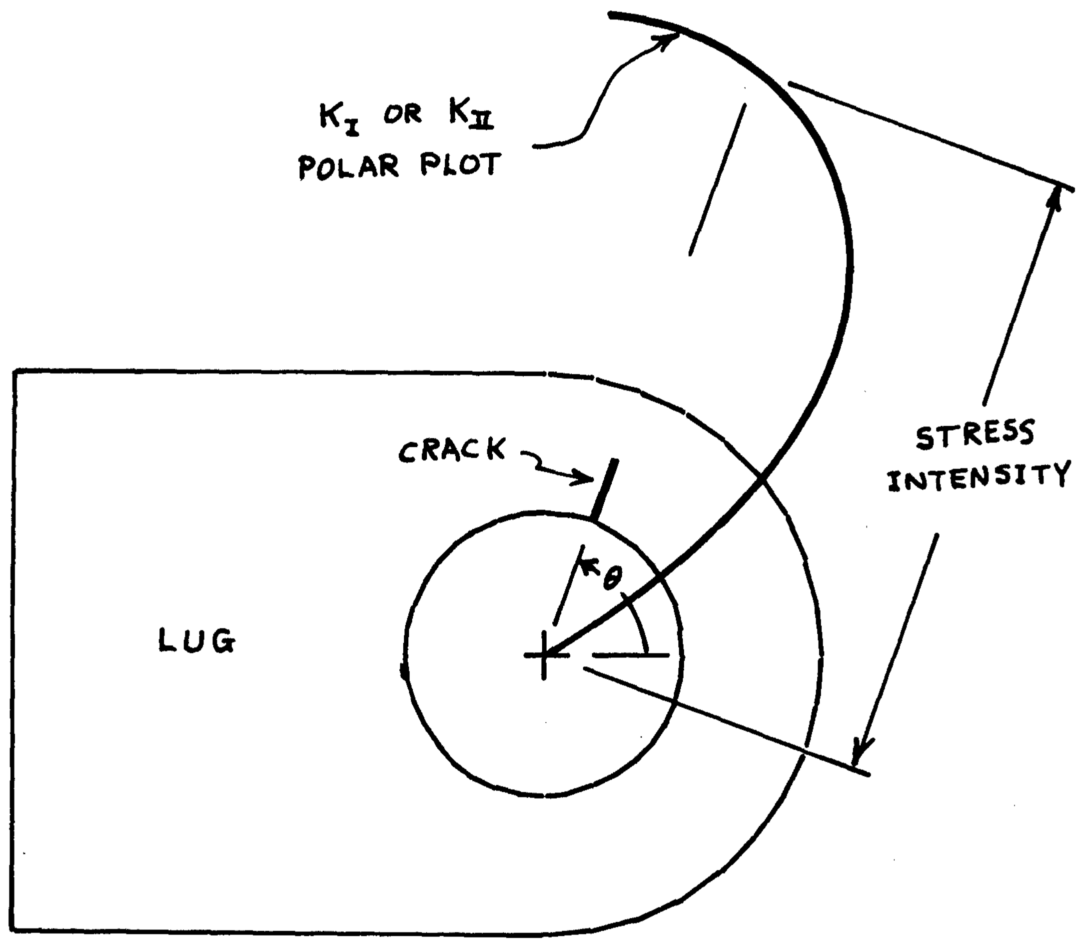


FIG. 20 INTERPRETATION OF BUTTERFLY PLOTS

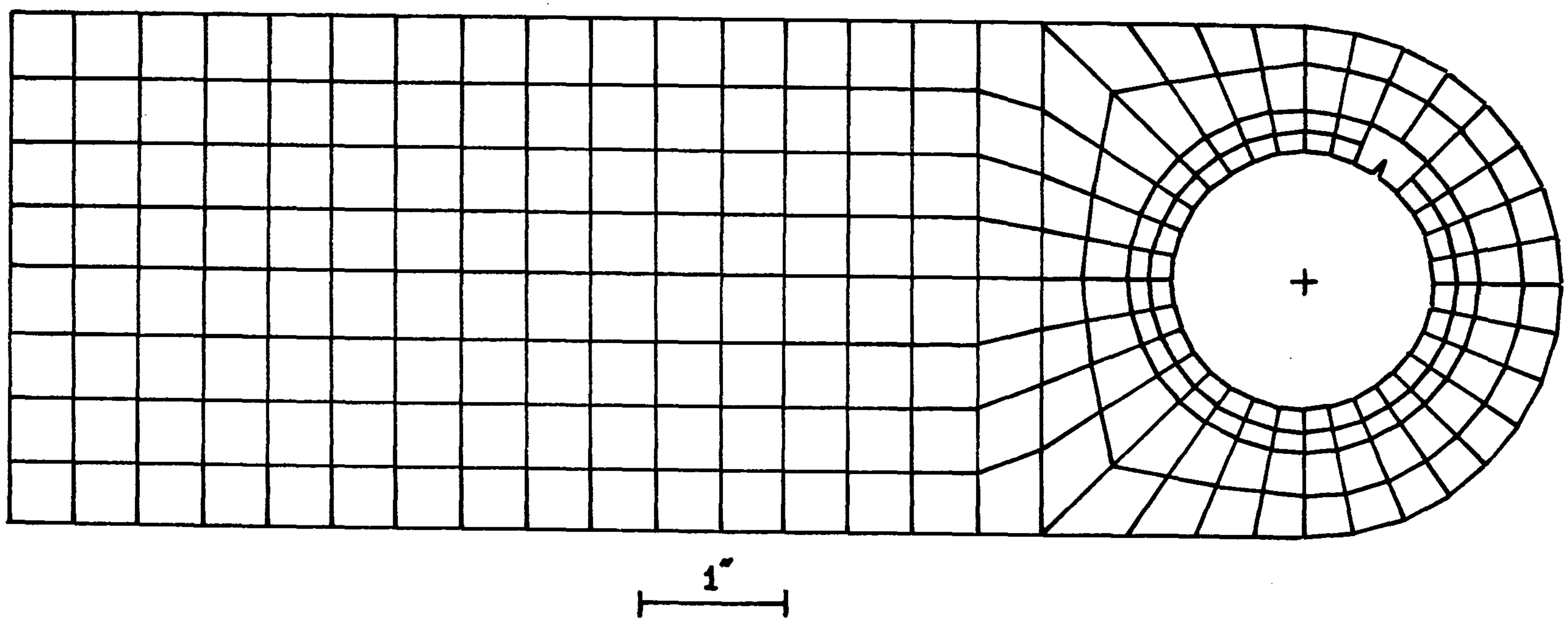


FIG. 21 SCALE MESH PLAN FOR ENGINE PYLON TRUSS LUG

STRESS CONTOURS IN UNCRACKED STRUCTURE
(0.5 KSI INTERVAL)

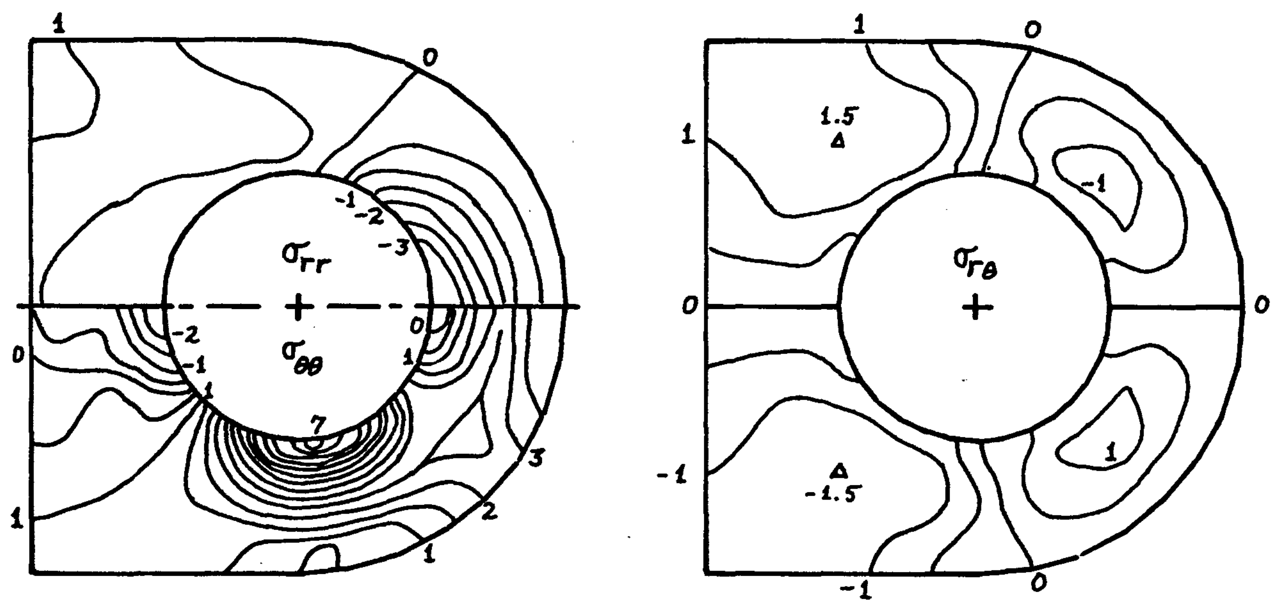


FIG. 22 STRESS CONTOURS FOR ENGINE PYLON TRUSS LUG (TENSION BEARING, COSINE PRESSURE)

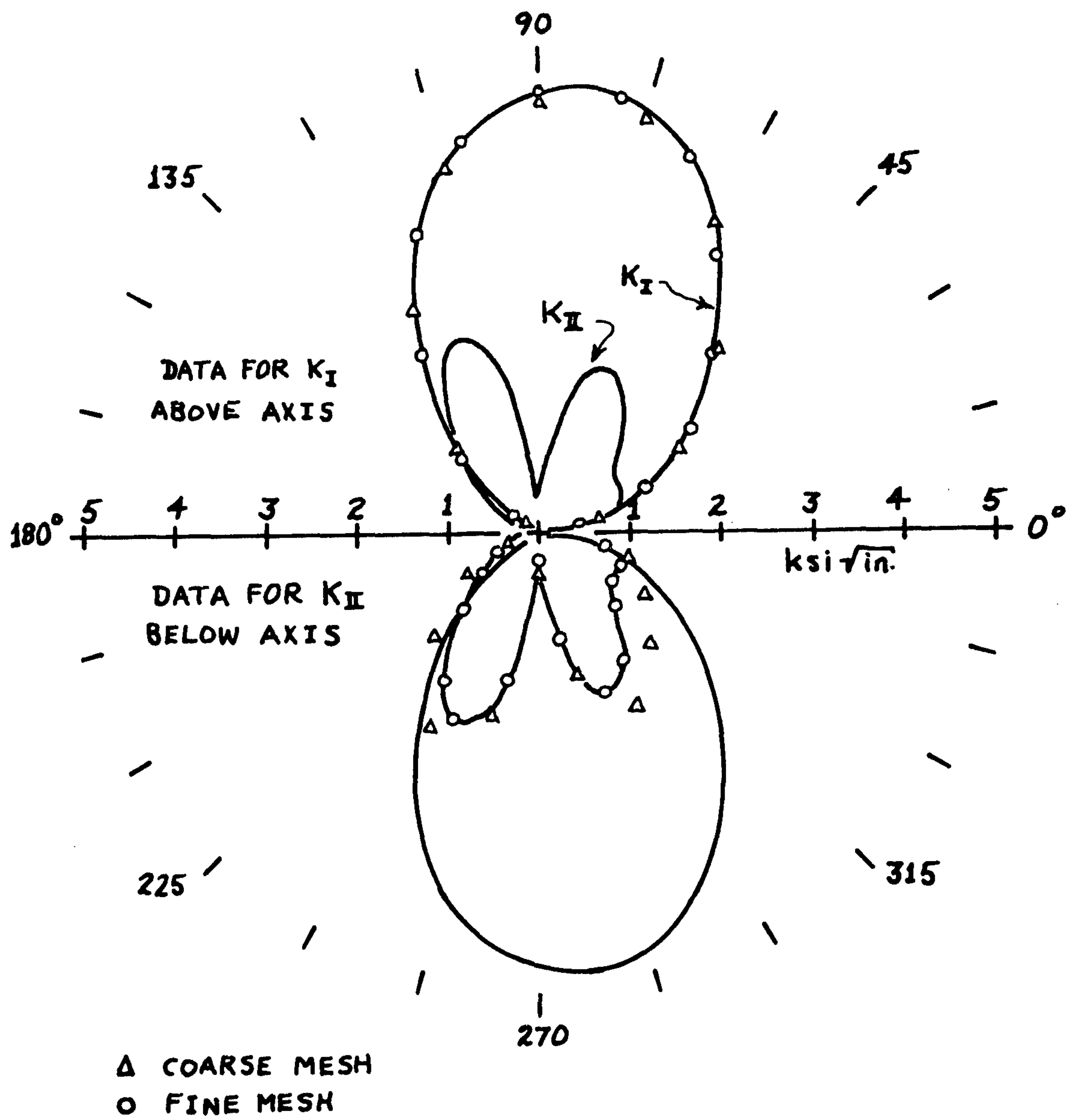


FIG. 23 BUTTERFLY PLOT FOR ENGINE PYLON TRUSS LUG (TENSION BEARING, COSINE PRESSURE)

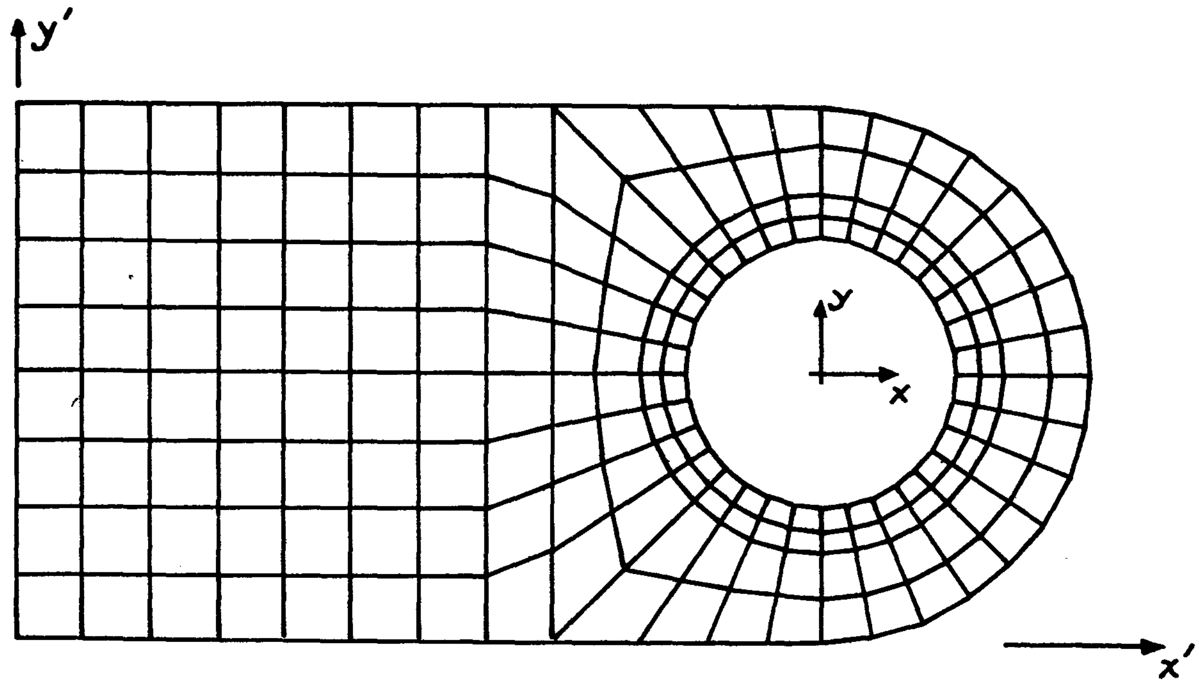


Note: x'y' axes refer to comparison of results with engineering beam theory (Fig. 29).

FIG. 24 SCALE MESH PLAN FOR 7-INCH ENGINE PYLON TRUSS LUG

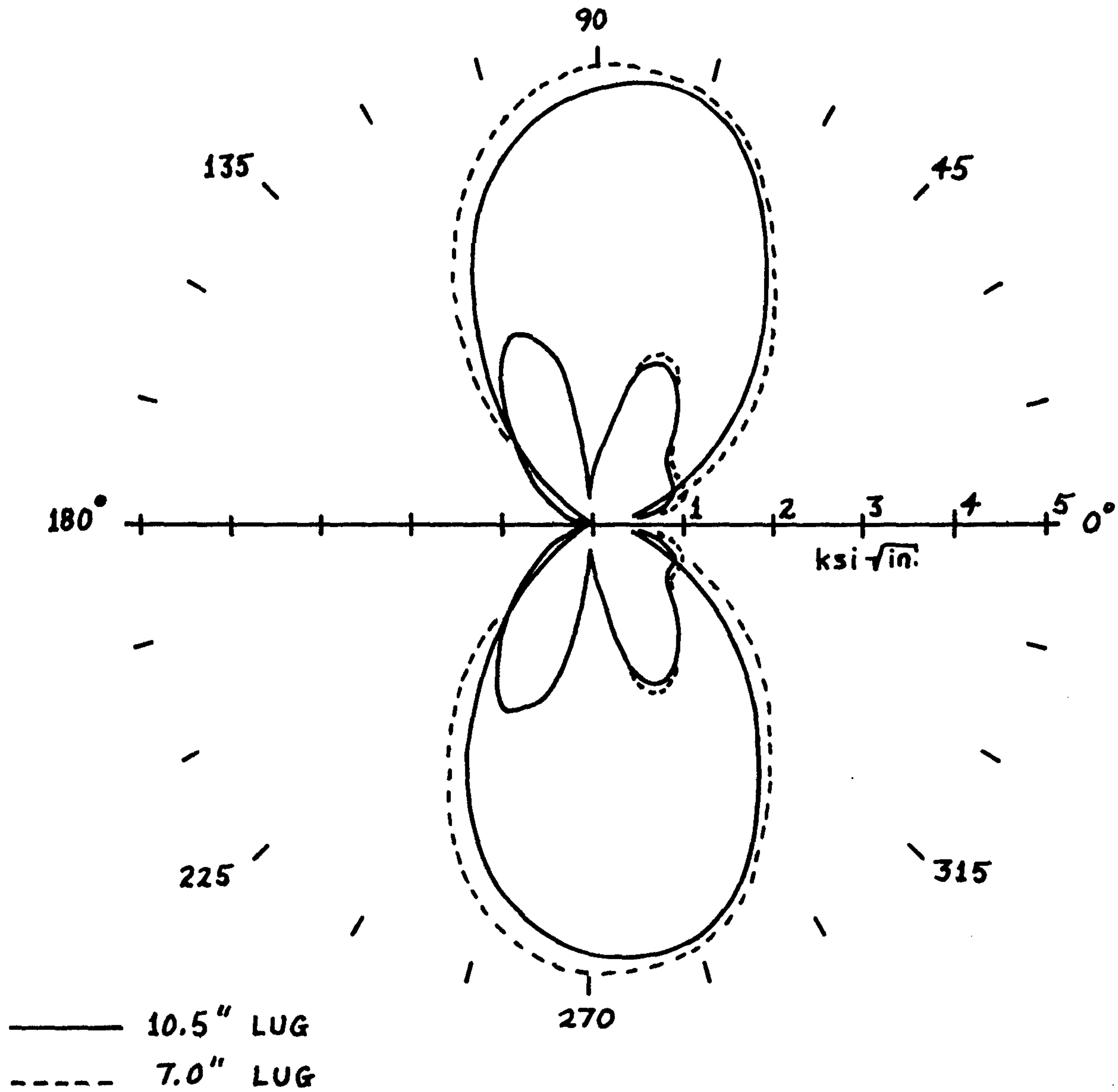


FIG. 25 EFFECT OF SHANK LENGTH ON STRESS INTENSITY
(TENSION BEARING, COSINE PRESSURE)

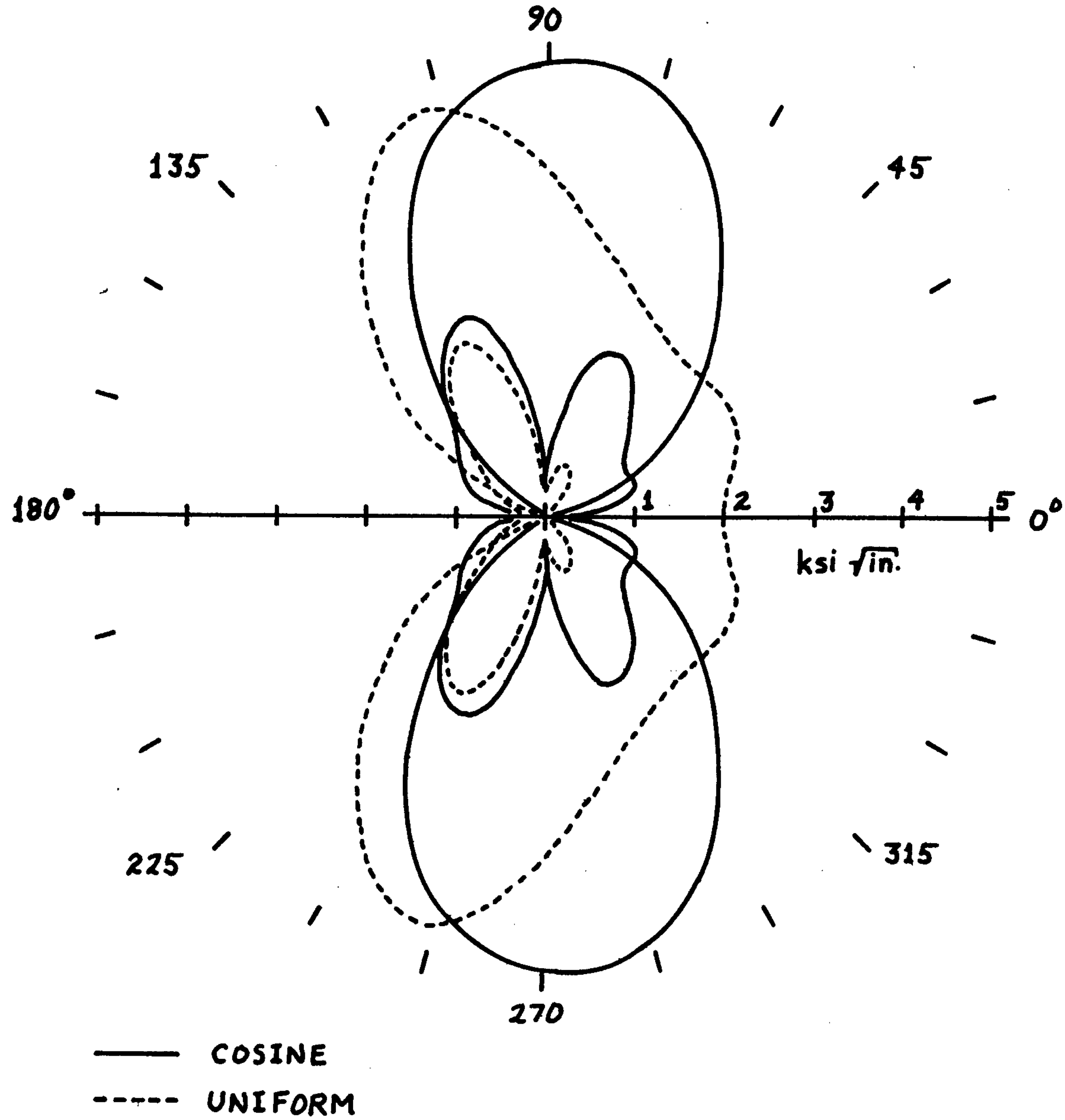


FIG. 26 COMPARISON OF COSINE AND UNIFORM PRESSURE DISTRIBUTIONS (TENSION BEARING)

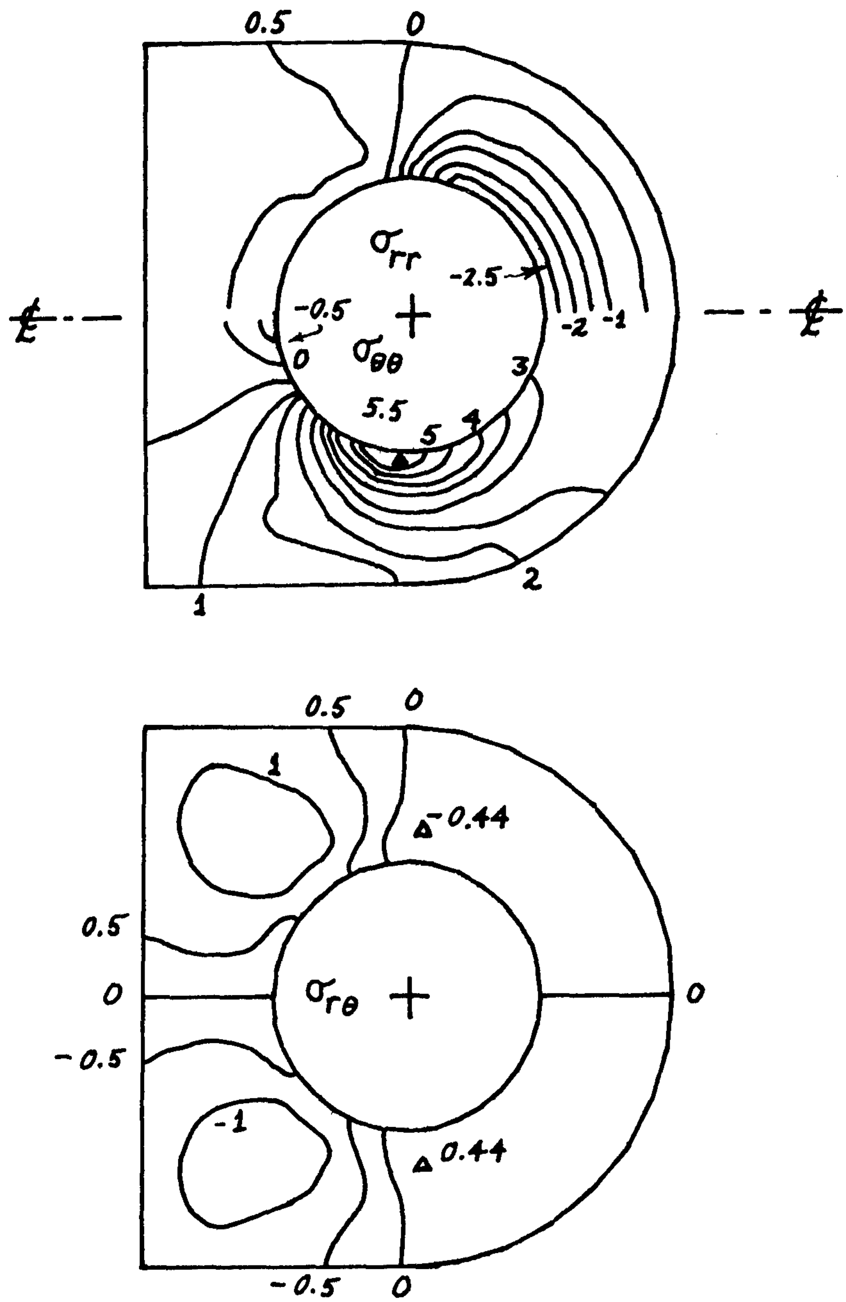


FIG. 27 STRESS CONTOURS FOR 7-INCH ENGINE PYLON TRUSS LUG (TENSION BEARING, UNIFORM PRESSURE)

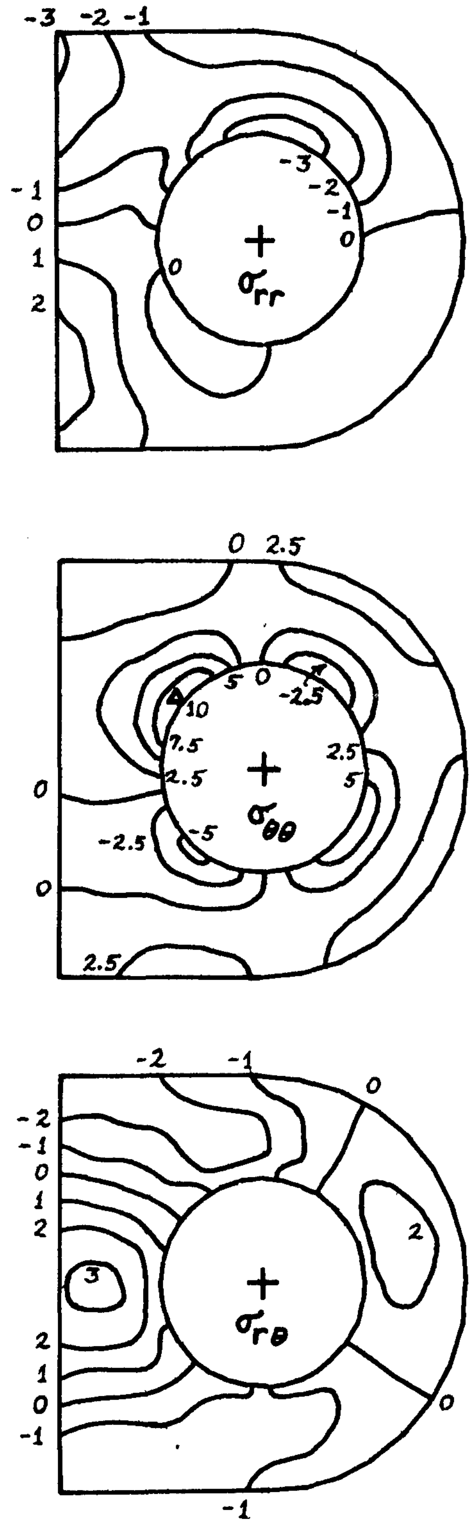


FIG. 28 STRESS CONTOURS FOR 7-INCH ENGINE PYLON TRUSS LUG (POSITIVE SHEAR BEARING, COSINE PRESSURE)

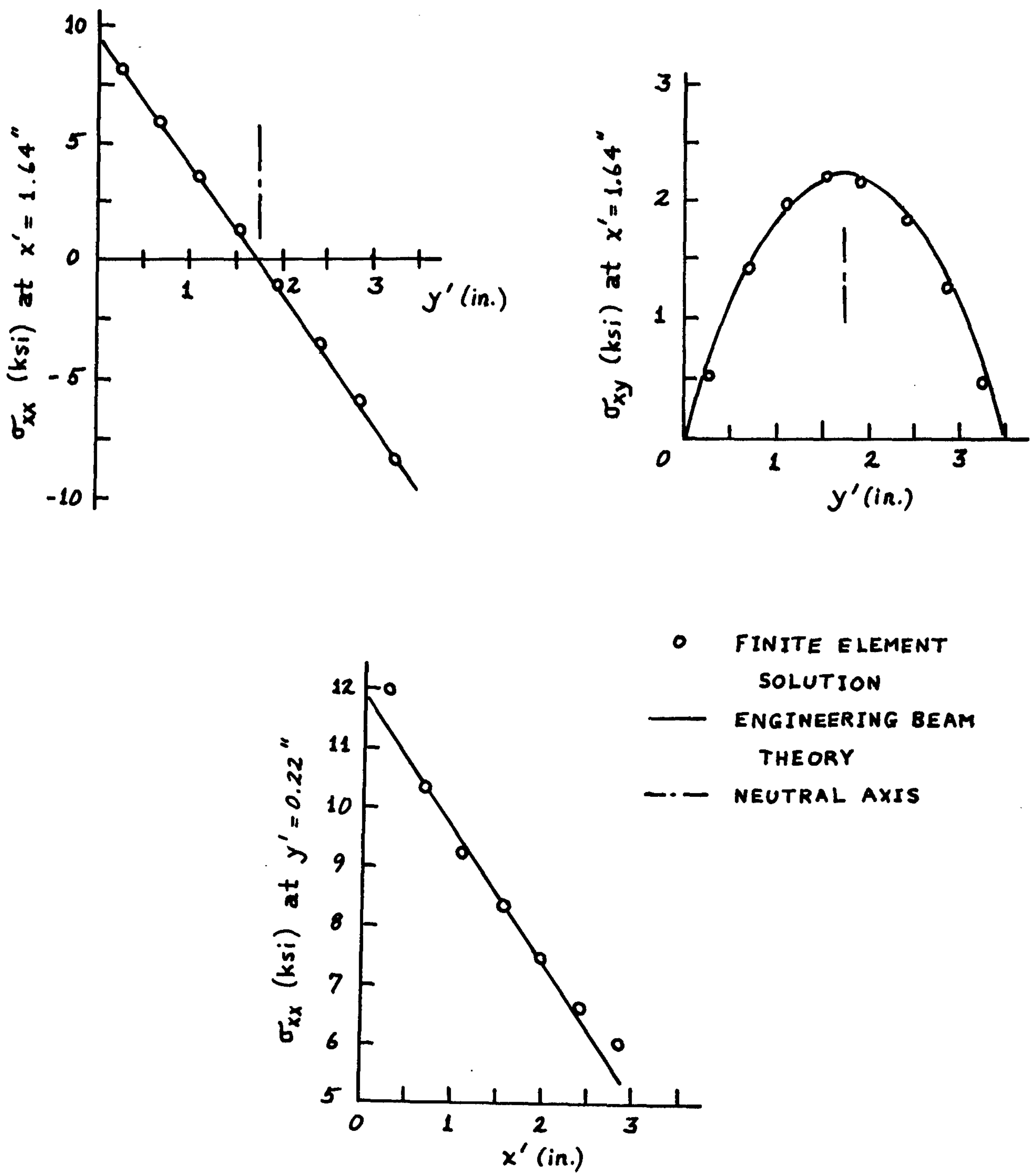


Note: See Fig. 24 for location of x'y' axes

FIG. 29 COMPARISON OF FINITE ELEMENT RESULTS WITH ENGINEERING BEAM THEORY (POSITIVE SHEAR BEARING, COSINE PRESSURE)

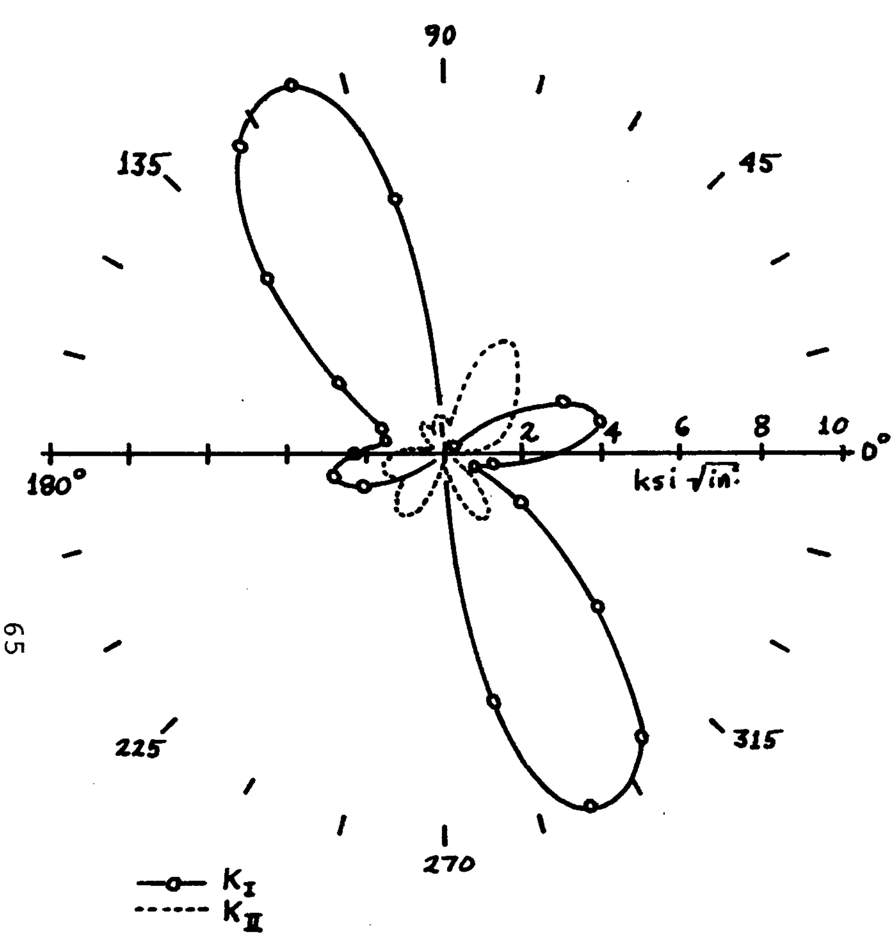


FIG. 30 BUTTERFLY PLOTS FOR 7-INCH ENGINE PYLON TRUSS LUG (POSITIVE SHEAR BEARING, COSINE PRESSURE)

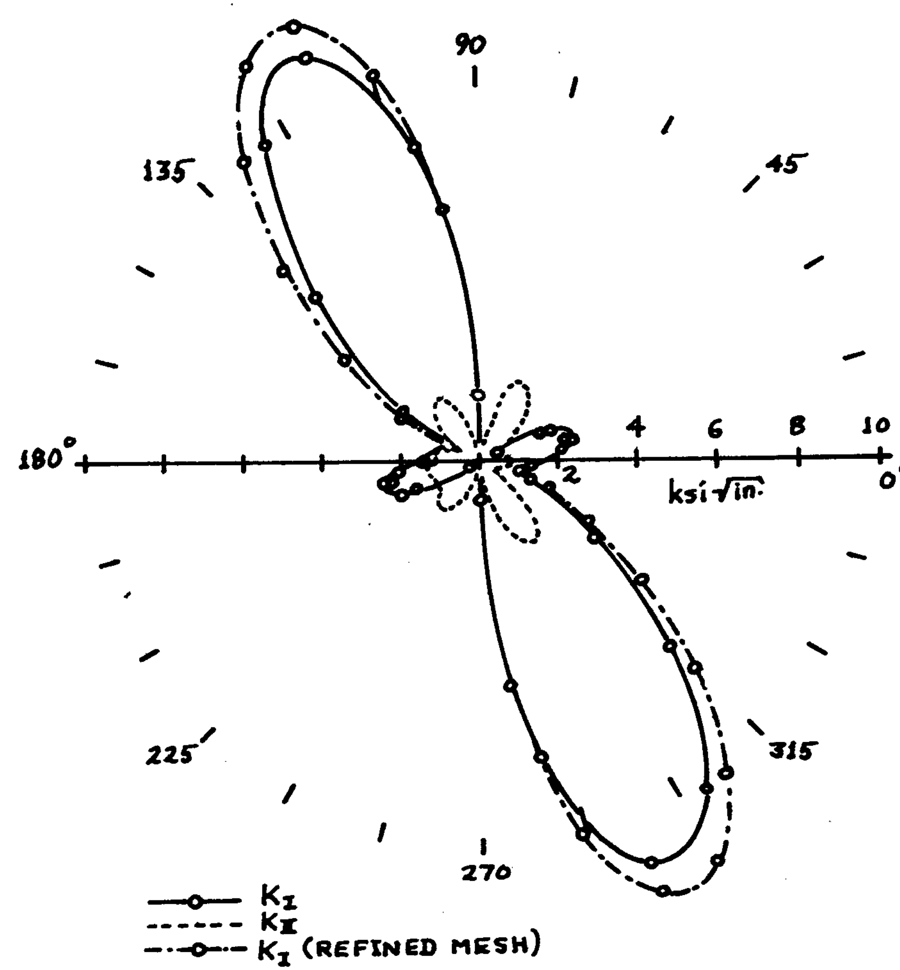


FIG. 31 BUTTERFLY PLOTS FOR 7-INCH PYLON TRUSS LUG (POSITIVE SHEAR BEARING, UNIFORM PRESSURE)

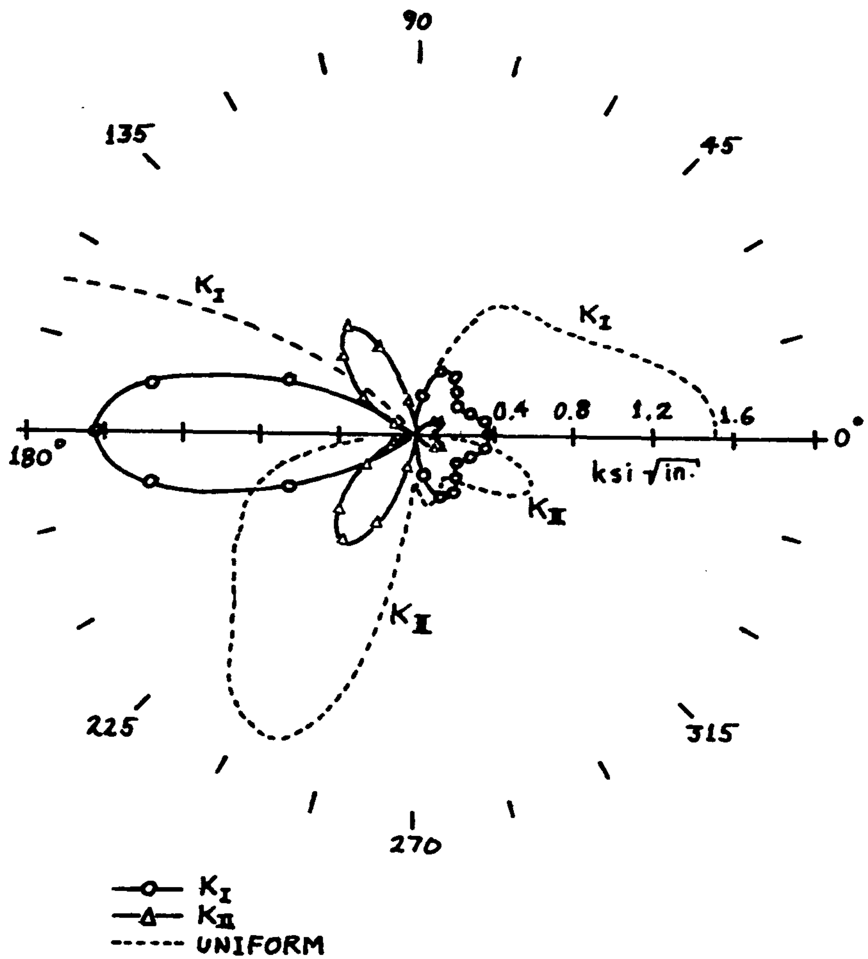


FIG. 32 BUTTERFLY PLOTS FOR 7-INCH ENGINE PYLON TRUSS LUG (COMPRESSION BEARING, COSINE PRESSURE)

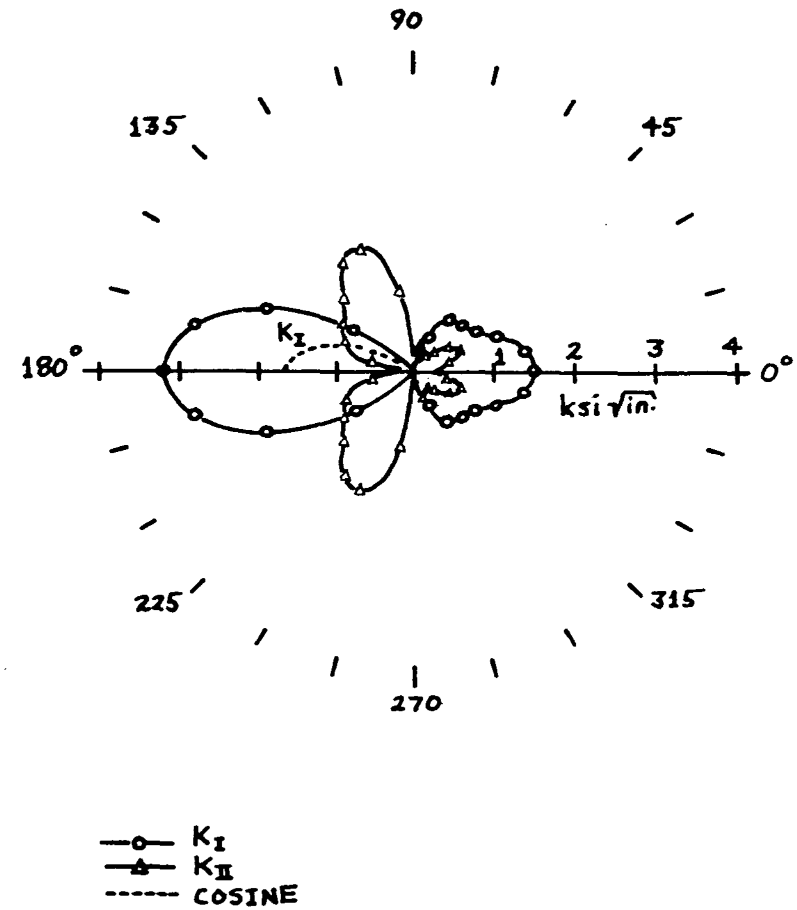


FIG. 33 BUTTERFLY PLOTS FOR 7-INCH ENGINE PYLON TRUSS LUG (COMPRESSION BEARING, UNIFORM PRESSURE)

# APPENDIX A

```
C***************************************************************************
C                                                                          *
C ATTACHMENT LUG PROCEDURE (LUG)                                           *
C                                                                          *
C PROCEDURE LUG IS A FINITE-ELEMENT ANALYSIS PROGRAM FOR STRESS ANALYSIS AND/OR*
C CALCULATION OF NASA/ASTM STANDARD STRESS INTENSITY FACTORS IN A ONE- OR TWO- *
C MATERIAL LUG SUBJECTED TO A BEARING LOAD.                                *
C                                                                          *
C PROCEDURE LUG AUTO-GENERATES A STRUCTURE MODEL REPRESENTING AN ATTACHMENT LUG*
C PARALLEL TO THE X-AXIS.  THE LEFT (VERTICAL) EDGE OF THE LUG IS BUILT IN.   *
C THE LUG BEGINS WITH CONSTANT WIDTH (Y-DIRECTION) AND FAIRS INTO A SEMI-  *
C CIRCULAR SHAPE ON THE RIGHT.  AN INTEGRALLY BONDED ISOTROPIC BUSHING (MATL *
C #1) IS CONCENTRIC WITH THE SEMI-CIRCLE.  THE LUG (MATL #2) MAY BE ISOTROPIC *
C OR ORTHOTROPIC WITH MATERIAL AXES INCLINED AT AN ARBITRARY ANGLE TO THE XY *
C AXIS SYSTEM.  A COSINE OR UNIFORM PRESSURE BEARING LOAD IS APPLIED TO THE *
C INNER SURFACE OF THE BUSHING, CENTERED ON THE LINE OF ACTION OF THE      *
C RESULTANT BEARING FORCE.  THE BEARING FORCE IS INPUT AS A TENSION COMPONENT *
C (PARALLEL TO X, POSITIVE TO RIGHT) AND A SHEAR COMPONENT (PARALLEL TO Y, *
C POSITIVE UP).  PLANE STRESS IS ASSUMED.  MULTIPLE CASES MAY BE RUN BY    *
C REPEATING CARDS 2 THRU 7 OF THE INPUT DATA CARD STACK.                   *
C                                                                          *
C INPUT DATA CARD STACK:                                                   *
C   1.    NCASES                                               (I5)        *
C   2.    TITLE                                                (20A4)      *
C   3.    IANL, LOAD, MODE, NT                                 (4I5)       *
C   4.    DI, DB, W, H, T, CSIZE                               (6E10.0)    *
C   5.    E1, V1                                               (2E10.0)    *
C   6.    E2, V2                                               (2E10.0)    *
C         OR                                                               *
C         EL2, ELT2, ET2, G2, THETA                            (5E10.0)    *
C   7.    TENSN, SHEAR                                         (2E10.0)    *
C                                                                          *
C EXPLANATION:                                                             *
C NCASES = TOTAL NO. OF CASES TO BE RUN                                    *
C TITLE = ANY DESCRIPTIVE INFORMATION FOR THIS CASE                        *
C IANL = ANALYSIS OPTION: 1 = STRESS ANALYSIS AND FULL PRINT               *
```

```
C                        2 = STRESS INTENSITY ANALYSIS; PLACE CRACK AT       *
C                        ANGULAR INTERVALS FROM 0 TO 360 DEGREES AROUND THE  *
C                        BUSHING; PRINT ONLY K1 AND K2 VERSUS ANGLE.         *
C                                                                            *
C LOAD = LOAD OPTION: 1 = COSINE BEARING                                     *
C                     2 = UNIFORM BEARING                                    *
C                                                                            *
C MODE = MATERIAL MODE OPTION: 1 = ISOTROPIC LUG                             *
C                              2 = ORTHOTROPIC LUG                           *
C                                                                            *
C NT = TOTAL NO. OF DIVISIONS IN 45-DEGREE INTERVAL AROUND BUSHING; 8*NT DIVS *
C      WILL OCCUR AROUND ENTIRE BUSHING.  (MESH IS AUTO-GENERATED FROM NT.)  *
C      NT VALUES FROM 2 TO 4 CAN BE CHOSEN.                                  *
C                                                                            *
C DI = BUSHING I.D.                                                          *
C DB = BUSHING O.D.                                                          *
C W = LUG WIDTH                                                              *
C H = LUG LENGTH, ROOT TO TIP                                                *
C T = LUG THICKNESS                                                          *
C CSIZE = CRACK LENGTH (USED ONLY IF IANL = 2)                               *
C CDIR = ANGLE (DEGREES) FROM RADIAL DIRECTION TO CRACK DIRECTION, POSITIVE  *
C        CCW (USED ONLY IF IANL = 2)                                         *
C                                                                            *
C E1, V1 = BUSHING YOUNGS MODULUS, POISSON RATIO                             *
C E2, V2 = SAME FOR LUG (ONLY IF MODE = 1)                                   *
C FOR MODE = 2:                                                              *
C EL2, ELT2, ET2, G2 = LUG ELASTIC MODULI                                    *
C THETA = ANGLE FROM X-AXIS TO L-AXIS, POSITIVE CCW (DEGREES)                *
C                                                                            *
C TENSN, SHEAR = BEARING FORCE COMPONENTS                                    *
C                                                                            *
C PROCEDURE LUG REQUIRES THE FOLLOWING SUBROUTINES:                          *
C   1.   ASRL FEABL/V2:                                                      *
C        ASMLTV,ECON,FACT,ORK,SETUP,SIMULQ,XTRACT                            *
C   2.   ASRL EGL:                                                           *
C        CTFORM,QUAD4,PCRK59                                                 *
```

```
C   3.   IBM SCIENTIFIC SUBROUTINE PACKAGE (SSP):                            *
C        SINV,MFSD                                                          *
C                                                                            *
C NOTE TO PROGRAM USERS: PROCEDURE LUG IS WRITTEN IN ANS STANDARD FORTRAN-4  *
C AND SHOULD RUN ON ANY HARDWARE WITH 180 KBYTES (45000 DECIMAL WORDS, 127710 *
C OCTAL WORDS) OF CORE MEMORY.  FULL (132-POSITION) LINE PRINTER IS REQUIRED. *
C IF STRESS ANALYSIS (IANL = 1) IS EXECUTED, JOB CONTROL INSTRUCTIONS MUST BE *
C SUPPLIED TO SET UP FORTRAN UNIT NUMBER 20 AS A SCRATCH FILE WITH 200 RECORDS *
C OF UNFORMATTED DATA (30 DECIMAL WORDS PER RECORD).  PROCEDURE LUG WILL      *
C WRITE TO AND READ FROM FORTRAN FILE 20 AS A SEQUENTIAL DATASET.  FORTRAN    *
C UNIT NUMBERS 5 FOR CARD READER AND 6 FOR PRINTER ARE ASSUMED; TO MODIFY,    *
C REPROGRAM CARDS 49 AND 50.                                                 *
C                                                                            *
C SPONSORED BY: U.S. AIR FORCE FLIGHT DYNAMICS LABORATORY                    *
C               WRIGHT-PATTERSON AIR FORCE BASE, OHIO 45433                  *
C TECH MONITOR: JAMES RUDD (AFFDL/FBR)                                       *
C                                                                            *
C PROGRAMMED BY: AEROELASTIC AND STRUCTURES RESEARCH LABORATORY              *
C                41-219 M.I.T.   CAMBRIDGE, MASS. 02139                      *
C PROGRAM MGR9:  OSCAR ORRINGER (617)-253-2430                               *
C                                                                            *
C COPYRIGHT (C) 1974  MASSACHUSETTS INSTITUTE OF TECHNOLOGY                  *
C                                                                            *
C*****************************************************************************
      DIMENSION TITLE(20)                                              LUG 0001
      DATA LDATA /22350/                                               LUG 0002
      DIMENSION RE(22350), IN(22350)                                   LUG 0003
      EQUIVALENCE (RE(1), IN(1))                                       LUG 0004
      COMMON /IO/ KR, KW, KP, KT1, KT2, KT3                            LUG 0005
      COMMON /SIZE/ NET, NDT                                           LUG 0006
      COMMON /BEGIN/ ICON,IKOUNT,ILNZ,IMASTR,IQ,IK                     LUG 0007
      COMMON /E N D/ LCON,LKOUNT,LLNZ,LMASTR,LQ,LK                     LUG 0008
C ELEMENT-LEVEL STORAGE                                                LUG 0009
      DIMENSION EXY(18), TEMP(4), C(3,3), CB(3,3), CL(3,3), NOD(4),    LUG 0010
     2 ANG(4), Q(18), SM(171), B(3,9), SXY(3), SRT(3), BCR(2,18),      LUG 0011
     3 LDUMY(4), SCALE(66,2)                                           LUG 0012
```

```
      EQUIVALENCE (B(1,1), C(1,1))
C STORAGE FOR STRESS INTENSITY RESULTS
      DIMENSION ONE(48), TWO(48), ANGLE(48)
      DATA TEMP/4*0./, NOD/4*0/, CB/9*0./, PI/3.141593/
C READ/PRINT CONTROL
  500 FORMAT(16I5)
  501 FORMAT(8E10.3)
  502 FORMAT(20A4)
  600 FORMAT(4(1X,30(4H****),/),/,36H0FEABL-2 WING ATTACH LUG PROGRAM FO
     2R,I4,6H CASES,/,4(1X,30(4H****),/))
  601 FORMAT(5H1CASE,I4,1H:,1X,20A4)
  602 FORMAT(6H0MODE=,I2,33H (1=ISOTROPIC, 2=ORTHOTROPIC LUG),/,1X,8HTOT
     2AL OF,I3,25H ELEMENTS AROUND PIN HOLE,/,1X,10HHOLE I.D.=,E10.3,5X,
     313HBUSHING O.D.=,E10.3,5X,10HLUG WIDTH=,E10.3,2X,11HLUG LENGTH=,
     4 E10.3,2X,10HTHICKNESS=,E10.3)
  603 FORMAT(21H0BUSHING MATERIAL: E=,E10.3,4H NU=,E10.3)
 6041 FORMAT(21H0ISOTROPIC LUG:    E=,E10.3,4H NU=,E10.3)
 6042 FORMAT(44H0ORTHOTROPIC LUG WITH MATERIAL AXES INCLINED,E10.3,18H D
     2EG AND C MATRIX=,3X,3E15.3,/,2(75X,3E15.3,/))
  605 FORMAT(17H0APPLIED TENSION=,E10.3,15H LB. AND SHEAR=,E10.3,4H LB.)
  606 FORMAT(1H0,10(4H****),/,39H0INDEFINITE MATRIX; THIS CASE CANCELLED
     2,/,1X,10(4H****))
  607 FORMAT(25H1STRESS ANALYSIS FOR CASE,I4,1X,20A4,/,5H0LNUM,4X,18HCEN
     2TROID LOCATION,12X,18HCARTESIAN STRESSES,20X,14HPOLAR STRESSES,/,
     3 7X,10H----XC----,2X,10H----YC----,2X,10H----XX----,2X,10H----YY--
     4--,2X,10H----XY----,2X,10H----RR----,2X,10H----TT----,2X,10H----RT
     5----,/,1X,25(4H****),/,1X,15HPART A: BUSHING)
  608 FORMAT(1X,11HPART B: LUG)
  609 FORMAT(1X,I4,8(2X,E10.3))
  610 FORMAT(28H1STRESS INTENSITIES FOR CASE,I4,1X,20A4,//,4H POS,7X,10H
     2--ANGLES--,2X,10H----K1----,2X,10H----K2----,/,1X,46(1H*))
  611 FORMAT(1X,I3,7X,E10.3,2X,E10.3,2X,E10.3)
  612 FORMAT(17H0ANALYSIS OPTION=,I2,14H; LOAD OPTION=,I2)
  613 FORMAT(14H0CRACK LENGTH=,E10.3,12H; DIRECTION=,E10.3)
      SQPI = SQRT(PI)
C DEVICE CODES
```

```
      KR = 5
      KW = 6
      READ (KR,500) NCASES
      WRITE (KW,600) NCASES
C CASE LOOP
      DO 32 ICASE = 1,NCASES
      KT1 = KW
      READ (KR,502) TITLE
      WRITE (KW,601) ICASE, TITLE
      READ (KR,500) IANL,LOAD,MODE,NT
C IANL = 1 (STRESS ANALYSIS; NO CRACK) OR 2 (STRESS INTENSITY ANALYSIS
C        WITH CRACK SEQUENCED AROUND PIN HOLE)
C LOAD = 1 (COSINE BEARING) OR 2 (CONSTANT BEARING) OVER 180-DEG ARC
C MODE = 1 (ISOTROPIC LUG) OR 2 (ORTHOTROPIC LUG)
C NT = DIVISIONS PER 45 DEG AROUND PIN HOLE
      NT2 = 2*NT
      NT2P1 = NT2+1
      NT3P1 = 3*NT+1
      NT4P1 = 4*NT+1
      NT5P1 = 5*NT+1
      NT6P1 = 6*NT+1
      NT8 = 8*NT
      MAXLOC = 1
      IF (IANL .EQ. 2) MAXLOC = NT8
      AINC = 0.25*PI/NT
      READ (KR,501) DI, DB, W, H, T, CSIZE, CDIR
      AAA2 = 0.
      AAA3 = -PI/2.
      AAA4 = AINC/2.
      TWOPI = 2./PI
      DO 100 I = 3,NT8,2
      AAA2 = AAA2+AINC
      AAA3 = AAA3+AINC
      AAA1 = TWOPI*(SIN(AAA3+AAA4)-SIN(AAA3-AAA4))
      IP1 = I+1
      CA2 = COS(AAA2)
```

```
      SA2 = SIN(AAA2)
      SCALE(I,1) = AAA1*CA2
      SCALE(IP1,1) = AAA1*SA2
      SCALE(I,2) = AAA4*CA2
  100 SCALE(IP1,2) = AAA4*SA2
      SCALE(1,1) = 0.
      SCALE(1,2) = 0.5*AAA4
      SCALE(2,1) = 0.
      SCALE(2,2) = 0.
      SCALE(NT8+1,1) = 0.
      SCALE(NT8+2,1) = 0.
      SCALE(NT8+1,2) = -0.5*AAA4
      SCALE(NT8+2,2) = 0.
C DI = PIN HOLE DIAMETER
C DB = BUSHING O.D.
C W = LUG WIDTH
C H = LUG LENGTH
C T = PART THICKNESS
C CSIZE = CRACK SIZE
C CDIR = CCW ANGLE FRCM BEARING SURFACE OUTWARD NORMAL TO LINE OF
C        CRACK (DEGREE MEASURE)
      WRITE (KW,612) IANL, LOAD
      WRITE (KW,602) MCDE, NT8, DI, DB, W, H, T
      IF (IANL .EQ. 2) WRITE (KW,613) CSIZE, CDIR
      RI = 0.5*DI
      RB = 0.5*DB
      RL = 0.5*W
      A = H-W
C BUSHING MATERIAL (ALWAYS ISOTROPIC)
      READ (KR,501) E, V
      WRITE (KW,603) E, V
      CB(1,1) = E/(1.-V*V)
      CB(2,1) = V*CB(1,1)
      CB(1,2) = CB(2,1)
      CB(2,2) = CB(1,1)
      CB(3,3) = 0.5*E/(1.+V)
```

```
      G = CB(3,3)                                                       LUG 0121
      ETA = (3.-V)/(1.+V)                                               LUG 0122
C LUG MATERIAL                                                          LUG 0123
      GO TO (1,2), MCDE                                                 LUG 0124
C ISOTROPIC                                                             LUG 0125
    1 READ (KR,501) E, V                                                LUG 0126
      WRITE (KW,6041) E, V                                              LUG 0127
      CL(1,1) = E/(1.-V*V)                                              LUG 0128
      CL(1,2) = V*CL(1,1)                                               LUG 0129
      CL(2,2) = CL(1,1)                                                 LUG 0130
      CL(3,3) = C.5*E/(1.+V)                                            LUG 0131
      GO TO 3                                                           LUG 0132
C ORTHOTROPIC                                                           LUG 0133
    2 READ (KR,501) CL(1,1), CL(1,2), CL(2,2), CL(3,3), THETA           LUG 0134
C THETA = MATERIAL AXIS INCLINATICN (DEGREES)                           LUG 0135
    3 CL(2,1) = CL(1,2)                                                 LUG 0136
      CL(1,3) = 0.                                                      LUG 0137
      CL(2,3) = 0.                                                      LUG 0138
      CL(3,1) = 0.                                                      LUG 0139
      CL(3,2) = 0.                                                      LUG 0140
      GO TO (6,4), MODE                                                 LUG 0141
    4 WRITE (KW,6042) THETA, CL                                         LUG 0142
      IF (THETA .EQ. 0.) GO TO 6                                        LUG 0143
C SPECIAL TRANSFCRMATICN FOR CL                                         LUG 0144
      DO 5 I = 1,3                                                      LUG 0145
      DO 5 J = 1,3                                                      LUG 0146
    5 C(I,J) = CL(I,J)                                                  LUG 0147
      THETA = -THETA                                                    LUG 0148
      CALL CTFORM(THETA,C,CL)                                           LUG 0149
C APPLIED LOADS                                                         LUG 0150
    6 READ (KR,501) TENSN, SHEAR                                        LUG 0151
      WRITE (KW,605) TENSN, SHEAR                                       LUG 0152
      IF (IANL .EQ. 1) GO TO 4000                                       LUG 0153
      TENSN = TENSN/T                                                   LUG 0154
      SHEAR = SHEAR/T                                                   LUG 0155
      T = 1.0                                                           LUG 0156
```

```
 4000 CONTINUE                                                            LUG 0157
C TOPOLOGY PARAMETERS AND HOUSEKEEPING; BEGIN BY SIZING THE MESH TO       LUG 0158
C KEEP ELEMENT ASPECT RATIOS CLOSE TO UNITY                               LUG 0159
      E = PI*(RI+RB)/NT8                                                  LUG 0160
      NRB = (RB-RI)/E+0.5                                                 LUG 0161
      E = PI*(RB+RL)/NT8                                                  LUG 0162
      NRL = (RL-RB)/E+0.5                                                 LUG 0163
      E = 0.5*W/NT                                                        LUG 0164
      NA = A/E+0.5                                                        LUG 0165
      IF (NRB .LE. 1) NRB = 2                                             LUG 0166
      IF (NRL .LE. 0) NRL = 1                                             LUG 0167
      IF (NA .LE. 0) NA = 1                                               LUG 0168
      NRBP1 = NRB+1                                                       LUG 0169
      NRBP2 = NRB+2                                                       LUG 0170
      NR = NRB+NRL                                                        LUG 0171
      NNR = NR+1                                                          LUG 0172
      NDR = 2*NNR                                                         LUG 0173
      NETB = NT8*NRB                                                      LUG 0174
      NETBP1 = NETB+1                                                     LUG 0175
      NM1 = NT8*NR+2*NT*NA                                                LUG 0176
      NET = NM1                                                           LUG 0177
      IF (IANL .EQ. 2) NET = NM1+1                                        LUG 0178
      NDT = 2*(NT8*NNR+NA*NT2P1)                                          LUG 0179
      NDW = 4*NT+2                                                        LUG 0180
      LIST = 9*NM1                                                        LUG 0181
      IF (IANL .EQ. 2) LIST = LIST+19                                     LUG 0182
      IF (IANL .EQ. 1) GO TO 2002                                         LUG 0183
      DO 2001 LOC = 1,MAXLOC                                              LUG 0184
      ONE(LOC) = 0.                                                       LUG 0185
 2001 TWO(LOC) = 0.                                                       LUG 0186
C CRACK LOCATION LOOP                                                     LUG 0187
 2002 DO 2011 LOC = 1,MAXLOC                                              LUG 0188
      CALL SETUP(LDATA,NDW,LIST,RE,IN)                                    LUG 0189
C ELEMENT CONNECTIONS (THREE STAGES)                                      LUG 0190
C STAGE 1: BUSHING                                                        LUG 0191
      LP = IMASTR                                                         LUG 0192
```

```
      L = IMASTR+NET
      DO 8 J = 1,NT8
      DO 8 I = 1,NRB
      IN(LP) = L
      K = NDR*(J-1)+2*I-1
      M = K+NDR
      IF (J .EQ. NT8) M = 2*I-1
      DO 7 N = 1,4
    7 IN(L+N-1) = K+N-1
      IN(L+4) = M+2
      IN(L+5) = M+3
      IN(L+6) = M
      IN(L+7) = M+1
      LP = LP+1
    8 L = L+8
C STAGE 2: SURROUNDING LUG AREA
      DO 10 J = 1,NT8
      DO 10 I = NRBP1,NR
      IN(LP) = L
      K = NDR*(J-1)+2*I-1
      M = K+NDR
      IF (J .EQ. NT8) M = 2*I-1
      DO 9 N = 1,4
    9 IN(L+N-1) = K+N-1
      IN(L+4) = M+2
      IN(L+5) = M+3
      IN(L+6) = M
      IN(L+7) = M+1
      LP = LP+1
   10 L = L+8
C STAGE 3: LUG FOOT (TRACK NUMBERING IN A DATA VECTOR OVERLAY, WHICH
C WILL END WITH CONSTRAINED DOF #S IN CORRECT BLOCK)
      IN(1) = NT8*NDR+1-NDW
      DO 11 J = 2,NDW
   11 IN(J) = IN(J-1)+1
      DO 15 J = 1,NA
```

```
C ADVANCE THE LINE
      DO 12 K = 1,NDW
   12 IN(K) = IN(K)+NDW
      DO 15 I = 1,NT2
      IN(LP) = L
      K = 2*I-1
      DO 13 N = 1,4
   13 IN(L+N-1) = IN(K+N-1)
      IN(L+4) = IN(L+2)-NDW
      IN(L+5) = IN(L+3)-NDW
      IN(L+6) = IN(L)-NDW
      IN(L+7) = IN(L+1)-NDW
      IF (J .GT. 1) GO TO 14
C SPECIAL CASE FCR FIRST LINE OF ELEMENTS IN THE FOOT
      K = (3*NT+I)*NDR-1
      IN(L+4) = K+NDR
      IN(L+5) = K+1+NDR
      IN(L+6) = K
      IN(L+7) = K+1
   14 LP = LP+1
      L = L+8
   15 CONTINUE
      IF (IANL .EQ. 1) GO TO 2005
C CRACK ELEMENT CVERLAY: BEGIN BY DUMMYING FOUR QUAD4 ELEMENTS OVERLAID
C BY THE PCRK59
      K = NRB*(LCC-1)
      LDUMY(1) = K+1-NRB
      LDUMY(2) = K+1
      LDUMY(3) = K+2-NRB
      LDUMY(4) = K+2
C POINTER AND DCF FOR PCRK59
      IN(LP) = L
      K = NDR*(LCC-1)+1
      IN(L) = K+4
      IN(L+1) = K+5
      IN(L+2) = K+4+NDR
```

```
      IN(L+3)  = K+5+NDR
      IN(L+4)  = K+2+NDR
      IN(L+5)  = K+3+NDR
      IN(L+6)  = K+NDR
      IN(L+7)  = K+1+NDR
      IF (LOC .NE. MAXLOC) GO TO 3000
C READJUST TOP EDGE DOF IF THE PCRK59 RECONNECTS WITH THE NUMBERING
C START LINE
      IN(L+2)  = 5
      IN(L+3)  = 6
      IN(L+4)  = 3
      IN(L+5)  = 4
      IN(L+6)  = 1
      IN(L+7)  = 2
 3000 CONTINUE
C LAPPED NODE
      IN(L+8)  = K
      IN(L+9)  = K+1
      LAPX = IQ+K-1
      LAPY = IQ+K
C MOVED NODE
      IN(L+10)  = K+2
      IN(L+11)  = K+3
      MOVX = IQ+K+1
      MOVY = IQ+K+2
      DO 2003 N = 1,6
 2003 IN(L+11+N)  = K-1+N-NDR
      IF (LOC .NE. 1) GO TO 2005
C SPECIAL CASE WHEN PCRK59 OVERLAYS NUMBERING START LINE
      LDUMY(1)  = 2*NT8-1
      LDUMY(3)  = 2*NT8
      M = NDR*(NT8-1)+1
      DO 2004 N = 1,6
 2004 IN(L+11+N)  = M-1+N
 2005 CONTINUE
      CALL ORK(LDATA,RE,IN)
```

```
C GLOBAL COORDINATE ALGORITHM: OVERLAY IN FORCE/DISPLACEMENT VECTOR FOR LUG 0301
C LATER CONVENIENCE (THREE STAGES SIMILAR TO CONNECTIONS)               LUG 0302
C STAGE 1: BUSHING                                                      LUG 0303
      E = (RE-RI)/NRB                                                   LUG 0304
      DO 16 J = 1,NT8                                                   LUG 0305
      THETA = (J-1)*AINC                                                LUG 0306
      DO 16 I = 1,NRBP1                                                 LUG 0307
      K = NDR*(J-1)+2*(I-1)                                             LUG 0308
      R = RI+(I-1)*E                                                    LUG 0309
      RE(IQ+K) = R*COS(THETA)                                           LUG 0310
   16 RE(IQ+1+K) = R*SIN(THETA)                                         LUG 0311
C STAGE 2: SURROUNDING LUG, BY OUTER EDGE + INTERPOLATION               LUG 0312
      DO 22 J = 1,NT8                                                   LUG 0313
      THETA = (J-1)*AINC                                                LUG 0314
      K = J*NDR-2                                                       LUG 0315
      IF (J .GT. NT2P1 .AND. J .LT. NT6P1) GO TO 17                     LUG 0316
C FIRST AND FOURTH QUADRANTS (CIRCULAR ARC)                             LUG 0317
      RE(IQ+K) = RL*COS(THETA)                                          LUG 0318
      RE(IQ+1+K) = RL*SIN(THETA)                                        LUG 0319
      GO TO 21                                                          LUG 0320
   17 IF (J .GT. NT4P1) GO TO 19                                        LUG 0321
C SECOND QUADRANT                                                       LUG 0322
      IF (J .GT. NT3P1) GO TO 18                                        LUG 0323
      RE(IQ+K) = -RL*TAN(THETA-0.5*PI)                                  LUG 0324
      RE(IQ+1+K) = RL                                                   LUG 0325
      GO TO 21                                                          LUG 0326
   18 RE(IQ+K) = -RL                                                    LUG 0327
      RE(IQ+1+K) = RL*TAN(PI-THETA)                                     LUG 0328
      GO TO 21                                                          LUG 0329
C THIRD QUADRANT                                                        LUG 0330
   19 IF (J .GT. NT5P1) GO TO 20                                        LUG 0331
      RE(IQ+K) = -RL                                                    LUG 0332
      RE(IQ+1+K) = -RL*TAN(THETA-PI)                                    LUG 0333
      GO TO 21                                                          LUG 0334
   20 RE(IQ+K) = -RL*TAN(1.5*PI-THETA)                                  LUG 0335
      RE(IQ+1+K) = -RL                                                  LUG 0336
```

```
C INTERPOLATION
   21 L = NDR*(J-1)+2*NRB
      E =  (RE(IQ+K)-RE(IQ+L))/NRL
      V =  (RE(IQ+1+K)-RE(IQ+1+L))/NRL
      DO 22 I = NRBP2,NR
      L = L+2
      RE(IQ+L)  = RE(IQ+L-2)+E
   22 RE(IQ+1+L)  = RE(IQ-1+L)+V
C STAGE 3: LUG FOOT
      K = NT8*NDR
      E = A/NA
      V = W/NT2
      DO 23 J = 1,NA
      DO 23 I = 1,NT2P1
      RE(IQ+K)  = -(RL+J*E)
      RE(IQ+1+K)  = RL-(I-1)*V
   23 K = K+2
      IF (IANL .EQ. 1) GO TO 2006
C CHANGE COORDINATES OF MOVED NODE TO LAPPED NODE
      RE(MOVX)  = RE(LAPX)
      RE(MOVY)  = RE(LAPY)
C ANGLE TO CRACK; TIP COORDINATES
      E =  (LOC-1)*AINC
      ANGLE(LOC)  = 180.*E/PI
      CDIR = PI*CDIR/180.
      XTIP = RE(LAPX)+CSIZE*COS(CDIR+E)
      YTIP = RE(LAPY)+CSIZE*SIN(CDIR+E)
 2006 CONTINUE
C GENERATION/ASSEMBLY
      IF (IANL .EQ. 1)  REWIND 20
      DO 24 K = 1,18
   24 Q(K)  = 0.
      DO 26 L = 1,NM1
      IF (IANL .EQ. 1) GO TO 2007
C SKIP DUMMY QUAD4 ELEMENTS IN OVERLAY
      IF (L .EQ. LDUMY(1)  .OR. L .EQ. LDUMY(2)  .OR. L .EQ. LDUMY(3)
```

```
     2 .OR. L .EQ. LDUMY(4)) GO TO 26
 2007 CONTINUE
      CALL XTRACT(L,8,EXY,RE,IN)
C ... THUS RETRIEVING THE PROPER COORDINATES (CLEVER!!)
      E = 0.
      V = 0.
      DO 25 N = 1,4
      E = E+0.25*EXY(2*N-1)
   25 V = V+0.25*EXY(2*N)
      EXY(11) = EXY(8)
      EXY(10) = EXY(7)
      EXY(8) = EXY(6)
      EXY(7) = EXY(5)
      EXY(5) = EXY(4)
      EXY(4) = EXY(3)
      IF (L .LE. NETB) CALL QUAD4(EXY,T,TEMP,CB,0,NOD,ANG,Q,SM,B,L,KW)
      IF (L .GT. NETB) CALL QUAD4(EXY,T,TEMP,CL,0,NOD,ANG,Q,SM,B,L,KW)
      IF (IANL .EQ. 1) WRITE (20) B, E, V
      CALL ASMLTV(L,8,SM,Q,RE,IN)
   26 CONTINUE
      IF (IANL .EQ. 1) GO TO 2008
C ASSEMBLE THE PCRK59
      CALL XTRACT(NET,18,EXY,RE,IN)
      CALL PCRK59(2,G,ETA,XTIP,YTIP,EXY,SM,BCR)
      CALL ASMLTV(NET,18,SM,Q,RE,IN)
 2008 CONTINUE
C GET RID OF NODAL COORDINATES
      DO 27 K = IQ,LQ
   27 RE(K) = 0.
      IF(SHEAR .EQ. 0. .AND. TENSN .EQ. 0. ) GO TO 288
      IF(SHEAR .EQ. 0.) GO TO 282
C APPLY SHEAR
      IFLAG = 1
      J3 = 0
      J4 = 0
      AAA1 = SHEAR
```

```
      AAA2 = 0.
      AAA3 = SHEAR
      AAA4 = 0.
      IF(SHEAR) 280,282,281
C NEGATIVE SHEAR
  280 NSEG = 2
      J1 = NT4P1
      J2 = NT8
      J3 = 1
      J4 = 1
      GO TO 285
C POSITIVE SHEAR
  281 NSEG = 1
      J1 = 1
      J2 = NT4P1
      GO TO 285
C APPLY TENSION
  282 IF(TENSN .EQ. 0.) GO TO 288
      J3 = 0
      J4 = 0
      IFLAG = 0
      AAA1 = 0.
      AAA2 = TENSN
      AAA3= 0.
      AAA4 = -TENSN
      IF(TENSN) 283,288,284
C NEGATIVE TENSION
  283 NSEG = 1
      J1 = NT2P1
      J2 = NT6P1
      GO TO 285
C POSITIVE TENSION
  284 NSEG = 2
      J1 = NT6P1
      J2 = NT8
      J3 = 1
```

```
      J4 = NT2P1                                                       LUG 0445
  285 I = -1                                                           LUG 0446
      JL = J1                                                          LUG 0447
      JU = J2                                                          LUG 0448
      DO 287 ISEG = 1,NSEG                                             LUG 0449
      DO 286 ILINE = JI,JU                                             LUG 0450
      I = I+2                                                          LUG 0451
      IP1 = I+1                                                        LUG 0452
      KX = IQ+NDR*(ILINE-1)                                            LUG 0453
      RE(KX) = RE(KX)+AAA1*SCALE(I,LOAD)+AAA2*SCALE(IP1,LOAD)          LUG 0454
  286 RE(KX+1) = RE(KX+1)+AAA3*SCALE(IP1,LCAD)+AAA4*SCALE(I,LOAD)      LUG 0455
      JL = J3                                                          LUG 0456
      JU = J4                                                          LUG 0457
  287 CONTINUE                                                         LUG 0458
      IF(IFLAG .EQ. 1) GO TO 282                                       LUG 0459
  288 IF(IANL .EQ. 1) GO TO 289                                        LUG 0460
C APPLY HALF OF LCAD AT EACH NODE AT CRACK OPENING                      LUG 0461
      RE(MOVX) = 0.5*RE(LAPX)                                          LUG 0462
      RE(MOVY) = C.5*RE(LAPY)                                          LUG 0463
      RE(LAPX) = RE(MOVX)                                              LUG 0464
      RE(LAPY) = RE(MOVY)                                              LUG 0465
C LOADING IS CCMPLETE                                                  LUG 0466
  289 CALL BCCN(RE,IN)                                                 LUG 0467
C SCLUTION (POSITIVE-DEFINITE MATRIX)                                  LUG 0468
      ISGN = 0                                                         LUG 0469
      CALL FACT(ISGN,RE,IN)                                            LUG 0470
      IF (ISGN .EQ. 1) GO TO 29                                        LUG 0471
      WRITE (KW,606)                                                   LUG 0472
      GC TO 32                                                         LUG 0473
   29 IF (IANL .EQ. 1) KT1 = 0                                         LUG 0474
      CALL SIMULQ(E,RE,IN)                                             LUG 0475
      IF (IANL .EQ. 2) GO TO 2009                                      LUG 0476
C STRESS SOLUTICN                                                      LUG 0477
      REWIND 20                                                        LUG 0478
      WRITE (KW,607) ICASE, TITLE                                      LUG 0479
      DO 31 L = 1,NET                                                  LUG 0480
```

```
      CALL XTRACT(L,8,Q,RE,IN)
      READ (20) E, E, V
      H = E**2+V**2
      DO 30 I = 1,3
      SXY(I) = 0.
      DO 30 J = 1,8
   30 SXY(I) = SXY(I)+B(I,J)*Q(J)
      CSQ = E*E/H
      SSQ = V*V/H
      SC = E*V/H
      SRT(1) = SXY(1)*CSQ+SXY(2)*SSQ+2.*SXY(3)*SC
      SRT(2) = SXY(1)*SSQ+SXY(2)*CSQ-2.*SXY(3)*SC
      SRT(3) = SC*(SXY(2)-SXY(1))+(CSQ-SSQ)*SXY(3)
      IF (L .EQ. NETEP1) WRITE (KW,608)
   31 WRITE (KW,609) L, E, V, SXY, SRT
      GO TO 2011
C STRESS INTENSITY SCLUTICN
 2009 CALL XTRACT(NET,18,Q,RE,IN)
      DO 2010 J = 1,18
      ONE(LOC) = CNE(LOC)+BCR(1,J)*Q(J)
 2010 TWO(LOC) = TWO(LOC)+BCR(2,J)*Q(J)
C CONVERT TO NASA/ASTM STANDARD STRESS INTENSITIES
      ONE(LOC) = SQPI*CNE(LOC)
      TWO(LOC) = ABS(SQPI*TWO(LOC))
C END OF LOCATICN LOOP
 2011 CONTINUE
      IF(IANL .EQ. 1) GO TO 32
      WRITE (KW,610) ICASE, TITLE
      WRITE (KW,611) (LOC, ANGLE(LOC), ONE(LOC), TWO(LOC),
     2 LOC = 1,MAXLCC)
C END OF CASE
   32 CONTINUE
      STOP
      END
```



☆ U. S. GOVERNMENT PRINTING OFFICE: 1976 — 657-630/425